RESPONSE OF MULTI-STORY BUILDINGS UNDER EARTHQUAKE EXCITATION

A THESIS

Presented to

The Faculty of the Division of Graduate

Studies and Research

By

Tzu-I Hsu

In Partial Fulfillment

of the Requirements for the Degree

Doctor of Philosophy in the School

of Engineering Science and Mechanics

Georgia Institute of Technology

March, 1976

D-254 3-a

RESPONSE OF MULTI-STORY BUILDINGS

UNDER EARTHQUAKE EXCITATION

Approved:

M. C. Bernard, Chairman

J. J. Goode

W. W. King

C. E. S. Ueng

Date approved by Chairman: 2-23-76

This Thesis is

dedicated to my wife

Day-Luan

ACKNOWLEDGMENTS

The author wishes to express his sincere gratitude and appreciation to his thesis advisor, Dr. M. C. Bernard, for his suggestion of the topic and his helpful assistance and guidance throughout this research work.

Appreciation is also extended to Dr. J. J. Goode, Dr. W. W. King and Dr. C. E. S. Ueng, members of the reading committee, for their valuable suggestions. The helpful comments of Dr. B. J. Goodno is also gratefully acknowledged.

The author wishes to thank Dr. M. E. Raville, Director of the School of Engineering Science and Mechanics, who arranged financial assistance during the period of his study at the Georgia Institute of Technology.

The author's deepest appreciation goes to his wife, Day-Luan, for her love, patience, devotion and encouragement during the entire period of this study.

Finally, the author would like to thank his mother who for many years has offered her guidance to make his life meaningful.

TABLE OF CONTENTS

TABLE OF CONTENTS (Continued)

LIST OF TABLES

LIST OF ILLUSTRATIONS

LIST OF ILLUSTRATIONS (Continued)

LIST OF ILLUSTRATIONS (Continued)

LIST OF SYMBOLS

a, b	Parameters of the envelope function
c_j, c_{ij}	Damping coefficients
c^*_j, c^*_{ij}	Generalized damping coefficients
d	Proportional constant
$D(t)$	Envelope function
$E[\ ]$	Expected value
$\bar{F}_j$	Frequencies of ground acceleration, real positive numbers
F_j	Frequencies of ground acceleration, random variables
$F(t)$	Forcing function
g	Acceleration of gravity
$G(t)$	Stationary random process
$h_j(t)$	Impulse response functions
i	Imaginary unit $= \sqrt{-1}$
$I(t)$	Intensity function
$[I]$	Identity matrix
$\{I_o\}$	Unit column vector
j	Integer
k_j, k_{ij}	Spring constants
k^*_j, k^*_{ij}	Generalized stiffnesses
$\bar{k}_j$	Complex stiffnesses
k_e	Equivalent spring constant
$[L]$	Equivalent modal matrix
m_j	Masses

LIST OF SYMBOLS (Continued)

m_j^*	Generalized masses
n,N	Integers
$\bar{N}(t)$	Time varying ratio
N_o	Number of zero crossings per second
N_m	Number of maxima per second
$p_j(t)$	Forcing functions
$p_j^*(t)$	Generalized forcing functions
$p_{\{X\}}(x;t)$	Probability density function
$P_X\{x\}$	Probability distribution function
$P(t)$	Forcing function
$[Q^{(e)}(t)]$	Effective earthquake force matrix
$Q(t)$	Restoring force
$Q_j(t)$	Base shear forces
$Q_T(t)$	Total base shear force
$R_X(t_1,t_2)$	Autocorrelation function
$R_{XY}(t_1,t_2)$	Cross-correlation function
S_a	Spectral acceleration response
S_d	Spectral displacement response
S_v	Spectral pseudo-velocity response
$S_X(\omega)$	Power spectral density function
t	Time
T_j,T	Periods of vibration
$U_j(t)$	Normal coordinates
$\ddot{U}_j^{(e)}(t)$	Effective acceleration

LIST OF SYMBOLS (Continued)

$V_j(t)$	Story shear force
$v_j^{(D)}$	Critical story shear force
$X_o(t), X_g(t)$	Ground displacement
$\dot{X}_g(t)$	Ground velocity
$\ddot{X}_g(t)$	Ground acceleration
$X_j(t)$	Absolute displacements
$Y_j(t)$	Relative displacements
$y_j^{(D)}$	Critical relative displacements
α	Parameter of the envelope function
β	Coefficient
$\Gamma_X(t_1, t_2)$	Autocovariance function
$\Gamma_{XY}(t_1, t_2)$	Cross-covariance function
γ_i, γ	Structural damping factors
$\delta(t)$	The Dirac-delta function
δ_{mn}	The Kronecker delta
δ_j	Participation factors
Δ	Error of linearization
λ	Ratio of N_o/N_m
Θ_j	Phase angles of ground acceleration, random variables
θ_j	Phase angles of ground acceleration, real positive numbers
$\mu_X(t)$	Mean function
μ_d	Parameter of acceleration autocorrelation function
ξ_j, ξ	Damping ratios
$\rho(\tau)$	Normalized autocorrelation function

LIST OF SYMBOLS (Continued)

$\sigma_X(t)$	Standard deviation
$\bar{\sigma}_X(t_1, t_2)$	Average root-mean-square value
$\sigma_X^2(t)$	Variance function
τ	Time difference
$\{\phi_j\}$	Normalized modal vector
$[\Phi]$	Mode shape matrix
ω_j	Undamped natural circular frequency
ω_a	Parameter of ground acceleration autocorrelation function

SUMMARY

This research presents a method for the simulation of earthquake ground motion as well as a procedure for obtaining the dynamic response of multi-story shear buildings subjected to simulation earthquake excitation. The earthquake disturbance is simulated as a modulated nonstationary random process in which the stationary random process is expressed directly in terms of random functions. Then, a mathematical model is used to represent a tall building structure which includes not only viscous damping but also structural damping. The governing equations of motion of the building model are derived subsequently and then analyzed by the normal mode method. Finally, random vibration theory is employed in obtaining the dynamic response of buildings to the simulated earthquake excitation.

The earthquake acceleration model is simulated by a nonstationary random process which consists of a product of a deterministic envelope time function and a stationary random process. The probability density function of the random frequencies of the earthquake acceleration process is obtainable from the characteristics of the normalized autocorrelation function during the time of the strongest motion. The parameters of the stationary random process are obtained from those of the filtered processes which are used by Shinozuka and Sato and Amin and Ang in their work on simulation processes for earthquake ground motion. Thus, the input random process is actually a combination of the currently developed filtered process and modulated process.

The response spectral curves of the simulation process are plotted and compared. It is found that the simulated stochastic process satisfies Levy's criteria for simulation processes and thus is a suitable model for representing earthquake acceleration. It has also been shown that the simulated random process is a Gaussian process. Hence, the response is also a Gaussian process so long as linear systems are of concern.

A multi-story linear, damped shear building model on firm foundation is used almost entirely in the dynamic response analysis. Absolute viscous damping is included in the theoretical treatment for modal analysis of the governing equations of motion. As a result, the forcing functions of the equations of motion are expressed in terms of not only ground acceleration but also ground velocity. Thus, the correlations of acceleration and velocity processes of ground motion are actually involved in the dynamic response analysis.

Nonlinear models for tall buildings can be devised by taking into account the actual nonlinear nature of the shear forces in the columns. This has been investigated in the later stage of the thesis work. However it is concluded that the earthquake representation being used here is sufficiently complicated that if it is used as the input process for a nonlinear model the subsequent analysis would become extremely tedious, if not impossible.

Finally, the statistics of the response of the building structure such as the mean-square response, the probability density functions and the probability of the largest response exceeding an inadmissible value, are determined by means of random vibration theory.

CHAPTER I

INTRODUCTION

The dynamic analysis approach to the design of structures to withstand strong ground motion divides itself generally into three parts. They are the characterization of an input earthquake excitation, the specification of a structural model and the analysis of the dynamic response. As long as an input and a structure are specified, the analysis can be made leading to the solution of the problem.

The design earthquake input excitation for the site under consideration is usually prescribed in three ways. The first one consists in representation of values describing seismic loading by means of some deterministic function of time. It is obviously understood, however, that this approach has nothing in common with actual erratic and complex earthquake accelerograms. Thus, a dynamic response analysis based on this approach becomes unrealistic. The second, semi-empirical approach consists of representing the strong motion by the strongest earthquakes which had taken place in the past and which are typical for the seismic region considered. However, since the record of the next earthquake will be entirely different from the last one, or any previous or other future one in duration and shape, it is obvious that using any particular earthquake record from the past in place of the ground acceleration to obtain the response of structures to future earthquakes is improper. The inability to know from past records the

nature of future earthquakes suggests that possibly a statistical or probabilistic approach should be employed using random function theory. This goes to the development of the third approach which is based on probabilistic methods. This approach has been widely used recently in the representation of earthquake excitation. In this research, considerable effort will be put on the simulation of earthquake excitation model by means of the third approach.

There are many mathematical models available for representing real buildings in the dynamic analysis of structures to earthquakes. These vary from the simple linear elastic types to those which are complex and nonlinear. We shall confine our attention to a multi-story building, since other types of structures can be dealt with in a similar framework. Dissipation or damping in a structure is a very important factor in limiting its response to seismic disturbance. Two types of damping, viscous damping and structural damping, will be considered in the proposed structural model. Their effect on structural response will be examined. A linear multi-story shear building will be used mostly in the research. It is obvious, however, that the significance of the nonlinear behavior of a structure increases as the deformation increases. Moreover, nonlinearities in the deformation may have some influences on response of structures. Thus, a nonlinear structural model will also be investigated in this study.

The analysis of structural response can be achieved as long as the input process and the structural model are prescribed. It was mentioned that a probabilistic approach is realistic in representing earthquake excitation. Therefore, the theory of random vibration will

be employed in solving this kind of problem.

The normal mode method will be employed for the evaluation of the dynamic response. The statistics of the response of a building structure, such as the mean-square response, the probability density functions and the probability of the largest response exceeding an inadmissible value, can then be determined. These statistical quantities, which may not be precisely obtained in a deterministic approach, are essentially important factors in recent structural design.

CHAPTER II

LITERATURE REVIEW

Introduction

The dynamic analysis approach to the design of structures to withstand strong ground motion has been recognized by engineers for many years, but it is only recently that significant advances have been made. These advances result from the introduction of stochastic processes to structural analysis. Generally, one-degree-of-freedom structural models have always been used for response analysis. It is understood that the choice of structural models and the corresponding methods of approach depend entirely on the characteristics of the buildings to be designed. Due to the complicated expressions for the equations of motion, multi-story buildings of modern construction have seldom been analyzed by using stochastic processes to represent the earthquake ground motion. A brief review of the literature on the earthquake excitation models, structural models and the current state of the art on the subject will be described in this chapter.

Earthquake Excitation Models

The idea of "random" earthquakes was firstly proposed by G. W. Housner [1]* in 1947. He assumed that the ground acceleration during an earthquake could be considered composed of random pulses of fixed magnitude arriving randomly in time. He showed that the spectral curves

*Numbers in brackets correspond to references on p. 158.

computed by the true earthquake record and by the simulated model have the same fluctuation about the mean. Subsequently, a number of simulation processes have been developed to represent random earthquakes. Following is a review of these idealizations which are classified according to different simulation approaches.

Idealization of Earthquakes as Segments of White Noise

Using an analog computer, Bycroft [2] studied the use of a white noise process to represent earthquake ground motion. By comparing his average maximum response values with Housner's standard spectra curves [3], Bycroft concluded that white noise is a suitable representation for earthquakes. Rosenblueth and Bustamante [4] also used white noise simulation for earthquakes. Their model for an earthquake was composed of a series of velocity impulses of random amplitude. They found that, if the average velocity spacing in the actual earthquake accelerogram is considerably smaller than the natural period of any particular structure being considered, a white noise ground acceleration process may be assumed. Although ideal white noise is physically impossible, since it corresponds to an infinite variance value of the random process, it is still a good model because of its mathematical simplicity.

Idealization of Earthquakes as a Linear Filtered Process

Mathematical representation for filtered processes may be expressed as [5, p. 143)]

$$P[\ddot{X}_g(t)] = S(t) \qquad (2\text{-}1)$$

where

$$P = \sum_{m=0}^{M} b_m \frac{d^m}{dt^m}$$

is a linear differential operator and the b_m are real constants. $S(t)$ is the input process for the filter. $\ddot{X}_g(t)$ is the output random process which is here taken to be the earthquake ground motion. In general, shot noise is used as the input process for the filter. A random process $S(t)$ is called shot noise, if its mean and covariance function are given by

$$\mu_S(t) = 0 \tag{2-2}$$

and

$$\Gamma_S(t_1,t_2) = I(t_1)\ \delta(t_2 - t_1),\ t_2 > t_1 \tag{2-3}$$

where

$$\mu_S(t) = E[S(t)]$$

$$= \int_{-\infty}^{\infty} s\ p_{\{S\}}(s;t)ds \tag{2-4}$$

and

$$\Gamma_S(t_1,t_2) = E[\{S(t_1) - \mu_S(t_1)\}\{S(t_2) - \mu_S(t_2)\}] \tag{2-5}$$

in which $p_{\{S\}}(s;t)$ is called the probability density function of the random process $S(t)$.

$I(t)$ is called the intensity function and $\delta(t)$ is the Dirac-delta function. In case $I(t)$ is a constant, $S(t)$ becomes the well-known white noise process. By choosing different forms of intensity functions and the orders of the filter, different processes may be simulated. This idea was probably first established by Lin [6]. He used a first order linear filter and a half period sine intensity

function to produce a nonstationary random process as earthquake acceleration. The variance function of such a process looks like that of the typical earthquake record. Later on, Amin and Ang [7] used a second order linear filter to generate earthquake excitation with an intensity function given by

$$I(t) = \begin{cases} I_o\left(\frac{t}{t_1}\right)^2, & 0 \le t \le t_1 \\ I_o, & t_1 \le t \le t_2 \\ I_o \exp\left[-c(t-t_2)\right], & t \ge t_2 \end{cases} \qquad (2\text{-}6)$$

where I_o and c are constants, t_1 and t_2 are specified time instants. This simulation has been shown to be in good agreement with past earthquake records. Shinozuka and Sato [8] generated ground acceleration by passing white noise through a second order filter and then multiplying by a time-varying function to introduce nonstationarity. The filter and time-varying function are chosen so as to resemble average results from available records such as response spectra and variance as a function of time. Levy [9] commented upon Shinozuka and Sato's simulation process emphasizing possible differences with information taken from actual records. Levy also used a computer simulation. The filter input in his model is generated by applying suitable weighting functions to white noise in order to produce a correlated input which then is time multiplied and passed through a filter, to produce ground acceleration. At the same time, Ruiz and Penzien [10] put the local soil condition into the parameters of the filter. The ground motion is then simulated by a nonstationary filtered shot noise.

Physical interpretation of the filtered processes may be viewed as passing a random process through bedrock as the filter to produce ground motion. This kind of simulation seems to be in good agreement with past earthquake records statistically and geologically.

Idealization of Earthquakes as a Gaussian Process with Given Power Spectral Density

It is obvious that local geology affects the free surface motion of the ground. Kanai [11] analyzed the power spectral density functions of many accelerograms and suggested that the power spectral density function of the ground acceleration takes the form

$$S_{\ddot{X}_g}(\xi_g, \omega_g, \omega) = \frac{1 + 4\xi_g^2\left(\frac{\omega}{\omega_g}\right)^2}{\left[1 - \left(\frac{\omega}{\omega_g}\right)^2\right]^2 + 4\xi_g^2\left(\frac{\omega}{\omega_g}\right)^2} S_o \qquad (2\text{-}7)$$

where ξ_g and ω_g are the ground damping factor and the predominant frequency, respectively, and S_o is a constant. It is quite obviously understood that a random process that possesses a spectral density function in the form of Equation (2-7) is a stationary random process. Cauchey and Stumpf [12] used this spectral density function to study the transient response of a linear system under earthquake excitation. Penzien, Kaul and Berge [13] also used the same formula to study the response of offshore towers to random strong earthquakes and sea waves. Housner and Jennings [14], on the other hand, proposed model accelerograms which are sections of a stationary Gaussian random process with a power spectral density obtained from the average of the undamped velocity spectra of recorded ground accelerations. Eight pseudo-earthquakes of thirty seconds duration were generated on the digital

computer, and the velocities, displacements, and velocity spectra were calculated.

Simulation of earthquakes as member functions of a Gaussian random process with given power spectral density has the advantage that the dynamic response analysis of a linear structural system under earthquake excitation can be easily achieved because of the stationarity assumption in the simulation process. This kind of simulation, however, cannot exhibit the nonstationary characteristics of strong ground motion.

Idealization of Earthquakes as a Nonstationary Random Process Consisting of a Finite Sum of Modulated Processes

From a random function [15], Bogdanoff, Goldberg and Bernard [16] assumed earthquake acceleration takes the form

$$\ddot{X}_g(t) = \begin{cases} \sum_{j=1}^{n} t\, a_j\, e^{-\alpha_j t} \cos(\bar{F}_j\, t + \Theta_j), & t > 0 \\ 0, & t \le 0 \end{cases} \tag{2-8}$$

where the a_j and the $\bar{F}_j$ are given sets of real positive numbers with $\bar{F}_1 < \bar{F}_2 < \cdots < \bar{F}_n$, and $\Theta_1, \Theta_2, \cdots, \Theta_n$ are n independent random variables uniformly distributed over the interval $(0,2\pi)$. This simulation essentially exhibits the nonstationary behavior of strong ground motion. Later on, Goldberg, Bogdanoff and Sharpe [17] studied some simple linear and nonlinear systems by using a somewhat different form as earthquake input process. It is defined by

$$\ddot{X}_g(t) = \begin{cases} \sum_{j=1}^{n} t\, a_j\, e^{-\alpha_j t} \cos(F_j\, t + \Theta_j), & t > 0 \\ 0, & t \le 0 \end{cases} \tag{2-9}$$

where $F_1, F_2, \cdots, F_n$ are considered as independent random variables uniformly distributed over the interval (6,46) and (6,36). The F_j are also independent of the Θ_j. And the Θ_j are independent random variables uniformly distributed over the interval $(0,2\pi)$ as assumed in [16]. The introduction of random frequencies as well as random phases, they pointed out, while not producing substantial differences in appearance of member functions, does influence the extreme value distribution in comparison to the model proposed in [16]. Hence, in the design of a structure to resist an earthquake, the latter input process seems more plausible than that of the former. However, how to assign values to the parameters, α_j and a_j, to represent a particular earthquake was not mentioned. Moreover, the lengthy expressions for response makes analysis of structures of more than one-degree-of-freedom difficult.

Idealization of Earthquakes as a Nonstationary Modulated Process

This simulation consists of a product of a deterministic time function $D(t)$ and a stationary random process $G(t)$. Mathematically,

$$\ddot{X}_g(t) = D(t)\, G(t) \tag{2-10}$$

where $\ddot{X}_g(t)$ is the simulation random process for earthquake ground acceleration. Simulation may be made by selection of $D(t)$ and the corresponding parameters and by selection of $G(t)$. Simulation in this way can produce as many sample functions as desired and can be consistent with past earthquake records. This simulation has been widely used recently. Iyengar [18,19] used

$$D(t) = (a_1 + a_2\, t)\exp(-\,pt) \tag{2-11}$$

and took G(t) to be a Gaussian stationary random process with zero mean and variance equal to unity. The spectral density of G(t) is given by

$$S_G(\omega) = A_1 \exp(-\omega^2 c^2) + A_2 \omega^2 \exp(-4\omega^2 c^2) \qquad (2\text{-}12)$$

where a_1, a_2, p, A_1, A_2 and c are parameters which can be determined from a particular earthquake to be considered. Robert [20] used a half-sine pulse and a rectangular pulse as envelope functions. The corresponding correlation function of the stationary random process is characterized by a Dirac-delta function. Barnoski and Maurer [21] used a unit step function as the envelope function and assumed G(t) to be Gaussian with zero mean value and a correlation function given by

$$R_G(\tau) = R_o \exp(-\mu_d|\tau|) \cos \omega_d \tau \qquad (2\text{-}13)$$

where μ_d and ω_d are positive constants and R_o is the strength of the correlation function. It is obvious that the modulated random processes proposed in [20] and [21] are only approximate models for easy computations in evaluation of the mean-square response of linear structural systems. It should be noted, however, that a reasonable simulation process should satisfy some criteria statistically based on past earthquake records. The criteria of simulation process will be summarized later. Jennings, Housner and Tsai [22], on the other hand, simulated the envelope function by

$$D(t) = \begin{cases} t^2/16 & , \ 0 \le t \le 4 \\ 1.0 & , \ 4 \le t \le 35 \\ \exp\left[-0.0357\,(t-35)\right] & , \ 35 \le t \le 80 \\ 0.05 + 0.0000938\,(120 - t)^2 & , \ 80 \le t \le 120 \\ 0 & , \ t > 120 \end{cases} \qquad (2\text{-}14)$$

and generated $G(t)$ by passing a Gaussian white noise process through a second order filter. Recently, Saragoni and Hart [23] proposed a simulation procedure which is accomplished by modeling the modulated stochastic process as a segmented nonstationary random process. In their model, the time axis is subdivided into continuous time regions each having a unique, but stationary power spectral density function. It is recognized that the stochastic processes proposed in [22] and [23] are actually a combination of the filtered processes and the modulated processes. The modulated process is widely used recently not only because it is a reasonable representation for earthquake but also because its simple mathematical form enables easy evaluation of structural response.

Structural Models and Methods of Analysis

The rational design and construction of structures to withstand earthquakes requires a knowledge not only of the forces caused by ground motion, but also of the types of structures to be used in the analysis. The difficulty of precisely evaluating the appropriate physical properties of structures has been overcome by using mathematical models to represent real buildings. The literature on structural models

is voluminous. However, linear or nonlinear, single- or multi-degree-of-freedom, and lumped or distributed systems can be classified, respectively, according to material properties, motion behaviors and the characters of structures [24].

Damping is an important factor in the dynamic response analysis of structures. The damping in a system is associated with the dissipation of energy. It is a complex phenomenon. Fortunately, mathematical models for damping are provided for engineering application. Damping models are listed by Hurty and Rubinstein [25] as (1) structural damping, (2) viscous damping, (3) Coulomb damping, and (4) negative damping. However, only the former two have been mostly considered in a structure. Structural damping is due to internal friction within the material or at connections between elements of a structural system [26]. The damping forces are assumed to be proportional to the elastic forces in the system, as long as the system remains elastic, and are opposite in direction to the velocity vectors. Symbolically, the relationship between the structural damping force F_s and the elastic force F_e is given by [25]

$$F_s = i \gamma F_e \tag{2-15}$$

where γ is called the structural damping factor.

Structural damping has been widely used for the representation of energy dissipation of structures in both ordinary and random vibration theory [5,25,27]. The value of the structural damping coefficient usually lies between 0.01 to 0.05 for most engineering materials. Viscous damping is due to the vibration of the structural system in

a viscous medium. The viscous damping force F_v is sometimes assumed to be proportional to the velocity. Mathematically,

$$F_v = c\,\dot{y} \tag{2-16}$$

where c is the viscous damping coefficient.

Generally speaking, column stiffness and mass distribution characterize various structural models. Following is a brief description of the structural models and methods of analysis of structures to resist earthquakes.

Single-Degree-of-Freedom Systems:

Linear Systems. This is the simplest dynamic model which reveals the essential parameters relating structural response to earthquake disturbance. Figure 1 is a schematic representation of the deformed shape assumed by an idealized one-story structure whose rigid foundation undergoes a displacement equal to the earthquake motion of the ground. According to D'Alembert's principle, the equation of motion may be written as

$$m\,\ddot{y} + c\,\dot{y} + k\,y = -\,m\,\ddot{x}_g \tag{2-17}$$

where m = the mass of the structure,

k = the shear stiffness of the columns,

c = the damping coefficient,

y = the displacement of the mass relative to the ground,

and x_g = the horizontal displacement of the ground.

If damping is small (underdamped case), as is normally encountered in building structures, the solution for the response y at any time t after

starting from rest, is given by the Duhamel integral [28]

$$y(t) = \frac{1}{\omega'} \int_0^t \ddot{x}_g(\tau) \exp[-\xi\omega(t-\tau)]\sin\omega'(t-\tau)d\tau \qquad (2\text{-}18)$$

where ω = the natural undamped frequency of vibration of the structure

$$= \left(\frac{k}{m}\right)^{1/2}$$

ξ = fraction of critical damping

$$= c/2\ (km)^{1/2}$$

and $\omega' = \omega(1 - \xi^2)^{1/2}$.

The statistical properties of the response can be obtained by use of the random vibration theory [5,29] whenever the input process $\ddot{X}_g(t)$ is specified. However, in certain applications, we are interested in the maximum numerical value of certain response properties, some of which depend only on the natural period and degree of damping of the system. It is therefore of interest to construct curves that represent maximum numerical values of the response as function of the natural period or natural frequency of simple structures. Such plots are called response spectra. Thus, the velocity spectrum $S_v(\xi,\omega)$ is defined as

$$S_v(\xi,\omega) \equiv \left[\int_0^t \ddot{x}_g(\tau) \exp[-\xi\omega(t-\tau)] \sin\omega(t-\tau)d\tau \right]_{max} \qquad (2\text{-}19)$$

It is apparent that the maximum displacement depends on the spectral velocity divided by the circular frequency. This ratio is called the spectral displacement and is denoted by S_d [30]. Thus, the spectral displacement is defined by

$$S_d \equiv S_v/\omega \tag{2-20}$$

Similarly, the spectral acceleration is defined by

$$S_a \equiv \omega S_v \tag{2-21}$$

From above definitions, it is obvious that the spectral velocity depends on three factors: (1) the characteristics of the ground acceleration $\ddot{X}_g(t)$, (2) the damping ratio of the structure ξ, and (3) the circular frequency of the structure ω. Thus, for any given earthquake input, and for any specified structural damping ratio, it is possible to determine the spectral velocity as function of structural frequency or period $T = 2\pi/\omega$. The velocity spectrum for the N-S component of the El Centro, California earthquake is presented in Figure 2. Each of the curves on this graph was derived by evaluating the spectral velocity resulting from the earthquake acceleration history recorded at El Centro in May 18, 1940, considering the indicated damping ratio for a succession of different periods of vibration in the range of interest [3]. The analysis for each combination of damping and period gave a single point on the curve. The complete graphs were obtained by connecting the sequence of computed points appropriately by straight lines. It is noted here that the sharp peaks and valleys in the response spectrum curves shown in Figure 2 are due to local resonances in the ground motion record. Such irregularities are not of fundamental significance and may be smoothed out by averaging the response spectra of a number of different earthquake records. An average velocity spectrum for ground motion in the 1940 El Centro earthquake intensity is shown in

Figure 3. Multiplying these average velocity response spectra by the circular frequency yields the corresponding set of acceleration response spectra, as shown in Figure 4, while dividing by the circular frequency leads to the displacement response spectra of Figure 5.

Nonlinear Systems. Nonlinear behavior of a structure may be due to stress-strain relations, large deformations, conditions of failure, or combination of these causes. Motion of a general type of nonlinear system with a single-degree-of-freedom is governed by the differential equation

$$m\ddot{x} + Q(y, \dot{y}) = P(t) \qquad (2\text{-}22)$$

where

m = mass

x = absolute displacement of mass

$y = x - x_g$

Q = resistance function (restoring force), including effect of damping

x_g = ground displacement

P = external force

t = time

Obviously, the well-known Duffing equation may be obtained simply by taking $Q(y,\dot{y}) = \alpha\,\dot{y} + a\,y + b\,y^3$ and is always treated as a basic equation in the analysis of nonlinear structures [17].

Analyses of nonlinear systems have been studied extensively [31]. The step-by-step numerical integration procedure is plausible by using digital computers [32]. The nonlinear equations of motion can also be

linearized by the method of equivalent linearization [33] or the perturbation method [34], so long as the nonlinear terms in the governing equations are small.

Multi-Degree-of-Freedom Systems:

The dynamical analysis of framed structures is considerably simplified by considering a multi-story rectilinear frame consisting of integrally connected columns and girders without diagonal bracing. The masses are lumped or concentrated at the floor levels. Thus, the effective mass at a given floor includes not only the mass of that floor and the additional mass of materials and objects standing upon the floor but also one-half the mass of the columns and walls and partitions immediately above and below that floor. Generally speaking, each mass may have up to six degrees of freedom, three of which correspond to translations and three to rotations. However, most problems in earthquake-resistant design are simplified without undue error by assuming that each mass has but one degree of freedom. Depending on the behavior of columns under loading, the linear or nonlinear properties are thus classified.

Linear Systems. A linear structure is based on the assumption that the columns are relatively flexible and have linear behavior. This type of building is generally called a "shear type building". The damping in a multi-story linear structure may include either viscous damping or structural damping or both. The equations of motion for a multi-degree-of-freedom system may be expressed as

$$[M]\{\ddot{y}\} + [C]\{\dot{y}\} + [K]\{y\} = \{P(t)\} \qquad (2\text{-}23)$$

where [M], [C] and [K] are mass matrix, damping matrix and stiffness matrix of the system, respectively. {P} is the forcing function vector. The normal mode method is generally used for the analysis of multi-degree-of-freedom systems. In this method, a linear transformation is employed to change the matrix coupled equations of motion to an uncoupled system [35]. According to this concept, a multi-story structure can be represented by a number of equivalent one-degree-of-freedom systems. However, damped systems do not in general have natural modes of vibration. The necessary and sufficient condition for a damped linear structure to have classical normal modes is that there exists a transformation which diagonalizes the damping matrix and uncouples the equations of motion [36,37]. In general, for an n degrees of freedom system there are n of these equivalent systems; they are characterized by the n natural periods and the associated mode shapes in which the actual structure may vibrate.

Nonlinear Systems. The simplest model is the shear building in which all floors are assumed rigid and the inter-story shear is assumed to have an elasto-plastic force-deformation relationship [40]. Other mathematical models employ a combination of the elasto-plastic rigid frame and the bilinear form of shear force-deformation relationship [10,41]. Of course, it is evident that the choice of any particular mathematical model is strongly dependent upon the physical characteristics of the building being analyzed.

The most convenient technique for evaluating the dynamic response of a nonlinear structure is by means of a step-by-step integration procedure. To carry out the step-by-step analysis, the response history

is divided into very short time increments. During each increment, the structure is assumed to be linearly elastic; however, between increments the properties are modified in accordance with the current condition of deformation. Thus, the nonlinear response is obtained as a sequence of linear response of successively differing systems.

Distributed Systems. For some structures whose masses are distributed, the lumped-parameter approach gives only an approximation to the system. Structures such as beams, bars, plates and shells are distributed-parameter systems, and may be viewed as having an infinite number of degrees of freedom and hence as limiting cases of those structures mentioned in the preceeding paragraphs. The ordinary differential equations that we established in terms of matrices, now become partial differential equations, in which the independent variables are time and the space coordinates. Shinozuka [42] gave an example for a beam column structure to earthquake excitation.

State of the Art

This part will include recent developments on earthquake simulation and structural models and will also show how the simulated earthquakes have been used as inputs for the multi-story building models.

Simulation Processes

Simulation of earthquakes as sample functions of a stochastic process has been a research topic for almost three decades. White noise was first tried [1,2,4]. Gaussian processes with given power spectral densities were then used [12,13,14]. Later on, the

nonstationarity of strong earthquake motion was taken into consideration. A literature review has shown that the modulated process and the filtered process are the ones most widely used as simulation processes for earthquakes at the present time [6,7,8,9,10,18,19,22,23].

The local geological condition at a certain place can be characterized by the parameters of the filter for a filtered process [10]. The magnitude of an earthquake can also be specified by the intensity function of the input process for the filter. However, it is clear that the analytical solution for more than one-degree-of-freedom systems will involve considerable algebraic difficulties for the filtered processes.

The advantage of a modulated process as simulation of earthquakes is its mathematical simplicity. The process is formed simply by the product of an envelope function and a stationary process. The nonstationarity of earthquakes is characterized by the envelope function. The modulated process can be constructed by selection of an envelope function and a stationary random process such that the involved parameters satisfy certain conditions for the simulation processes. Modulated processes have been widely used in the dynamic analysis for both single-and multi-degree-of-freedom systems recently [19,20,21].

It is worth noting that the small number of existing records of strong motion earthquakes permits only a general inference of whether or not a simulation process is consistent with the statistics of past earthquakes. Levy's proposed criteria are the most recent to come to our attention and can be used as a qualitative basis for judging the acceptability of a simulation process [9]. He requires the simulation

process to satisfy the following criteria:

1. Response Spectra -

   Response spectra curves of a one-degree-of-freedom linear system subjected to earthquake simulation process should be similar to the spectra curves proposed by Housner [3].

2. Maximum Ground Acceleration -

   The simulated earthquake should indicate similar values for the maximum ground acceleration to that of former earthquakes.

3. Nonstationarity -

   Nonstationarity of ground motion should resemble past observation; in particular, the acceleration variance functions should ascend to a maximum and then decay to zero with increasing time. The significance of nonstationarity of earthquake motion was extensively studied by Amin and Ang [43].

4. Autocorrelation Function -

   The degree of correlation between closely spaced ordinates generated from the model should agree with the information that can be obtained from the records. Thus, the normalized autocorrelation functions for the ground acceleration, with stationarity assumed during the time of strongest motion, should exhibit the same characteristics and tend to fit the envelopes that have been determined for real earthquakes.

Structural Models

The introduction of random processes as earthquake excitation models has become significant only recently. However, the structural models used in the dynamic response analyses have had a long history

and can be found in any vibration textbook, for example, in that by Newmark and Rosenblueth [24]. Generally, any structural model used in the deterministic dynamic response analysis can also be used in the probabilistic analysis [5]. A literature review shows that one-degree-of-freedom linear systems have been widely used in the analysis for simulation processes. This is due to the fact that not only the response of one-degree-of-freedom structures can be easily obtained but also response spectra curves are all related to one-degree-of-freedom structures.

Modern structures are almost all high-rise buildings and should be treated as multi-degree-of-freedom systems. The lumped shear type building is mostly used in the design process because of its mathematical simplicity. It is customary to assume that the masses are concentrated at the floor levels, and the columns act like springs of oscillators. In many ways the assumption that structural systems possess no damping is a mathematical convenience rather than a reflection of real physical evidence. The viscous damping for a building structure is taken proportional either to the absolute velocity of each floor mass or to the relative velocity of each floor with respect to the adjacent floor. For example, Douglas [44] and Blume [45] used a structural model based on relative viscous damping, Newmark studied the dynamic response of multi-story buildings using an absolute viscous model [46], while Eringen considered both relative and absolute viscous damping in his tall building model [39]. The energy dissipation of the interfloor is due to structural damping, such as friction between various structural members. It is evident that external damping from air

leads us to take into account the damping based on absolute floor velocity. Lin's model seems a good representation for a tall shear building, since it includes both viscous and structural damping [5, p. 193].

Multi-story Structures Using Simulation Processes

It was pointed out that one-story structures are mostly used in the response analysis for simulation processes. So long as the statistical properties of the simulation process are given, the statistics of the response can be obtained by using the Duhamel integral representation. However, analysis of most high-rise buildings are always based on past earthquake records as input functions [44,45,46]. This is equivalent to a deterministic analysis. A literature review has shown that only few investigations have been developed on dynamic response analysis of tall buildings using simulation processes so far. Ruiz and Penzien used a second order linear filtered process to analyze an eight-story lumped nonlinear shear building with equal viscous damping [10]. The nonlinear stress-strain relation of columns are assumed to be bilinear. Penzien and Kaul [47] used a stationary Gaussian process to obtain response of offshore towers to strong motion earthquakes. The offshore tower structure is assumed to be a lumped multi-degree-of-freedom system. By a combination of the normal mode method and the equivalent linearization technique, the uncoupled equation of motion was then obtained. Roberts [20], on the other hand, used a modulated process to analyze a ten-story lumped linear shear building. The stiffness in his building model were assumed to have proportional relations. Obviously the structural model proposed by

Roberts is only an ideal model for easy algebraic computations.

Recently, Housner [48], Clough [49,50], Newmark [51], Penzien [10,52,53] and a few other investigators [54,55] have developed nonlinear models for the structures in earthquake design. However, these people have almost entirely used either deterministic inputs or a trivial and inaccurate random representation. Thus, their results are quite questionable. Up to the present time, three basic methods have been used in the study of stochastically excited nonlinear systems. These are a method using the Fokker-Planck equations [53,56], a perturbation approach [34] and a statistical linearization approach [33,57]. However, the inputs of the nonlinear models used are all limited to filtered shot noise, shot noise or stationary white noise random processes. Very few investigations have been made which utilize these methods in the analysis of stochastic seismic response for the nonlinear structural models.

Thus, from the discussion above, it appears that substantial research remains to be done concerning the dynamic response analysis of multi-story buildings under earthquake excitation using modern developed simulation stochastic processes.

CHAPTER III

EARTHQUAKE GROUND MOTION SIMULATION

Motivations

It has been pointed out in the preceeding chapter that there are a number of models for representing earthquake ground motion. However, the better models are still too complex to be used as input processes in the analysis of complicated structures. A realistic and practical model will subsequently be proposed such that it contains the following three features:

1. Generating a Modulated Process in which the Stationary Random Process Is Expressed Directly in Terms of Random Functions - Recent developments in the simulation of earthquakes have been towards the use of modulated nonstationary random processes which are formed by products of deterministic envelope functions and stationary random processes. However, most simulation processes have thus far concentrated on the duplication of either correlation functions or spectral density functions of the corresponding stationary random processes rather than on the generation of ensembles of member functions [18,20,21,22,23]. Simulation in this way always results in the difficulty of generating artificial accelerograms directly. Thus, it seems preferable to express the stationary random process of the modulated process directly in order to obtain better insight into the artificial accelerograms in order to compare them to the actual earthquake records.

2. Obtaining Distributions of Random Frequencies of Earthquake Accelerations Statistically - The random functions proposed in [16] and [17] may be viewed as being composed of finite sums of modulated processes. It was Bogdanoff, Goldberg and Bernard [16] who first used a random function as a simulation process for earthquake acceleration. They assumed acceleration frequencies are real positive numbers. Later on, Goldberg, Bogdanoff and Sharpe [17] also used a random function for earthquake acceleration. However, the earthquake frequencies are assumed to be random variables uniformly distributed in the range of [6,46] and [6,36]. Penzien [58], on the other hand, suggested that the frequencies be distributed in the interval $(2\pi, 10\pi)$. This inconsistency in describing the distribution of random frequencies reveals the need for obtaining the actual distribution of random frequencies from past earthquake records.

3. Simplifying Unnecessary Arbitrary Constants in an Input Model - A simulation model should be simple enough to allow the specification of its parameters in relation to the intensity and characteristics of a known earthquake. However, the models proposed by Goldberg, etc. [16,17] obviously contain too many unnecessary arbitrary constants. These constants not only make the analysis of a complex structure complicated but also are difficult to determine based on the statistics of past earthquake records.

Earthquake Acceleration Model

Due to the shortcomings of the existing simulation input models outlined in the preceeding paragraph, a simplified and modified random

process based on a random function somewhat different from that presented in references [16] and [17] will be proposed for earthquake acceleration. Here earthquake acceleration is given in the following form:

$$\ddot{X}_g(t) = \begin{cases} \sum_{j=1}^{n} t\, a_j\, e^{-\alpha_j t} \cos(F_j t + \Theta_j), & t > 0 \\ 0, & t \le 0 \end{cases} \qquad (3\text{-}1)$$

where $a_1, a_2, \cdots, a_n$ and $\alpha_1, \alpha_2, \cdots, \alpha_n$ are real positive numbers; $\Theta_1, \Theta_2, \cdots, \Theta_n$ are n independent random variables uniformly distributed over the interval $(0,2\pi)$. Also we assume n is a large positive integer. The acceleration frequencies $F_1, F_2, \cdots, F_n$ are independent random variables also independent of $\Theta_1, \Theta_2, \cdots, \Theta_n$. In this proposed model, we assume the random frequencies $F_1, F_2, \cdots, F_n$ are identically distributed in a more general range $(0,\infty)$ with some probability density function $p_F(f)$ rather than uniformly distributed over the interval $(6,36)$ and $(6,46)$ as suggested in [17]. The probability density function $p_F(f)$ will be established later.

From the central limit theorem, it is understood that n must be a large positive integer such that $\ddot{X}_g(t)$ is a Gaussian process. Consequently, the random process $\ddot{X}_g(t)$ will contain 2n real positive numbers for a_j and α_j. These 2n constants not only make the response results lengthy for further analysis but also are difficult to be determined from earthquake data. Therefore, some simplification seems necessary. To this end, Equation (3-1) may be rewritten as

$$\ddot{X}_g(t) = \begin{cases} {}_1\ddot{X}_g(t) + {}_2\ddot{X}_g(t) + \cdots + {}_n\ddot{X}_g(t), & t > 0 \\ 0, & t \le 0 \end{cases} \tag{3-2}$$

where

$${}_j\ddot{X}_g(t) = D_j(t)\ G_j(t) \tag{3-3}$$

in which

$$D_j(t) = a_j\ t\ e^{-\alpha_j t} \tag{3-4}$$

$$G_j(t) = \cos(F_j\ t + \Theta_j) \tag{3-5}$$

and

$$j = 1,2,\cdots,n$$

The $D_j(t)$ are envelope functions and the $G_j(t)$ are stationary random processes of the modulated processes ${}_j\ddot{X}_g(t)$. Thus, essentially, Equation (3-1) consists of a finite sum of modulated processes ${}_j\ddot{X}_g(t)$.

The influence of envelope functions upon the responses of linear structural systems has become an interesting research topic recently [59,60]. Obviously, from a statistical point of view, mean-square response is one of the most important criteria in structural design. Hence, by comparing mean-square responses resulting from different envelope functions but the same stationary random process, we can examine the effects of the envelope functions upon the responses of the structures. Based on this fact, Hasselman [60] used a staircase approximation in representing an envelope function to evaluate

the response of linear structures. He has shown that the mean-square response of linear systems to a modulated random process is rather insensitive to small variations in the envelope function. In other words, the variation of the envelope function has little influence upon the mean-square response of linear structures. This observation reflects that surprisingly good accuracy in mean-square response can be obtained even for crude approximations to the evelope functions. Based on this observation, we may put each set of fixed numbers in the envelope functions of Equation (3-1) equal; that is, by putting

$$\alpha_1 = \alpha_2 = \cdots = \alpha_n = \alpha$$

and

$$a_1 = a_2 = \cdots = a_n = a$$

From this simplication, Equation (3-1) becomes

$$\ddot{X}_g(t) = \begin{cases} D(t)\ G(t), & t > 0 \\ 0, & t \leq 0 \end{cases} \tag{3-6}$$

where

$$D(t) = b\ t\ e^{-\alpha t} \tag{3-7}$$

$$G(t) = (2/n)^{\frac{1}{2}} \sum_{j=1}^{n} \cos\ (F_j\ t + \Theta_j) \tag{3-8}$$

in which

$$b = a(n/2)^{\frac{1}{2}} \tag{3-9}$$

Obviously, D(t) is a well-defined deterministic envelope function so long as the parameters α, a and n are defined. The time modulating envelope function D(t) is used to control the process amplitude level and the time to the maximum acceleration. G(t) is a stationary random process expressed explicitly in terms of random functions. It should be noted that the introduction of the factor $(2/n)^{\frac{1}{2}}$ in front of the stationary random process is to make the variance of G(t) equal to unity. Figure 6 shows sample curves of the envelope function D(t) for several values of α. The trend of these curves shows that the envelope function is a slowly varying function, ascending to a maximum value $(b/\alpha)/e$ at time $1/\alpha$, then descending gradually to zero. Another feature of Figure 6 is that the coordinates decreases rapidly as α increases. This observation suggests that a large value of α corresponds to those earthquakes with short durations and a small value of α corresponds to those with long durations. Thus, we have modified the random function expressed in Equation (3-1) into the form of a recently developed modulated process in which the stationary random process is expressed directly in terms of random functions. The random process in the form of Equation (3-6) will be used for the earthquake acceleration simulation throughout this research. The only undefined quantity in the proposed input process is the probability density function $p_F(f)$ of the random frequencies F_j. This function will be determined later.

Statistics of the Simulation Process

In this section, the statistics of the stationary random process

$G(t)$ will be computed first. The results can then be used to determine the distribution of the random frequencies F_j.

Since n is assumed to be a large positive integer, from the central limit theorem [61], it is evident that the random process $G(t)$ is approximate a Gaussian process. Therefore, the mean function and the variance function of $G(t)$ completely characterize such a process. Once $G(t)$ is specified, the statistics of the simulation process $\ddot{X}_g(t)$ can then be easily determined. It is well known that the most important reason for the use of Gaussian random processes is that the class of Gaussian random processes is closed under linear operation; i.e., linear functions of Gaussian random processes remain Gaussian distributed. This feature will be used for establishing the response distributions of linear structural systems.

The mean function of $G(t)$, denoted by $\mu_G(t)$, may be obtained by performing ensemble average over the sample space, i.e.,

$$\mu_G(t) = E[G(t)]$$

$$= (2/n)^{\frac{1}{2}} E\left\{\sum_{j=1}^{n} [\cos(F_j t + \Theta_j)]\right\}$$

$$= (2/n)^{\frac{1}{2}} \sum_{j=1}^{n} \{E[\cos(F_j t + \Theta_j)]\} \qquad (3\text{-}10)$$

here use has been made by the fact that the operations of mathematical expectation and summation are commutative.

By expanding the compound cosine function, we have

$$\mu_G(t) = (2/n)^{\frac{1}{2}} \sum_{j=1}^{n} E[\cos(F_j t)\cos \Theta_j - \sin(F_j t)\sin \Theta_j] \qquad (3\text{-}11)$$

Since the F_j and the Θ_j are assumed to be independent random variables, the above equation can be written as

$$\mu_G(t) = (2/n)^{\frac{1}{2}} \sum_{j=1}^{n} \{E[\cos(F_j t)]\, E[\cos \Theta_j] - E[\sin(F_j t)]$$

$$\times\, E[\sin \Theta_j]\} \qquad (3\text{-}12)$$

Now, from the assumption that the Θ_j are identically uniformly distributed over the interval $(0,2\pi)$, we obtain the following two relations:

$$E[\cos \Theta_j] = \int_0^{2\pi} \frac{1}{2\pi} \cos \theta_j \, d\theta_j = 0 \qquad (3\text{-}13)$$

and

$$E[\sin \Theta_j] = \int_0^{2\pi} \frac{1}{2\pi} \sin \theta_j \, d\theta_j = 0 \qquad (3\text{-}14)$$

Substituting Equations (3-13) and (3-14) into Equation (3-12), we obtain

$$\mu_G(t) = 0 \qquad (3\text{-}15)$$

Equation (3-15) states that the mean function of $G(t)$ vanishes and thus is independent of the distribution of the random frequencies F_j.

The autocovariance function $\Gamma_G(t_1,t_2)$ of $G(t)$ at two instants of time t_1 and t_2 is given by

$$\Gamma_G(t_1,t_2) = E\{[G(t_1) - \mu_G(t_1)][G(t_2) - \mu_G(t_2)]\}$$

$$= E[G(t_1)\, G(t_2)]$$

$$= R_G(t_1,t_2) \qquad (3\text{-}16)$$

where $R_G(t_1,t_2)$ is the autocorrelation function of $G(t)$. The autocovariance function and the autocorrelation function are equal, because the mean function $\mu_G(t)$ vanishes.

Substituting Equation (3-8) into the expression for $R_G(t_1,t_2)$, we obtain

$$R_G(t_1,t_2) = E[G(t_1)\, G(t_2)]$$

$$= (2/n) \sum_{j=1}^{n} \sum_{k=1}^{n} E[\cos(F_j t_1 + \Theta_j) \cos(F_k t_2 + \Theta_k)]$$

$$= (2/n) \sum_{j=1}^{n} \sum_{k=1}^{n} E[\cos(F_j t_1) \cos(F_k t_2) \cos\Theta_j \cos\Theta_k$$

$$+ \sin(F_j t_1) \sin(F_k t_2) \sin\Theta_j \sin\Theta_k$$

$$- \cos(F_j t_1) \sin(F_k t_2) \cos\Theta_j \sin\Theta_k$$

$$- \sin(F_j t_1) \cos(F_k t_2) \sin\Theta_j \cos\Theta_k]$$

$$= (2/n) \sum_{j=1}^{n} \sum_{k=1}^{n} \{E[\cos(F_j t_1) \cos(F_k t_2)]$$

$$\times\ E[\cos\Theta_j \cos\Theta_k]$$

$$+ E[\sin(F_j t_1)\ \sin(F_k t_2)]\ E[\sin \Theta_j\ \sin \Theta_k]$$

$$- E[\cos(F_j t_1)\ \sin(F_k t_2)]\ E[\cos \Theta_j\ \sin \Theta_k]$$

$$- E[\sin(F_j t_1)\ \cos(F_k t_2)]\ E[\sin \Theta_j\ \cos \Theta_k]\} \qquad (3\text{-}17)$$

where we have used the fact that the F_j and the θ_j are independent random variables. Since the Θ_j are uniformly distributed in the interval $(0,2\pi)$, the following relations hold:

$$\left.\begin{aligned} E[\cos \Theta_j\ \cos \Theta_k] &= 0 \\ E[\sin \Theta_j\ \cos \Theta_k] &= 0 \\ E[\sin \Theta_j\ \sin \Theta_k] &= 0 \end{aligned}\right\} \quad \text{for } j \neq k \qquad (3\text{-}18)$$

$$E[\cos^2 \Theta_j] = \int_0^{2\pi} \frac{1}{2\pi} \cos^2\theta_j d\theta_j = \frac{1}{2} \qquad (3\text{-}19)$$

$$E[\sin^2 \Theta_j] = \int_0^{2\pi} \frac{1}{2\pi} \sin^2\theta_j d\theta_j = \frac{1}{2} \qquad (3\text{-}20)$$

and

$$E[\sin \Theta_j\ \cos \Theta_j] = 0$$

Upon substitution of the above relations into Equation (3-17), the autocorrelation function $R_G(t_1,t_2)$ can then be written as

$$R_G(t_1,t_2) = (1/n) \sum_{j=1}^{n} E[\cos(F_j \tau)] \qquad (3\text{-}21)$$

where

$$\tau = t_2 - t_1$$

Equation (3-21) reveals that the autocorrelation function of the random process G(t) is a function of the time difference τ only. This fact together with the zero expectation prove that G(t) is a weakly stationary random process. In order to obtain an explicit expression for the autocorrelation function of G(t), it is necessary to know the probability density function $p_F(f)$ of the random frequencies F_j. It was pointed out that $p_F(f)$ can be obtained from the statistics of past earthquake records. To this end, it is necessary to introduce the idea of normalized autocorrelation functions for the ground acceleration.

It is obvious that the simulation process expressed by Equation (3-6) is a nonstationary random process. However, from the empirical analyses of past accelerograms, Barstein [62], Shinozuka and Sato [8] and Amin and Ang [7] observed the stationarity may be assumed during the time of the strongest motion. The distribution of the random frequencies can then be derived from this observation. Barstein [62] introduced the idea of a normalized autocorrelation function for the ground acceleration. The so-called normalized autocorrelation function $\rho(\tau)$ is obtained by dividing the autocorrelation function of a nonstationary random process by the corresponding stationary mean-square value. It is given in the following expression based on the filtered processes [7,8]:

$$\rho(\tau) = \exp(-\mu_d|\tau|)\left[\cos(\omega_d\tau) \mp \frac{\mu_d}{\omega_d}\sin(\omega_d|\tau|)\right] \qquad (3\text{-}22)$$

where μ_d and ω_d are parameters of the filters. The plus sign appearing

in the second term of the above formula is for the process proposed by Amin and Ang [7] while the minus sign is for the process suggested by Shinozuka and Sato [8]. Later on, Levy [9] concluded that the normalized autocorrelation functions may be chosed in such a way that they are qualitatively similar to the empirical functions. Based on his suggestion, the normalized autocorrelation function of the proposed simulation process may be assumed in the following formulation without loss of generality:

$$\rho(\tau) = R_G(\tau)/R_G(0)$$

$$= \exp(-\mu_d|\tau|)\cos(\omega_d\tau) \qquad (3\text{-}23)$$

where $R_G(\tau)$ is the autocorrelation function of the stationary random process $G(t)$. It can be easily shown that $R_G(0)$ is equal to unity. Therefore, the normalized autocorrelation function is equal to the autocorrelation function for the proposed simulation process; i.e.,

$$\rho(\tau) = R_G(\tau) \qquad (3\text{-}24)$$

Thus, the autocorrelation function of the stationary random process $G(t)$ is obtainable as

$$R_G(\tau) = \exp(-\mu_d|\tau|)\cos(\omega_d\tau) \qquad (3\text{-}25)$$

Figure 7 shows a normalized autocorrelation function expressed by Equation (3-25) as well as envelopes of empirical functions developed by Amin and Ang [7]. It is found that the proposed normalized autocorrelation function not only is qualitatively similar to the empirical

functions but also falls within the envelope of the empirical functions. Thus, the autocorrelation function simulated in this way is consistent with past earthquake accelerograms statistically and can be used to obtain the probability density function of the random frequencies of the earthquake acceleration model.

Substituting Equation (3-24) into Equation (3-21) and using the definition of expectation, we obtain

$$\exp(-\mu_d|\tau|)\cos(\omega_d\tau) = \int_0^\infty \cos(f\tau)\, p_F(f)\, df \tag{3-26}$$

Equation (3-26) is a Fredholm integral equation of the first kind with unknown function $p_F(f)$ [63]. The function $R_G(\tau)$ defined by the left-hand side of Equation (3-26) may be recognized as the Fourier cosine transform of $p_F(f)$. Since $R_G(\tau)$ is piecewise differentiable and

$$\int_0^\infty |\exp(-\mu_d|\tau|\cos(\omega_d\tau)|d\tau \le \int_0^\infty \exp(-\mu_d|\tau|)\, d\tau$$
$$< \infty \tag{3-27}$$

Equation (3-26) can be inverted uniquely into the form

$$p_F(f) = (2/\pi)\int_0^\infty \cos(f\tau)\exp(-\mu_d\tau)\cos\omega_d\tau d\tau \tag{3-28}$$

Carrying out the integration, we obtain

$$p_F(f) = \frac{2\mu_d}{\pi}\,\frac{\omega_d^2 + \mu_d^2 + f^2}{(\omega_d^2 + \mu_d^2 + f^2)^2 - 4\omega_d^2 f^2} \tag{3-29}$$

It can be easily proved that

$$\int_0^\infty p_F(f)\, df = 1 \tag{3-30}$$

Figure 8 shows the proposed probability density function $p_F(f)$ of the random frequencies F_j for some specified values of μ_d and ω_d suggested by Amin and Ang [7]. The probability density function used by Goldberg et al. [17] is also plotted in Figure 8 for comparison. It is apparent that only after carefully studying many strong ground motion accelerograms that these parameters can be established for the various ground conditions commonly encountered in engineering practice.

Therefore, we conclude that the proposed simulation process is completely specified by Equations (3-6), (3-7) and (3-8) together with Equation (3-29). Thus, essentially, the proposed random process is a combination of the filtered process and the modulated process. It actually has the advantages of both processes.

The power spectral density function $S_G(\omega)$ of the stationary random process $G(t)$ can be obtained from the well-known Wiener-Khintchine theorem which asserts that for a weakly stationary random process, the autocorrelation function and the spectral density function are related to each other by Fourier transforms [61]. From this theorem, we have

$$S_G(\omega) = \frac{1}{2\pi}\int_{-\infty}^{\infty} R_G(\tau)\, \exp(-i\omega\tau)d\tau$$

$$= \frac{1}{2n\pi}\, E\left[\sum_{j=1}^{n}\int_{-\infty}^{\infty} \cos(F_j\tau)\, \exp(-i\omega\tau)d\tau\right] \tag{3-31}$$

Carrying out integration, we have

$$S_G(\omega) = \frac{1}{2n} E\left\{ \sum_{j=1}^{n} [\delta(\omega + F_j) + \delta(\omega - F_j)] \right\} \tag{3-32}$$

where $\delta(\omega)$ is the Dirac-delta function. Since the random variables F_j are assumed to be identically distributed in the interval $(0,\infty)$ with probability density function $p_F(f)$, the spectral density function $S_G(\omega)$ can be evaluated from Equation (3-32)

$$S_G(\omega) = \frac{1}{2} p_F(\omega) \tag{3-33}$$

Equation (3-33) shows that the spectral density function of the stationary random process is just one half of the probability density function of the random frequencies and is independent of the distribution of the random phases. This equation also reveals that the distribution of the random frequencies F_j are obtainable from the spectral density function of the stationary random process of a modulated random process. Substituting Equation (3-29) into Equation (3-33), we obtain

$$S_G(\omega) = \frac{\mu_d}{\pi} \frac{\omega_d^2 + \mu_d^2 + \omega^2}{(\omega_d^2 + \mu_d^2 + \omega^2)^2 - 4\omega_d^2\omega^2} \tag{3-34}$$

Equation (3-34) can also be written in the following form

$$S_G(\omega) = \frac{1 + \left(\frac{\omega}{\omega_g}\right)^2}{\left[1 - \left(\frac{\omega}{\omega_g}\right)^2\right]^2 + 4\xi_g^2\left(\frac{\omega}{\omega_g}\right)^2} S_o \tag{3-35}$$

where

$$S_o = \frac{\mu_d}{\pi(\mu_d^2 + \omega_d^2)}$$

$$\xi_g^2 = \frac{\mu_d^2}{\omega_d^2 + \mu_d^2}$$

$$\omega_g^2 = \omega_d^2 + \mu_d^2$$

It is worth noting that power spectral density functions expressed in the form similar to Equation (3-35) are usually used in literature for the simulation of stationary random processes of strong ground motion [11,64]. Figure 9 shows the spectral density functions expressed by Equation (3-35) and those proposed by Iyengar [18]. From these curves, we see immediately that they have one common property: they build up in magnitude at the beginning, after attaining the maximum, they decay as frequencies become large.

Now, we have established some fundamental properties of the stationary random process G(t). By use of these properties, we can obtain statistics of the modulated nonstationary random process $\ddot{X}_g(t)$ for the simulation of earthquake acceleration.

The mean function of $\ddot{X}_g(t)$, denoted by $\mu_{\ddot{X}_g}(t)$, is given by

$$\mu_{\ddot{X}_g}(t) = E[\ddot{X}_g(t)]$$

$$= D(t)\ \mu_G(t) \qquad (3\text{-}36)$$

Since the mean function of G(t) vanishes, we immediately obtain

$$\mu_{\ddot{X}_g}(t) = 0 \tag{3-37}$$

The autocovariance function $\Gamma_{\ddot{X}_g}(t_1,t_2)$ of the random process $\ddot{X}_g(t)$ at two instants of time t_1 and t_2 can be obtained as

$$\Gamma_{\ddot{X}_g}(t_1,t_2) = E\{[\ddot{X}_g(t_1) - \mu_{\ddot{X}_g}(t_1)][\ddot{X}_g(t_2) - \mu_{\ddot{X}_g}(t_2)]\}$$

$$= E[\ddot{X}_g(t_1)\ \ddot{X}_g(t_2)]$$

or

$$\Gamma_{\ddot{X}_g}(t_1,t_2) = R_{\ddot{X}_g}(t_1,t_2) \tag{3-38}$$

where $R_{\ddot{X}_g}(t_1,t_2)$ is the autocorrelation function of the random process $\ddot{X}_g(t)$. Equation (3-38) states that the autocorrelation function is equal to the autocovariance function for the simulation process. By substituting Equation (3-6) for $\ddot{X}_g(t)$, we have

$$R_{\ddot{X}_g}(t_1,t_2) = D(t_1)\ D(t_2)\ E[G(t_1)\ G(t_2)]$$

$$= D(t_1)\ D(t_2)\ R_G(t_1,t_2)$$

$$= D(t_1)\ D(t_2)\ R_G(\tau) \tag{3-39}$$

where

$$\tau = t_2 - t_1$$

Substituting Equation (3-25) into Equation (3-39), we obtain

$$R_{\ddot{X}_g}(t_1,t_2) = D(t_1)\, D(t_2)\, \exp(-\mu_d|\tau|)\, \cos(\omega_d\tau) \tag{3-40}$$

Obviously, it is easily to show that

$$R_{\ddot{X}_g}(t_1,t_2) = R_{\ddot{X}_g}(t_2,t_1) \tag{3-41}$$

Equation (3-41) shows that the autocorrelation function is symmetric with respect to different time instants t_1 and t_2. Since the autocorrelation function of the process $\ddot{X}_g(t)$ is function of t_1 and t_2, not of the difference τ, the nonstationarity of the simulation process is thus apparent.

The variance function, or the mean-square function, of $\ddot{X}_g(t)$ denoted by $\sigma^2_{\ddot{X}_g}(t)$, can be obtained by setting $t_1 = t_2 = t$ in Equation (3-40). Thus, we obtain

$$\sigma^2_{\ddot{X}_g}(t) = D^2(t) \tag{3-42}$$

or

$$\sigma_{\ddot{X}_g}(t) = D(t) \tag{3-43}$$

where $\sigma_{\ddot{X}_g}(t)$ is the standard deviation of the simulation process $\ddot{X}_g(t)$. Equation (3-42) states that the variance function of the random process is equal to the square of the deterministic envelope function $D(t)$ and is independent of the stationary random process $G(t)$. Figure 6 also shows the standard deviations or the root-mean-square functions for

different values of α. These curves show that they ascend to a maximum and then decay to zero with increasing time. These curves actually have similar shapes to those obtained from past earthquake record [7,18] and by simulation processes [6,9,16].

Estimation of Parameters

The random process for the ground acceleration strongly depends on the characteristics of the record and the local geological conditions. As mentioned previously, the distribution of the random frequencies F_j for the stationary random process $G(t)$ can be obtained from the parametric properties of the second order filter to meet the local geological requirements. However, there are still two other parameters, α and b which are to be determined for the envelope function. In order to obtain values for these parameters in the input process, we need some data from past earthquake record. Table 1 shows the characterization of eight past earthquake records. These records are taken from the reports of the U.S. Coast and Geodetic Survey [65] and Earthquake Engineering Research Laboratory, California Institute of Technology [66]. The details that can be used for stochastic analysis are the maximum absolute acceleration $(\ddot{x}_g)_m$ and the time to the maximum t_m. These two quantities are also shown in Table 1. From the records, we can also evaluate the rate of zero crossings N_o and the rate of maximum N_m. The values of N_o and N_m are taken by the average over the portion of strong motion. Their values are listed in Table 2. It is interesting to note from Table 2 that λ, the ratio of the rate of zero crossing to the rate of maxima, lies approximately in the range 1.1 to

1.3, in spite of the wide range, 0.17g to 1.27g, of the maximum absolute acceleration.

The parameter α can be estimated by observing that the root-mean-square curves have a maximum at or near the time t_m for which the absolute maximum acceleration is attained in the original record. This observation has been indicated by Iyengar [18] from a number of earthquake data analyses. We also note that the root-mean-square function of the proposed input process is equal to the envelope function $D(t)$ of the modulated process. All these facts enable us to determine α. Differentiating $D(t)$ yields

$$\frac{d\,D(t)}{d\,t} = b(1 - \alpha\, t)e^{-\alpha t} \tag{3-44}$$

Hence, $D(t)$ reaches a maximum at the time t_m'

$$t_m' = \frac{1}{\alpha} \tag{3-45}$$

or

$$\alpha = \frac{1}{t_m'} \tag{3-46}$$

However, it has been mentioned that

$$t_m' = t_m \tag{3-47}$$

Therefore,

$$\alpha = \frac{1}{t_m} \tag{3-48}$$

Thus, α is obtainable from the time t_m. The values of the α's for eight earthquake records listed in Table 1 are listed in Table 3.

In order to solve for b, one more equation connecting the absolute maximum acceleration and the average root-mean-square value of a stationary random process should be employed. It has been pointed out that the earthquake motion may be considered as a stationary random process during the portion of the strongest motion. Under this assumption, therefore, in an interval (t_1,t_2) containing t_m as the middle point, the random process $\ddot{X}_g(t)$ may be considered stationary with an average root-mean-square value defined by

$$\bar{\sigma}_{\ddot{X}_g}(t_1,t_2) = \bar{D}(t_1,t_2)$$

$$= \frac{1}{t_2 - t_1} \int_{t_1}^{t_2} D(t)\, dt \qquad (3\text{-}49)$$

Substituting Equation (3-7) for D(t) into Equation (3-49), we obtain

$$\bar{\sigma}_{\ddot{X}_g}(t_1,t_2) = \frac{b}{\alpha^2(t_2 - t_1)} [(e^{-\alpha t_1} - e^{-\alpha t_2}) + \alpha(t_1 e^{-\alpha t_1} - t_2 e^{-\alpha t_2})] \qquad (3\text{-}50)$$

Carwright and Longuet-Higgins [67] established a formula relating the average of the highest relative maximum of a sample of N maxima in the interval (t_1,t_2) with the average root-mean-square value of the stationary random process. The formula is given by

$$\frac{(\ddot{x}_g)_m}{\bar{\sigma}_{\ddot{X}_g}(t_1,t_2)} \doteq \frac{[\ln(1-\epsilon^2)^{\frac{1}{2}}N]^{\frac{1}{2}} + 0.2886\,[\ln(1-\epsilon^2)^{\frac{1}{2}}N]^{-\frac{1}{2}}}{(1 - 0.5\epsilon^2)^{\frac{1}{2}}} \tag{3-51}$$

where

$$\epsilon^2 = [1 - (\lambda/2)^2]$$

$$\lambda = N_o/N_m$$

N_o = Number of zero crossings per second

N_m = Number of maxima per second

$\bar{\sigma}_{\ddot{X}_g}(t_1,t_2)$ = Average root-mean-square value in the interval (t_1,t_2) containing t_m.

Substituting Equation (3-50) into Equation (3-51), we obtain

$$b \doteq \frac{(\ddot{x}_g)_m \alpha^2 (t_2 - t_1)(1 - 0.5\epsilon^2)^{\frac{1}{2}}}{\{[\ln(1-\epsilon^2)^{\frac{1}{2}}N]^{\frac{1}{2}} + 0.2886[\ln(1-\epsilon^2)^{\frac{1}{2}}N]^{-\frac{1}{2}}\}}$$

$$\times \frac{1}{\{(e^{-\alpha t_1} - e^{-\alpha t_2}) + \alpha(t_1 e^{-\alpha t_1} - t_2 e^{-\alpha t_2})\}} \tag{3-52}$$

or

$$b \doteq \frac{(\ddot{x}_g)_m \alpha^2 (t_2 - t_1)[1 + (0.5\lambda)^2]^{\frac{1}{2}}}{\sqrt{2}\,\{[\ln(0.5\lambda N)]^{\frac{1}{2}} + 0.2886[\ln(0.5\lambda N)]^{-\frac{1}{2}}\}}$$

$$\times \frac{1}{\{(e^{-\alpha t_1} - e^{-\alpha t_2}) + \alpha(t_1 e^{-\alpha t_1} - t_2 e^{-\alpha t_2})\}} \tag{3-53}$$

The estimated values of the parameter b for the eight records are computed from Equation (3-53) and listed in Table 3. Figures 10 and 11 show the shape of the envelope functions with the values of b and α given in Table 3. Since the root-mean-square function is equal to the envelope function of the random process, nonstationarity of the random process is evident from these figures.

So far, we have shown how to find the parameters α and b for the envelope function of the simulation process. There are still two more parameters μ_d and ω_d to be determined. These two parameters control the correlation structure of the filtered process. It has been pointed out that, in the phase of the strongest motion, the filtered autocorrelation becomes essentially stationary. Under this assumption, the filtered parameters can be so chosen as to make the normalized autocorrelation functions of the filter output agree with those measured from the earthquake records. Figures 12 and 13 show the normalized autocorrelation functions for four earthquake records listed in Table 1. The data were obtained for a common time interval $2 \leq t \leq 15$ sec., which corresponds to the strong-phase durations of the acceleration traces [7]. These figures show a common property; for $\tau \leq 0.01$ second, the autocorrelation function is positive and decreases with τ, while for $\tau > 0.10$ second, the results are generally negative and tend to approach zero for large τ. From this observation, we can estimate the filtered parameters μ_d and ω_d.

The time τ' at which the autocorrelation function reaches zero at the first time is given by the equation

$$\rho(\tau') = e^{-\mu_d \tau'} \cos \omega_d \tau'$$

$$= 0 \qquad (3\text{-}54)$$

It immediately follows that

$$\omega_d = \frac{1}{\tau'} \frac{\pi}{2} \qquad (3\text{-}55)$$

The estimated values for the ω_d's are listed in Table 4. It is worth noting that all the ω_d's lie within the range from 10 to 25 sec^{-1} which was proposed by Bolotin [68]. The parameter μ_d reflects the decaying rate of the autocorrelation function; the less the magnitude of μ_d, the stronger the correlation. Barstein [62], who worked up the accelerograms of five earthquakes, suggested that the range for μ_d be six to 8.5 $sec.^{-1}$. Table 4 lists estimated values for τ', ω_d and μ_d for the earthquakes one to four in Table 1. The simulated normalized autocorrelation functions are shown in Figure 12 and 13. It is observed that the proposed curves fit well with the computed data in the interval $0 \leq \tau \leq 0.1$ second.

It is obviously understood from Equations (3-29) and (3-34) that the probability density function of the random frequencies and the power spectral density of the stationary random process are dependent on the filtered parameters μ_d and ω_d. Once these two parameters have been obtained, the distribution of the random variables F_j as well as the spectral density function $S_G(\omega)$ of the stationary random process $G(t)$ can be computed. Figure 14 shows the probability density functions of the random variables F_j for records one to four. These curves

show that the probability density function of the random frequencies increases as the frequency increases, attaining a maximum value in the range of 15 to 18 sec.$^{-1}$, and then decreases to zero with increasing frequency. This observation reflects the real earthquake phenomenon rather than an ideal assumption with uniform frequency distribution proposed by Goldberg et al. [17]. In other words, beyond the interval (6,46) there are some distributions for the random frequencies in our simulation process.

The power spectral density function of the stationary random process G(t) can be constructed in a frequency domain from Equation (3-35). The normalized power spectral density function $\hat{S}_G(\omega)$ is defined as

$$\hat{S}_G(\omega) = \frac{S_G(\xi_g, \omega_g; \omega)}{|S_G(\xi_g, \omega_g; \omega|_{max}} \tag{3-56}$$

A comparison of the shapes of the normalized power spectral density functions of G(t) and a model proposed by Tajimi [64] is shown in Figure 15. It is seen that these curves are similar in shape for both the stationary process of the nonstationary modulated process and Tajimi's stationary model.

Testing the Model

It has been pointed out that a simulation process for earthquake motion should be consistent with the statistics of past earthquakes. Among recent investigations on this respect, Levy's criteria [9] seems satisfied on a qualitative basis for judging the acceptability of a

simulation process. In this section, therefore, the earthquake acceleration model devised in the preceding sections will be analyzed to determine how well it satisfies Levy's criteria for simulation process. The first and the third records will be used in our analysis for comparison. Other records can be treated in a similar manner. Record one is selected because it reaches its maximum value in the first few seconds. Thus, it can be used as a sample function for this type of ground motion which is called ensemble I. Record three reaches its maximum at about one fifth of its duration and can be represented as a sample function for such kind of ground disturbance which is called ensemble II. All the corresponding parameters are listed in Table 5.

The following quantities are computed and compared with the corresponding quantities from Levy's work:

1. Response Spectra - The relative velocity response spectrum, $S_v(\xi,T_n)$, of the simulation process can be expressed as

$$S_v(\xi,T_n) = |W(\xi,T_n;t)|_{max} \tag{3-57}$$

where

$$W(\xi,T_n;t) = \int_o^t \ddot{x}_g(\tau)\, \exp\left[-\frac{2\pi}{Tn}\,\xi(t-\tau)\right]\sin\left[\frac{2\pi}{Tn}\,(t-\tau)\right] d\tau \tag{3-58}$$

Upon integration, we obtain

$$W(\xi,T_n;t) = \sum_{j=1}^{n} \frac{be^{-\frac{2\pi\xi t}{Tn}}}{\sqrt{2n}} \left\{\sin\left(\frac{2\pi t}{Tn} - \theta_j\right) I_c\left(-\alpha + \xi, f_j + \frac{2\pi}{Tn}; t\right)\right.$$

$$- \cos\left(\frac{2\pi t}{Tn} - \theta_j\right) I_s\left(-\alpha + \xi, f_j + \frac{2\pi}{Tn}; t\right)$$

$$+ \sin\left(\frac{2\pi t}{Tn} - \theta_j\right) I_c\left(-\alpha + \xi, f_j + \frac{2\pi}{Tn}; t\right)$$

$$+ \cos\left(\frac{2\pi t}{Tn} - \theta_j\right) I_s\left(-\alpha + \xi, f_j + \frac{2\pi}{Tn}; t\right)\Big\} \qquad (3\text{-}59)$$

$$I_c(p,q;t) = \int_0^t \tau\, e^{p\tau}\cos(q\tau)\, d\tau$$

$$= \frac{t\, e^{pt}}{p^2+q^2}\left[p\cos(qt) + q\sin(qt)\right] - \frac{e^{pt}}{(p^2+q^2)^2}$$

$$\times \left[(p^2 - q^2)\cos(qt) + 2pq\sin(qt)\right] + \frac{p^2 - q^2}{(p^2+q^2)^2} \qquad (3\text{-}60)$$

and

$$I_s(p,q;t) = \int_0^t \tau e^{p\tau}\sin(q\tau)d\tau$$

$$= \frac{t\, e^{pt}}{p^2+q^2}\left[p\sin(qt) - q\cos(qt)\right] - \frac{e^{pt}}{(p^2+q^2)^2}$$

$$\times \left[(p^2 - q^2)\sin(qt) - 2pq\cos(qt)\right] - \frac{2pq}{(p^2+q^2)^2} \qquad (3\text{-}61)$$

It is noted from Equation (3-58) that $W(\xi,Tn;t)$ is a function not only of the ground acceleration, $\ddot{x}_g(t)$, but also of ξ, the damping ratio;

of T_n, the period of vibration; and of t, the time at which the integral is evaluated. For a complete examination of $W(\xi,T_n;t)$, it is necessary to evaluate the integral in Equation (3-58) for all periods of vibration which are pertinent to the structural problem. In practice, the calculations are made for periods of vibration between 0.1 second and 3.0 seconds, and for several values of the damping ratio. When $W(\xi,T_n;t)$ is computed for particular values of ξ and T_n, there is obtained a time history, in Equation (3-59), of a sample oscillator of the specified period and damping ratio as it responds to the simulation process. This response passes through a maximum at some time prior to the end of the earthquake and it is this maximum value which is of interest for aseismic design. The spectrum will therefore consist of a plot of such maximum responses versus period of vibration, with damping ratio ξ, as a parameter and n is taken to be thirty. The velocity response spectra for two samples of ensemble I are shown in Figures 16 and 17. Figures 18 and 19 show the velocity response spectra for two samples of ensemble II. The average velocity response spectra are computed by taking averages over five sample velocity response spectra. They are shown in Figures 20 and 21 for ensemble I and ensemble II, respectively. The acceleration response spectrum is evaluated by the maximum values of $\omega_n W(\xi,T_n;t)$. The ordinate of the acceleration spectrum at any particular period may be taken to represent the maximum acceleration attained by a simple oscillator of that period when subjected to the simulation process. Figures 22 and 23 show samples of acceleration response spectra for ensembles I and II. The average acceleration response spectra are also shown in Figures 24 and 25. Similarly, the

displacement response spectrum is computed by the maximum values of $W(\xi,T_n;t)/\omega_n$. Its coordinate at any particular period may represent the maximum displacement attained by a simple structure of that period when subjected to the earthquake. Figures 26 and 27 show samples of displacement response spectra. The average displacement response spectra are also shown in Figures 28 and 29. Like the velocity spectrum the time response spectrum $S_t(\xi,T_n)$ is also typical of a strong motion record. It is the curve of the time at which the absolute relative velocity is the highest, plotted versus the natural period T_n for various values of damping ratio ξ. Iyengars [18], using a different simulation process, have found that for zero damping the curves are violently oscillatory. When damping is not zero there is a marked drop in the level with the sharp peaks and valleys getting replaced gradually by horizontal lines. It is further noted that unlike the velocity spectrum ordinates, the ordinates of the time response spectrum need not always decrease with damping. The time response spectra curves shown in Figures 30 and 31 in the simulation process satisfactorily exhibit all these features. Some conclusions can be summarized on the well-defined characteristics of response spectra curves. These are:

1) The zero damping curve is marked by abrupt oscillations, which indicates that the response is very sensitive to small differences in periods of vibrations. The introduction of damping makes the response much less sensitive to small changes of period.

2) The introduction of a small amount of damping causes a reduction in the maximum response.

3) Most of the spectra approximate rather closely a typical

form. There is no evidence that the location of the earthquake has any significant effect upon the shape of the spectrum. This fact can be easily seen from the smooth average response spectra curves. Figures 16 through 31 obtained from the simulation process show that they exhibit similar characteristics to those obtained from past earthquake records.

2. Maximum Ground Acceleration - Two samples of the simulation earthquake acceleration are shown in Figures 32 and 33 for ensembles I and II, respectively. These figures are plotted by the Univac 1108 Digital Computer. They show not only that they have similar values for maximum ground accelerations but also that they exhibit similar type of oscillation to record one and record three.

3. Nonstationarity - The root-mean-square functions of the simulation earthquakes are shown in Figures 10 and 11. Since these functions are dependent on time, nonstationarity of the simulation process is evident.

4. Autocorrelation Function - The normalized autocorrelation function for the simulated earthquake acceleration is expressed in Equation (3-24). Figures 12 and 13 show the normalized autocorrelation functions for record one through record four. It is obvious that they exhibit the same characteristics as the statistics obtained from the earthquake data.

Thus, Levy's criteria are actually satisfied for the simulated earthquake acceleration. It is recognized that the proposed random process possesses more advantages than the existing simulation models. Therefore, the random process expressed by Equation (3-6) will be used

as an input function to analyze the response of multi-story buildings to earthquake excitation.

CHAPTER IV

STRUCTURAL MODEL

Motivations

It is important to investigate the response analysis of an N-story building for the following reasons:

1. Modern structures are in many cases high-rise buildings and consequently multi-degree-of-freedom systems. Nevertheless, one-degree-of-freedom structural models for the most part are used in response analyses. A review of the literature has shown that most analyses of multi-story buildings are based on past earthquake records - a sense of deterministic analysis. Only a few investigations have approached the study of multi-story buildings under earthquakes from a probabilistic simulated random processes. Therefore, it is worth studying on the subject.

2. Structural damping may have some effects on the response of buildings. However, few investigators have taken this factor into consideration in the analysis of multi-story buildings (5,39). For this purpose, structural damping will be included in the proposed building model and its effects on the dynamic response will be examined.

3. The viscous damping in a multi-story building is sometimes assumed to be proportional to the relative velocity between floors in order to make the normal mode approach succeed. Some assumed relations among stiffness, damping and mass matrices may meet this requirement

[36,37,38]. However, other structural models may or may not have normal modes. For example, the tall building model proposed by Lin [5, p. 193] seems a good model for its reality in representing both viscous and structural damping, but only the impulse response function of the structure has been obtained by a finite-difference approach. No further results have been achieved. Thus, the feasibility of the normal mode method in regard to Lin's model appears worthy of further consideration.

Proposed Structural Model

The linear damped multi-story shear building to be analyzed is shown schematically in Figure 34. The following assumptions are made:

(1) The distributed mass of the structure is concentrated at floor levels. This is m_j.

(2) The floor slabs are infinitely rigid and do not rotate during deformations.

(3) The entire shear stiffness at any column level is concentrated in one linear elastic shear spring with stiffness k_j.

(4) The structure has linear absolute viscous damping measured with reference to the absolute velocity - not the velocity relative to the ground.

(5) Structural damping is included in the building model. The structural damping factor is denoted by γ_j.

(6) There is no foundation rotation.

It is worth mentioning here that the absolute-velocity proportional damping force has been used by Newmark and Jennings [46] in analyzing the linear response of multi-story buildings to the recorded

earthquakes, not simulation processes. The so-called rocking effect on buildings has also been extensively studied by Merrit and Housner [69]. They showed that the maximum shear force in a tall building subjected to earthquake ground motion is essentially unaffected by any degree of foundation rocking effect. Therefore, we restrict our analysis to buildings on firm foundations and thus neglect the rocking effect.

Linear models have continued to be used in earthquake design for, among others, the following two reasons:

(1) Since moderate earthquakes are much more frequent than high-intensity ones, structures subjected to such earthquakes can be designed considering a completely elastic response. Consequently, there have been many investigations developed recently in the analyses of the elastic response of structures to earthquakes. Examples can be found in the volumes of the "Proceedings of the Fourth World Conference on Earthquake Engineering" in 1969 (Vol. II, Sec. A3-1 - A3-171) and the "Proceedings of the Fifth World Conference on Earthquake Engineering" in 1974. Thus, elastic response analyses of structures to earthquakes remain worth studying. Therefore, the proposed work is mostly limited to the elastic response of buildings.

(2) It has been pointed out by Newmark and Rosenblueth [24] that some structures, such as nuclear reactors, may be required to have a negligible probability of exceeding the yield point even at the Modified Mercalli intensity scale of nine.* Hence, elastic response analysis may also be applied to such structures.

Nonlinear models for tall buildings can be devised by taking

*See footnote on page 60.

into account the actual nonlinear nature of the shear forces in the columns. This will also be investigated in the later stage of the proposed work. However, it is currently felt that the earthquake representation being used here is sufficiently complicated that if it is to be used as the input process for a nonlinear structure the subsequent analysis would become extremely tedious, if not impossible.

*General panic. Considerable damage in ordinary substantial buildings with partial collapse, great damage in poorly built structures, slight damage in specially designed brick structures, serious damage to reservoirs, underground pipes broken, conspicuous cracks in ground, and buildings shifted off foundations.

CHAPTER V

METHOD OF APPROACH

Equations of Motion

Referring to Figure 34 and applying D'Alembert's principle to each floor mass, we obtain a set of equations in terms of the absolute displacements of the floors. Let x_j be the absolute floor displacement; then the equations of motion become

$$m_j \ddot{x}_j - k_{j+1}(x_{j+1} - x_j) + k_j(x_j - x_{j-1}) - \bar{c}_{j+1}(\dot{x}_{j+1} - \dot{x}_j)$$

$$+ \bar{c}_j(\dot{x}_j - \dot{x}_{j-1}) + c_j \dot{x}_j = 0 , \quad j = 1,2,\ldots,N-1.$$

$$m_N \ddot{x}_N + k_N(x_N - x_{N-1}) + \bar{c}_N(\dot{x}_N - \dot{x}_{N-1}) + c_N \dot{x}_N = 0$$

$$x_0 = x_g(t) \tag{5-1}$$

where the $\bar{c}_j$ are equivalent structural damping coefficients; the m_j and the k_j are the mass and stiffness of the jth floor, respectively; $x_g(t)$ is the ground displacement. Mathematically, the equivalent structural damping coefficient and the stiffness are related by the following expression [25]:

$$\bar{c}_j \dot{x}_j = i \gamma_j k_j x_j \tag{5-2}$$

where the γ_j are the structural damping factors. Substituting Equation (5-2) into Equation (5-1), we obtain

$$m_j \ddot{x}_j - k_j(1 + i\gamma_j)x_{j-1} + [k_j(1 + i\gamma_j) + k_{j+1}(1 + i\gamma_{j+1})]x_j$$

$$- k_{j+1}(1 + i\gamma_{j+1})x_{j+1} + c_j \dot{x}_j = 0, \quad j = 1,2,\ldots,N-1.$$

$$m_N \ddot{x}_N + k_N(1 + i\gamma_N)x_N - k_N(1 + i\gamma_N)x_{N-1} + c_N \dot{x}_N = 0$$

$$x_0 = x_g(t) \tag{5-3}$$

Since the relative displacement is more significant than the absolute displacement for the dynamic response of a tall building structure, we shall use the relative displacement of each mass with respect to the foundation as a measure of the response. Let $y_j = x_j - x_0$, then the equations of motion in terms of relative displacements become

$$m_j \ddot{y}_j + c_j \dot{y}_j + k_j(1 + i\gamma_j)(y_j - y_{j-1}) - k_{j+1}(1 + i\gamma_{j+1})$$

$$x\,(y_{j+1} - y_j) = - m_j \ddot{x}_g - c_j \dot{x}_g, \quad j = 1,2,\ldots,N-1.$$

$$m_N \ddot{y}_N + c_N \dot{y}_N + k_N(1 + i\gamma_N)(y_N - y_{N-1}) = - m_N \ddot{x}_g - c_N \dot{x}_g$$

$$x_0 = x_g(t) \tag{5-4}$$

Although the physical meaning of this equation is not clear, it is still widely used as a model for the representation of a structure with structural damping because the solution results in good results [38]. Equation (5-4) can be rewritten in matrix form

$$[M]\{\ddot{Y}\} + [C]\{\dot{Y}\} + [\bar{K}]\{Y\} = - \ddot{x}_g[M]\{I_o\} - \dot{x}_g[C]\{I_o\} \tag{5-5}$$

where

$$[\backslash M \backslash] = \begin{bmatrix} m_1 & 0 & \cdots & 0 & \cdots & 0 \\ 0 & m_2 & \cdots & 0 & \cdots & 0 \\ \vdots & \vdots & & \vdots & & \vdots \\ 0 & 0 & \cdots & m_j & \cdots & 0 \\ \vdots & \vdots & & \vdots & & \vdots \\ 0 & 0 & \cdots & 0 & \cdots & m_N \end{bmatrix} \tag{5-6}$$

= N x N diagonal inertia matrix,

$$[\backslash C \backslash] = \begin{bmatrix} c_1 & 0 & \cdots & 0 & \cdots & 0 \\ 0 & c_2 & \cdots & 0 & \cdots & 0 \\ \vdots & \vdots & & \vdots & & \vdots \\ 0 & 0 & \cdots & c_j & \cdots & 0 \\ \vdots & \vdots & & \vdots & & \vdots \\ 0 & 0 & \cdots & 0 & \cdots & c_N \end{bmatrix} \tag{5-7}$$

= N x N diagonal viscous damping matrix,

and

$$[\bar{K}] = \begin{bmatrix} \bar{k}_1+\bar{k}_2 & -\bar{k}_2 & 0 & 0 & \cdots & 0 & 0 & 0 & \cdots & 0 & 0 \\ -\bar{k}_2 & \bar{k}_2+\bar{k}_3 & -\bar{k}_3 & 0 & \cdots & 0 & 0 & 0 & \cdots & 0 & 0 \\ 0 & -\bar{k}_3 & \bar{k}_3+\bar{k}_4 & -\bar{k}_4 & \cdots & 0 & 0 & 0 & \cdots & 0 & 0 \\ \vdots & \vdots & \vdots & \vdots & & \vdots & \vdots & \vdots & & \vdots & \vdots \\ 0 & 0 & 0 & 0 & \cdots & -\bar{k}_j & \bar{k}_j+\bar{k}_{j+1} & -\bar{k}_{j+1} & \cdots & 0 & 0 \\ \vdots & \vdots & \vdots & \vdots & & \vdots & \vdots & \vdots & & \vdots & \vdots \\ 0 & 0 & 0 & 0 & \cdots & 0 & 0 & 0 & \cdots & -\bar{k}_N & \bar{k}_N \end{bmatrix} \tag{5-8}$$

= N x N symmetric complex stiffness matrix,

in which $\bar{k}_j$, equal to $k_j(1 + i\gamma_j)$, is called the complex stiffness of the jth floor and $\{I_o\}$ denotes the identity vector.

Thus, we have obtained equations of motion in which the forcing functions are expressed in terms of both ground acceleration and ground velocity. It is understood that the dynamic response analysis of structures to this kind of input function requires not only the auto-correlation function of ground acceleration but also the cross-correlation function of ground acceleration and velocity.

The Normal Mode Method

By means of the normal mode method, a linear transformation is employed to change Equations (5-5) to a set of uncoupled equations of motion. According to this concept, a multi-story building structure can be represented by a number of equivalent one-degree-of-freedom systems. However, it is well-known that damped systems do not in general have natural modes of vibration. A survey of the literature has shown that a necessary and sufficient condition for a damped linear system to have classical normal modes is that there exists a transformation which diagonalizes the damping matrix and uncouples the equations of motion [36,37,38].

The multi-story building as shown in Figure 34 is assumed to satisfy the following conditions and consequently has natural modes of vibration:

(1) The external damping coefficients are small. Thus, the coupled damping in different modes can be disregarded. Also we assume equal viscous damping in all normal modes [10]; i.e.,

$$c^*_{ij} = d\ \delta_{ij} \tag{5-9}$$

where c^*_{ij} is the element of the generalized damping matrix.

(2) The structural damping factors γ_j are small quantities and all equal to γ.

According to vibration theory, we form a linear transformation

$$\{Y\} = [\Phi]\ \{U\} \tag{5-10}$$

where $\{U\}$ is the normal coordinate vector representing the vibration mode amplitude and $[\Phi]$ represents the normal modal matrix as deduced from the undamped homogeneous form of Equation (5-5). In other words, $[\Phi]$ is the matrix of normal modes associated with the eigenvalue problem

$$[M]\ [\Phi] = [K]\ [\Phi]\ [\Lambda] \tag{5-11}$$

where

$$[\Lambda] = [\Omega^{-2}] \tag{5-12}$$

in which the elements of the matrix $[\Omega]$ are called natural frequencies. Premultiplying Equation (5-5) by $[\Phi]^T$, where the superscript T denotes transpose of the matrix $[\Phi]$, we obtain

$$[\Phi]^T\ [\ M\ ]\ [\Phi]\ [\Phi]^{-1}\ \{\ddot{Y}\} + [\Phi]^T\ [\ c\ ]\ [\Phi]\ [\Phi]^{-1}\ \{\dot{Y}\}$$

$$+ [\Phi]^T\ [\bar{K}]\ [\Phi]\ [\Phi]^{-1}\ \{Y\}$$

$$= [\Phi]^T\ \{P\} \tag{5-13}$$

where

$$\{P\} = -\ \ddot{x}_g[\ M\ ]\{I_o\} - \dot{x}_g[\ C\ ]\{I_o\} \tag{5-14}$$

Converting to normal coordinates in accordance with Equation (5-10), we obtain the dynamic equations of motion expressed in terms of normal coordinates. That is,

$$[M^*]\{\ddot{U}\} + [C^*]\{\dot{U}\} + [K^*]\{U\} = \{P^*\} \tag{5-15}$$

where

$$[M^*] = [\Phi]^T [\grave{M}] [\Phi]$$

$$= [\grave{I}] \tag{5-16}$$

$$= \text{generalized mass matrix}$$

$$[K^*] = [\Phi]^T [\bar{K}] [\Phi]$$

$$= [\Phi]^T\{([\grave{I}] + i\gamma[\grave{I}])[K]\}[\Phi] \tag{5-17}$$

$$= \text{generalized complex stiffness matrix}$$

$$[C^*] = [\Phi]^T[\grave{C}][\Phi] \tag{5-18}$$

$$= \text{generalized damping matrix}$$

$$\{P^*\} = - \ddot{x}_g[\Phi]^T[\grave{M}]\{I_o\} - \dot{x}_g[\Phi]^T[\grave{C}]\{I_o\} \tag{5-19}$$

$$= \text{generalized force vector.}$$

Using the orthogonality of the normal modes, we have

$$[\Phi]^T[K][\Phi] = [\grave{\Omega}^2][M^*] \tag{5-20}$$

Since $[\Phi]$ is the normal mode matrix, the following relation holds:

$$[M^*] = [I] \tag{5-21}$$

$$= \text{Identity matrix}$$

Thus, we obtain

$$[\Phi]^T [K] [\Phi] = [\Omega^2] [I] \tag{5-22}$$

where the elements ω_j ($j = 1,2,\ldots,N$) of the matrix $[\Omega]$ are called natural frequencies. It is obvious that the ω_j cannot be zero in the building model, since at least one mass must be connected to the ground by a spring element (column) and a zero natural frequency would imply a stressless rigid-body translation which is impossible in our building model.

Since we assume the structure is lightly damped, we may disregard the coupled damping in different modes; that is,

$$[C^*] = [\Phi]^T [C] [\Phi]$$

$$= \text{diagonal matrix} \tag{5-23}$$

It then follows from Equation (5-9) that

$$[C^*] = d\,[I] \tag{5-24}$$

Equation (5-24) implies that the generalized damping matrix becomes a diagonalized matrix in normal coordinates. Letting

$$d\,[I] = 2[\Xi][\Omega][I] \tag{5-25}$$

we obtain

$$[C^*] = 2[\Xi][\Omega][I] \tag{5-26}$$

where the ξ_j are the viscous damping ratios and are defined by

$$\xi_j = \frac{d}{2\omega_j} \tag{5-27}$$

Using above relations among mass, stiffness and damping matrices, we can write the matrix Equation (5-15) in the following form:

$$\{\ddot{U}\} + 2[\Xi][\Omega]\{\dot{U}\} + (1 + i\gamma)[\Omega^2]\{U\} = \{P^*\} \tag{5-27}$$

subjected to the initial conditions

$$\{U(0^-)\} = 0 \tag{5-28}$$

and

$$\{\dot{U}(0^-)\} = 0 \tag{5-29}$$

Equations (5-27), (5-28) and (5-29) can also be written in the following familiar uncoupled form:

$$\ddot{u}_j + 2\omega_j\xi_j\dot{u}_j + (1 + i\gamma)\omega_j^2 u_j = p_j^* \tag{5-30}$$

subjected to the conditions

$$u_j(0^-) = 0 \tag{5-31}$$

and

$$\dot{u}_j(0^-) = 0 \tag{5-32}$$

where

$$p_j^*(t) = -\{\Phi_j\}^T(\ddot{x}_g(t)\,[M]\{I_o\} + d\,\dot{x}_g(t)\,[M]\{I_o\}) \tag{5-33}$$

in which

$$j = 1,2,\ldots,N \ .$$

Thus, the coupled matrix Equations of motion (5-15) have been transformed to an uncoupled system of Equations (5-30). The methods for solving one-degree-of-freedom systems can then be employed to solve Equation (5-30). And the corresponding relative displacements are subsequently given by Equation (5-10).

At this point it should be noted that an important advantage of the normal mode method is that an approximate solution may be obtained by including only part of the modal contributions in the superposition. In general, the lower modes make the principal contributions to the response, and good approximations can frequently be obtained by considering only the first few modes in the analysis.

In order that the Duhamel integral solution may be employed to solve Equation (5-30), we need to find the impulse response function of the structural system.

Impulse Response Functions

When the forcing function is replaced by a unit impulse excitation $\delta(t)$, the solution of Equation (5-30) is called the impulse response function $h_j(t)$ or the one-side Green's function [70]. It describes the influence on the value of $u_j(t)$ at time t of an impulse concentrated at t=0. In order to express the solution of Equation (5-30) with the initial conditions (5-31) and (5-32) as a Duhamel integral, we have to find the impulse response functions of the building model.

Equation (5-30) can be rewritten in the following self-adjoint form:

$$\frac{d}{dt}\left(e^{2\omega_j\xi_j t}\frac{du_j}{dt}\right) + e^{2\omega_j\xi_j t}\omega_j^2(1 + i\gamma)u_j = e^{2\omega_j\xi_j t}p_j^*(t) \quad (5\text{-}33)$$

According to the theory of differential equations, the impulse response function $h_j(t)$ is completely characterized by the following conditions [70]:

$$(1)\quad \frac{d}{dt}\left(e^{2\omega_j\xi_j t}\frac{dh_j}{dt}\right) + e^{2\omega_j\xi_j t}\omega_j^2(1 + i\gamma)h_j = 0$$

$$(2)\quad h_j(t)\Big|_{t=0} = 0$$

$$(3)\quad \frac{dh_j(t)}{dt}\Big|_{t=0^+} = 1$$

Solving for (1) with initial conditions (2) and (3), we obtain

$$h_j(t) = \frac{A_j - iB_j}{2(A_j^2 + B_j^2)\omega_j}e^{-\xi_j\omega_j t}\left\{e^{A_j\omega_j t}[\cos(B_j\omega_j t) + i\sin(B_j\omega_j t)]\right.$$

$$\left. - e^{-A_j\omega_j t}[\cos(B_j\omega_j t) - i\sin(B_j\omega_j t)]\right\}, \qquad t \geq 0$$

$$= 0, \qquad t < 0 \qquad (5\text{-}34)$$

Here it is understood that only the real part represents the actual motion. The real part of $h_j(t)$ is given by

$$h_j(t) = \frac{e^{-\xi_j \omega_j t}}{(A_j^2 + B_j^2)\omega_j} \{A_j \cos(B_j \omega_j t) \sinh(A_j \omega_j t)$$

$$+ B_j \sin(B_j \omega_j t) \cosh(A_j \omega_j t) , \quad t \geq 0$$

$$= 0 , \quad t < 0 \tag{5-35}$$

where

$$A_j = \pm \left\{ \frac{-(1-\xi_j^2) + [(1-\xi_j^2)^2 + \gamma^2]^{\frac{1}{2}}}{2} \right\}^{\frac{1}{2}} \tag{5-36}$$

and

$$B_j = [A_j^2 + (1 - \xi_j^2)]^{\frac{1}{2}} \tag{5-37}$$

Equation (5-35) can also be written in the following form:

$$h_j(t) = \frac{e^{-\xi_j \omega_j t}}{2(A_j^2 + B_j^2)\omega_j} \{e^{A_j \omega_j t} [A_j \cos(B_j \omega_j t) + B_j \sin(B_j \omega_j t)]$$

$$- e^{-A_j \omega_j t} [A_j \cos(B_j \omega_j t) - B_j \sin(B_j \omega_j t)]\} , \quad t \geq 0$$

$$= 0 , \quad t < 0 \tag{5-38}$$

As a special case, when the structural damping is absent, A_j vanishes. Thus, in this case

$$h_j(t) = \frac{e^{-\xi_j \omega_j t}}{\omega_j (1-\xi_j^2)^{\frac{1}{2}}} \sin[\omega_j (1-\xi_j^2)^{\frac{1}{2}} t] , \quad t \geq 0$$

$$= 0 , \quad t < 0 \tag{5-39}$$

That is, Equation (5-39) is reduced to a well-known expression for the impulse response function of a one-degree-of-freedom system without structural damping [25].

It is quite obvious that computation of the response variance functions will be tedious if Equation (5-35) or (5-38) is employed. However, since the structural damping factor is so small in the range of 0.01 to 0.05, A_j is also a small quantity. By making a series expansion of the exponential functions and neglecting the higher order terms, we can approximate the impulse response function in the following expression:

$$h_j(t) = \frac{e^{-\xi_j \omega_j t} \sin(B_j \omega_j t)}{B_j \omega_j} \tag{5-40}$$

where

$$B_j = \left\{ \frac{(1-\xi_j^2) + [(1-\xi_j^2)^2 + \gamma^2]^{\frac{1}{2}}}{2} \right\}^{\frac{1}{2}} \tag{5-41}$$

Equation (5-40) will be used as the impulse response function for the jth normal coordinate in our response analyses.

CHAPTER VI

STATISTICAL ANALYSIS OF RESPONSE

Statistics of the Forcing Function

The solution to Equation (5-30), expressed as a Duhamel integral in terms of the impulse response function, is

$$U_j(t) = \int_0^t P_j^*(\tau)\, h_j(t-\tau)\, d\tau \tag{6-1}$$

where $U_j(t)$ and $P_j^*(t)$ are random processes; $h_j(t)$ is the impulse response function given by Equation (5-40).

Let δ_j be the modal participation factor of the jth normal mode, then by definition [25]

$$\delta_j = \{\Phi_j\}^T [M] \{I_o\} / (\{\Phi_j\}^T [M] \{\Phi_j\}) \tag{6-2}$$

where $\{\Phi_j\}$ is the column vector of the normal modal matrix $[\Phi]$. Since

$$\{\Phi_j\}^T [M] \{\Phi_j\} = 1 \tag{6-3}$$

we obtain

$$\delta_j = \{\Phi_j\}^T [M] \{I_o\} \tag{6-4}$$

Thus, the forcing function $P_j^*(t)$ can be expressed in terms of the modal participation factor. That is

$$P_j^*(t) = - \delta_j [\ddot{X}_g(t) - d\, \dot{X}_g(t)] \tag{6-5}$$

It is worth noting that the forcing function $P_j^*(t)$ expressed in Equation (6-5) contains not only ground acceleration but also ground velocity. Nevertheless, so far only the earthquake ground acceleration has been simulated and only its statistical properties have been obtained. In order to establish a relation between ground velocity and ground acceleration, Berg and Housner [71] made an extensive study on a number of earthquake records and found that the ground velocity may be obtained simply by direct integration from the corresponding ground acceleration. Accordingly, the ground velocity, regarded as a random process, can be obtained from Equation (3-1) by integration

$$\dot{X}_g(t) = \int_0^t \ddot{X}_g(\tau)\, d\tau \tag{6-6}$$

Substituting the expression for $\ddot{X}_g(t)$ and carrying out the integration, we obtain

$$\dot{X}_g(t) = a \sum_{j=1}^{n} \left\{ \frac{t\, e^{-\alpha t}}{(\alpha^2 + F_j^2)} [F_j \sin(F_j t + \Theta_j) - \alpha \cos(F_j t + \Theta_j)] \right.$$

$$- \frac{e^{-\alpha t}}{(\alpha^2 + F_j^2)^2} [(\alpha^2 - F_j^2) \cos(F_j t + \Theta_j) - 2\alpha F_j$$

$$\left. \times \sin(F_j t + \Theta_j)] + \frac{1}{(\alpha^2 + F_j^2)^2} [(\alpha^2 - F_j^2) \cos \Theta_j \right.$$

$$\left. - 2\alpha F_j \sin \Theta_j] \right\} \tag{6-7}$$

where the F_j and the Θ_j are random variables with distributions defined in Chapter III.

Due to the lengthy expression for the ground velocity, direct calculation for its various moments will be elaborate. However, since the ground acceleration has been shown to be a Gaussian random process, so is the corresponding ground velocity. Thus, only the first and the second moments are required to define such a process. These moments can then be obtained from the properties of the ground acceleration. The expectation of $\dot{X}_g(t)$ is

$$\mu_{\dot{X}_g}(t) = E[\dot{X}_g(t)]$$

$$= E\left[\int_0^t \ddot{X}_g(\tau)\, d\tau\right]$$

$$= \int_0^t \mu_{\ddot{X}_g}(\tau)\, d\tau \qquad (6\text{-}8)$$

Here the commutation of expectation and integration has been made by the fact that the random variables F_j and Θ_j are independent of time. It has been shown that the expectation of $\ddot{X}_g(t)$ vanishes. Thus,

$$\mu_{\dot{X}_g}(t) = 0 \qquad (6\text{-}9)$$

The cross-correlation function of ground velocity and ground acceleration at two instants of time, t_1 and t_2, can be obtained by

$$R_{\dot{X}_g \ddot{X}_g}(t_1, t_2) = E\left[\dot{X}_g(t_1)\, \ddot{X}_g(t_2)\right] \qquad (6\text{-}10)$$

By use of Equation (6-6), we have

$$R_{\dot{X}_g \ddot{X}_g}(t_1,t_2) = E\left[\int_0^{t_1} \ddot{X}_g(\tau)\, \ddot{X}_g(t_2)\, d\tau\right]$$

$$= \int_0^{t_1} E\left[\ddot{X}_g(\tau)\, \ddot{X}_g(t_2)\right] d\tau$$

$$= \int_0^{t_1} R_{\ddot{X}_g}(\tau,t_2)\, d\tau \qquad (6\text{-}11)$$

where use has been made of the fact that the integration and expectation are commutative.

Similarly, we can easily show that

$$R_{\ddot{X}_g \dot{X}_g}(t_1,t_2) = \int_0^{t_2} R_{\ddot{X}_g}(t_1,\tau)\, d\tau \qquad (6\text{-}12)$$

and

$$R_{\dot{X}_g}(t_1,t_2) = \int_0^{t_2}\int_0^{t_1} R_{\ddot{X}_g}(\tau_1,\tau_2)\, d\tau_1\, d\tau_2 \qquad (6\text{-}13)$$

Thus, all the statistical properties of the ground velocity can be established from those of the ground acceleration. Consequently, the statistics of the forcing function $P_j^*(t)$ can be obtained.

The expectation of $P_j^*(t)$ is

$$\mu_{P_j^*}(t) = -\delta_j\left(\mu_{\ddot{X}_g}(t) - d\mu_{\dot{X}_g}(t)\right) \qquad (6\text{-}14)$$

Since

$$\mu_{\ddot{X}_g}(t) = \mu_{\dot{X}_g}(t)$$

$$= 0 \tag{6-15}$$

It immediately follows that

$$\mu_{P_j^*}(t) = 0 \tag{6-16}$$

The cross-correlation function of the forcing functions $P_j^*(t_1)$ and $P_k^*(t_2)$ at two time instants t_1 and t_2 is given by

$$R_{P_j^* P_k^*}(t_1,t_2) = \delta_j \delta_k \{R_{\ddot{X}_g}(t_1,t_2) + d\, R_{\ddot{X}_g \dot{X}_g}(t_1,t_2)$$

$$+ d\, R_{\dot{X}_g \ddot{X}_g}(t_1,t_2) + d^2 R_{\dot{X}_g}(t_1,t_2)\} \tag{6-17}$$

Substituting Equations (6-11), (6-12), and (6-13) into Equation (6-17), we have

$$R_{P_j^* P_k^*}(t_1,t_2) = \delta_j \delta_k \Big\{R_{\ddot{X}_g}(t_1,t_2) + d \int_0^{t_2} R_{\ddot{X}_g}(t_1,\tau)d\tau$$

$$+ d \int_0^{t_1} R_{\ddot{X}_g}(\tau,t_2)d\tau$$

$$+ d^2 \int_0^{t_2}\int_0^{t_1} R_{\ddot{X}_g}(\tau_1,\tau_2)d\tau_1 d\tau_2\Big\} \tag{6-18}$$

Using Equation (3-40) and carrying out the integration, we obtain

$$R_{P_j^* P_k^*}(t_1, t_2) = \beta \ \delta_j \delta_k \ R_{\ddot{X}_g}(t_1, t_2) \tag{6-19}$$

where

$$\beta = 1 + \frac{2d(\mu_d - \alpha)}{(\mu_d - \alpha)^2 + \mu_d^2} - \frac{d^2(\mu_d^2 - \alpha^2)}{[(\mu_d - \alpha)^2 + \omega_d^2][(\alpha + \mu_d)^2 + \omega_d^2]} \tag{6-20}$$

It is recognized here that the forcing function being a linear combination of ground acceleration and ground velocity is obviously a Gaussian process. Thus, Equation (6-16) and Equation (6-19) completely define the forcing function as the input process for the building structure.

Response Statistics

The solution of the jth normal coordinate of the multi-story building can be given by means of a Duhamel integral

$$U_j(t) = \int_0^t P_j^*(\tau) \ h_j(t-\tau) \ d\tau \tag{6-21}$$

where the impulse response function $h_j(t)$ is given by Equation (5-40) and the first and the second moments of the forcing function are given by Equations (6-16) and (6-19).

From an engineering design point of view, however, the relative displacement responses are more meaningful than the normal coordinate responses. They are related by the linear transformation

$$\{Y\} = [\Phi] \ \{U\} \tag{6-22}$$

Equation (6-22) can also be written in the following form:

$$Y_k(t) = \sum_{j=1}^{N} \varphi_{kj}\, U_j(t) \tag{6-23}$$

where φ_{kj} is the kth row and the jth column of the mode matrix.

It then follows that the expectation of the relative displacement at the kth floor is given by

$$\mu_{Y_k}(t) = E[Y_k(t)]$$

$$= E\Big[\sum_{j=1}^{N} \varphi_{kj}\, \mu_{U_j}(t)\Big] \tag{6-24}$$

$$= \sum_{j=1}^{N} \varphi_{kj}\, \mu_{U_j}(t)$$

where it has been possible to use the commutative rule for summation and expectation since the elements of the modal matrix are deterministic quantities. The expectation function $\mu_{U_j}(t)$ can be obtained from Equation (6-21)

$$\mu_{U_j}(t) = E\Big[\int_0^t P_j^*(\tau)\, h_j(t-\tau)\, d\tau$$

$$= \int_0^t E[P_j^*(\tau)]\, h_j(t-\tau)\, d\tau \tag{6-25}$$

Since

$$E[P_j^*(t)] = 0 \quad , \tag{6-26}$$

thus

$$\mu_{U_j}(t) = 0 \tag{6-27}$$

It then follows that

$$\mu_{Y_j}(t) = 0 \tag{6-28}$$

Equation (6-28) states that the expectation function of the relative displacement response vanishes at each floor.

The cross-correlation function of the relative displacements at the kth and the jth floors is easily obtained as

$$R_{Y_k Y_j}(t_1, t_2) = \sum_{m=1}^{N} \sum_{n=1}^{N} \varphi_{km}\, \varphi_{jn}\, R_{U_m U_n}(t_1, t_2) \tag{6-29}$$

In practice, we are interested in the mean-square response of the relative displacements. This can be easily done by setting $t_1 = t_2 = t$ and $k = j$. Denoting the mean-square function of the relative displacement at the jth floor by $\sigma^2_{Y_j}(t)$, we obtain

$$\sigma^2_{Y_j}(t) = \sum_{m=1}^{N} \sum_{n=1}^{N} \varphi_{jm}\, \varphi_{jn}\, R_{U_m U_n}(t) \tag{6-30}$$

Equation (6-30) can also be written in the following form:

$$\sigma^2_{Y_j}(t) = \sum_{n=1}^{N} \varphi^2_{jn} \sigma^2_{U_n}(t) + \sum_{m=1}^{N} \sum_{n=1}^{N} (1-\delta_{mn}) \varphi_{jm} \varphi_{jn} R_{U_m U_n}(t) \tag{6-31}$$

where δ_{mn} is the Kronecker delta defined as

$$\delta_{mn} = \begin{cases} 1, & m = n \\ 0, & m \neq n \end{cases} \tag{6-32}$$

Equation (6-31) reveals that the mean-square function of the relative displacement at the jth floor of a multi-story building can be computed by the mean-square functions and the cross-correlation functions of the normal coordinates. However, as it was pointed by Bolotin [72], in dynamic systems having a small damping the cross-correlation between the normal coordinates of the system may be neglected. In this case, the right-hand side of Equation (6-31) retains only the first term. It then follows that

$$\sigma_{Y_j}^2(t) = \sum_{n=1}^{N} \varphi_{jn}^2 \, \sigma_{U_n}^2(t) \tag{6-33}$$

The mean-square function of the normal coordinates can be obtained from Equation (6-1)

$$\sigma_{U_n}^2(t) = E\,[U_n^2(t)]$$

$$= E\left[\int_0^t \int_0^t P_n^*(\tau_1)\, P_n^*(\tau_2)\, h_n(t-\tau_1)\, h_n(t-\tau_2) d\tau_1 d\tau_2\right]$$

$$= \int_0^t \int_0^t R_{P_n^*}(\tau_1,\tau_2)\, h_n(t-\tau_1)\, h_n(t-\tau_2) d\tau_1 d\tau_2 \tag{6-34}$$

Substituting Equation (6-34) into Equation (6-33), we obtain

$$\sigma_{Y_j}^2(t) = \sum_{n=1}^{N} \varphi_{jn}^2 \int_0^t \int_0^t R_{P_n}^*(\tau_1,\tau_2)\, h_n(t-\tau_1)\, h_n(t-\tau_2) d\tau_1 d\tau_2 \tag{6-35}$$

Using the expression for the autocorrelation function of the forcing function from Equation (6-19), we obtain

$$\sigma^2_{Y_j}(t) = \beta \sum_{n=1}^{N} \varphi^2_{jn}\delta^2_n \int_0^t \int_0^t R_{\ddot{X}_g}(\tau_1,\tau_2)\, h_n(t-\tau_1)\, h_n(t-\tau_2)d\tau_1 d\tau_2 \qquad (6\text{-}36)$$

Equation (6-36) shows that the mean-square function of the relative displacement at the jth floor of a multi-story building subjected to earthquake can be obtained once the correlation function of the ground acceleration as well as the characteristics of the structure under consideration are known.

Equation (6-36) can also be written in the following form:

$$\sigma^2_{Y_j}(t) = \beta \sum_{n=1}^{N} \varphi^2_{jn}\delta^2_n \int_0^t \int_0^t D(\tau_1)\, D(\tau_2)\, R_G(\tau_1,\tau_2)\, h_n(t-\tau_1)$$

$$\times\, h_n(t-\tau_2)d\tau_1 d\tau_2 \qquad (6\text{-}37)$$

Carrying out the integration, we have

$$\sigma^2_{Y_j}(t) = \beta \sum_{n=1}^{N} \varphi^2_{jn}\delta^2_n\, I_n(t) \qquad (6\text{-}38)$$

where

$$I_n(t) = \int_0^t \int_0^t D(\tau_1)\, D(\tau_2)\, R_G(\tau_1,\tau_2)\, h_n(t-\tau_1)\, h_n(t-\tau_2)d\tau_1 d\tau_2 \qquad (6\text{-}39)$$

or

$$I_n(t) = 2\, b^2\, e^{-2\alpha t} \left\{ \sum_{i=1}^{3} \bar{A}_i(t)[C_i(2\epsilon, p_1 + p_2; t) + C_i(2\epsilon, 0; t)] \right.$$

$$+ \sum_{i=1}^{2} \bar{B}_i(t)[C_i(r,p_1;t) - C_i(r,p_2;t)]$$

$$+ \sum_{i=1}^{3} \bar{E}_i(t)\ [S_i(2\epsilon,p_1 + p_2;t)]$$

$$- \sum_{i=1}^{2} \bar{E}_i(t)\ [S_i(r,p_1;t) + S_i(r,p_2;t)]\Big\} \qquad (6\text{-}40)$$

in which

$$\epsilon = d/2 - \alpha$$

$$p_1 = \omega_n' + \omega_d$$

$$p_2 = \omega_n' - \omega_d$$

$$q = \epsilon - \mu_d$$

$$r = \epsilon + \mu_d$$

$$A_1 = q^2 + p_1^2$$

$$A_2 = q^2 + p_2^2$$

$$\bar{A}_1(t) = -\ (q/A_1 + q/A_2)t^2$$

$$\bar{A}_2(t) = 2\left(q/A_1 + q/A_2 + \frac{q^2-p_1^2}{A_1^2} + \frac{q^2-p_2^2}{A_2^2}\right) t$$

$$\bar{A}_3(t) = -\,(q/A_1 + q/A_2)$$

$$\bar{B}_1(t) = \left(\frac{a}{A_1} - \frac{a}{A_2}\right) t^2$$

$$\bar{B}_2(t) = 2\left(\frac{q}{A_2} - \frac{q}{A_1} + \frac{q^2-p_2^2}{A_2^2} - \frac{q^2-p_1^2}{A_1^2}\right) t$$

$$\bar{E}_1(t) = -\left(\frac{p_1}{A_1} + \frac{p_2}{A_2}\right) t^2$$

$$\bar{E}_2(t) = 2\left(\frac{p_1}{A_1} + \frac{p_2}{A_2} + \frac{2ap_2}{A_2^2} + \frac{2ap_1}{A_1^2}\right) t$$

$$\bar{E}_3(t) = -\left(\frac{p_1}{A_1} + \frac{p_2}{A_2}\right)$$

Further, the functions $S_i(n,p;t)$ and $C_i(n,p;t)$ are defined by

$$\begin{aligned} S_i(n,p;t) &= \int_0^t \tau^{i-1} e^{-n\tau} \sin p\tau \, d\tau \\ C_i(n,p;t) &= \int_0^t \tau^{i-1} e^{-n\tau} \cos p\tau \, d\tau \end{aligned} \qquad (6\text{-}41)$$

in which $i = 1,2,3$.

It is noted that

$$C_i(n,0;t) = \int_0^t \tau^{i-1} e^{-n\tau} \, d\tau$$

Upon integration, we obtain

$$S_1(n,p;t) = \frac{1}{n^2+p^2} \{e^{-nt}[-n \sin pt - p \cos pt] + p\}$$

$$S_2(n,p;t) = \frac{t\, e^{-nt}}{n^2+p^2} (-n \sin pt - p \cos pt)$$

$$- \frac{e^{-nt}}{(n^2+p^2)^2} [(n^2-p^2) \sin pt + 2pn \cos pt]$$

$$+ \frac{2pn}{(n^2+p^2)^2}$$

$$S_3(n,p;t) = e^{-nt} \left\{ \frac{t^2}{n^2+p^2} [-n \sin pt - p \cos pt] \right.$$

$$- \frac{2t}{(n^2+p^2)^2} [(n^2-p^2) \sin pt + 2np \cos pt]$$

$$+ \frac{2}{(n^2+p^2)^3} [(-n^3+3p^2n) \sin pt + (p^3-3pn^2)$$

$$\left. x \cos pt] \right\} - \frac{2}{(n^2+p^2)^3} (p^3 - 3pn^2)$$

$$C_1(n,p;t) = \frac{1}{n^2+p^2} \{e^{-nt} [-n \cos pt + p \sin pt] + n\}$$

$$C_2(n,p;t) = \frac{t\, e^{-nt}}{n^2+p^2} (-n \cos pt + p \sin pt) - \frac{e^{-nt}}{(n^2+p^2)^2} [(n^2 - p^2)$$

$$\times \cos pt - 2pn \sin pt] + \frac{n^2-p^2}{(n^2+p^2)^2}$$

and

$$C_3(n,p;t) = e^{-nt}\left\{\frac{t^2}{n^2+p^2}[-n\cos pt + p\sin pt] - \frac{2t}{(n^2+p^2)^2}\right.$$

$$\times [(n^2-p^2)\cos pt - 2np \sin pt]$$

$$\left. + \frac{2}{(n^2+p^2)^3}[(3p^2n - n^3) \times \cos pt + (3pn^2-p^3)\sin pt]\right\}$$

$$- \frac{2}{(n^2+p^2)^3}(3p^2n - n^3)$$

Thus, the mean-square function of the relative displacement can be computed by Equations (6-38) and (6-40) so long as the involved parameters corresponding to input characters and structural properties are specified.

We have obtained the first and the second moments of the relative displacement response $Y_j(t)$. The probability density function of $Y_j(t)$ can then be determined by

$$p_{Y_j}(y_j;t) = \frac{1}{(2\pi\sigma^2_{Y_j}(t))^{\frac{1}{2}}} \exp\left(-\frac{y_j^2}{2\sigma^2_{Y_j}(t)}\right) \qquad (6\text{-}42)$$

It has been mentioned that very valuable information to the engineer is the probability $P\{|Y_j| \geq h\,\sigma_{Y_j}\}$ that the relative displacement $Y_j(t)$ exceeds an undesirable amount $h\,\sigma_{Y_j}$, where σ_{Y_j} is the standard

deviation and h is known from the design considerations. For example, the quantity $h\sigma_{Y_j}$ could be a failure criteria that failure occurs when $|Y_j(t)|$ exceeds $h\sigma_{Y_j}$. The solution to this problem is provided by

$$P\{|Y_j| \geq h\sigma_{Y_j}\} = \int_{-\infty}^{-h\sigma_{Y_j}} p_{Y_j}(y_j;t)\, dy_j + \int_{h\sigma_{Y_j}}^{\infty} p_{Y_j}(y_j;t) dy_j \quad (6\text{-}43)$$

Since $Y_j(t)$ is a Gaussian process with probability density function given by Equation (6-42), we conclude that

$$P\{|Y_j| \geq h\sigma_{Y_j}\} = 1 - 2 \text{ erf } h \quad (6\text{-}44)$$

where the error function is defined as

$$\text{erf } x = \frac{1}{\sqrt{2\pi}} \int_0^x e^{-\eta^2/2}\, d\eta \quad (6\text{-}45)$$

Consequently, the probability of survival is then given by

$$P\{|Y_j| < h\sigma_{Y_j}\} = 2 \text{ erf } h \quad (6\text{-}46)$$

For practical design purposes, we shall consider the case in which the quantity $h\sigma_{Y_j}$ is independent of time. In this case

$$h\sigma_{Y_j}(t) = y_j^{(D)} \quad (6\text{-}47)$$

where $y_j^{(D)}$ denotes the design criteria for the relative displacement at the jth floor and is assumed to be a constant. For a nonstationary

input process, $\sigma_{Y_j}(t)$ should be function of time. As a result, h should also be time dependent. Hence, we conclude, from Equation (6-44), that the probability that the relative displacement $Y_j(t)$ exceeds an inadmissible amount $y_j^{(D)}$, a constant, will be time dependent.

In engineering applications, we are also interesting in the bound to which the probability of the relative displacement exceeds an amount. By Tchebycheff's theorem [61], this bound is given by

$$P\{|Y_j| \geq h\sigma_{Y_j}\} \leq \frac{1}{h^2} \tag{6-48}$$

For the case of constant $h\sigma_{Y_j}$ expressed by Equation (6-46), Equation (6-48) becomes

$$P\{|Y_j| \geq h\sigma_{Y_j}\} \leq \frac{\sigma_{Y_j}^2(t)}{\{y_j^{(D)}\}^2} \tag{6-49}$$

It is obvious that $p_{Y_j}(y_j;t)$ is symmetrical about the mean zero, Gauss' inequality [73] provides a better bound for $P\{|Y_j| \geq h\sigma_{Y_j}\}$, namely

$$P\{|Y_j| \geq h\sigma_{Y_j}\} \leq \frac{4}{9}\frac{\sigma_{Y_j}^2(t)}{\{y_j^{(D)}\}^2} \tag{6-50}$$

Thus, a bound for the probability of survival is obtained by

$$P\{|Y_j| < h\sigma_{Y_j}\} \geq 1 - \frac{4}{9}\frac{\sigma_{Y_j}^2(t)}{\{y_j^{(D)}\}^2} \tag{6-51}$$

Equation (6-50) shows that the smaller the ratio $\sigma_{Y_j}(t)/y_j^{(D)}$ the smaller the probability that, at t, $|Y_j|$ is in excess of $y_j^{(D)}$. It is noted that Equations (6-49) and (6-50) stress the importance of designing a structure with $\sigma_{Y_j}(t)/y_j^{(D)}$ as small as possible for all significant t, they do not enable us to calculate the probability appearing on the left hand side. The exact solution is given by Equation (6-44).

Another important response quantity for designing purpose is the shearing force. The shearing force $V_j(t)$ is defined as the elastic part of the force which acts in the walls and columns connecting the jth story to the (j-1)th story, i.e.,

$$V_j(t) = k_j[Y_j(t) - Y_{j-1}(t)] \tag{6-52}$$

It is obvious that $V_j(t)$ is a random process, since $Y_j(t)$ is a random process. Substituting Equation (6-23) into Equation (6-52), we obtain

$$V_j(t) = k_j \sum_{n=1}^{N} [\varphi_{jn} - \varphi_{(j-1)n}] U_n(t) \tag{6-53}$$

Equation (6-53) can be rearranged in the following form:

$$V_j(t)/k_j = \sum_{n=1}^{N} L_{jn} U_n(t) \tag{6-54}$$

where

$$L_{jn} = \varphi_{jn} - \varphi_{(j-1)n} \tag{6-55}$$

Here we see that Equation (6-54) has the same form as Equation (6-23) with L_{jn} replacing φ_{jn}. Thus, when the displacement statistics are calculated, we may in a straight-forward fashion calculate the shearing force statistics. The mean function and the variance function of the shearing force $V_j(t)$ are computed, respectively, as follows

$$\mu_{V_j}(t) = 0 \tag{6-56}$$

and

$$\sigma^2_{V_j}(t) = \beta k_j^2 \sum_{n=1}^{N} L^2_{jn}\, \delta_n^2\, I_n(t) \tag{6-57}$$

where $I_n(t)$ is given by Equation (6-40).

The probability of the shearing force $V_j(t)$ exceeding an inadmissible amount $v_j^{(D)}$ is given by

$$P\{|V_j(t)| \geq h\sigma_{V_j}\} \leq \frac{4}{9} \frac{\sigma^2_{V_j}(t)}{\{v_j^{(D)}\}^2} \tag{6-58}$$

where

$$v_j^{(D)} = h\sigma_{V_j}(t)$$

This equation also shows that the smaller the ratio $\sigma_{V_j}(t)/v_j^{(D)}$, the smaller the probability that, at time t, $|V_j(t)|$ is in excess of $v_j^{(D)}$.

It has been pointed out by Clough [74] that the earthquake

forces developed in the building structure may be evaluated most conveniently from its effective accelerations, which are given for each normal coordinate as the product of its frequency squared and the displacement amplitude

$$\ddot{U}_j^{(e)}(t) = \omega_j^2 U_j(t) \tag{6-59}$$

The distribution of acceleration through the structure then is given by

$$\{\ddot{Y}_j^{(e)}(t)\} = \{\Phi_j\} \ddot{U}_j^{(e)}(t) \tag{6-60}$$

which is the same form as the modal displacements.

The distribution of effective earthquake force is given by the product of the local masses and local acceleration, i.e.,

$$\{Q_j^{(e)}(t)\} = [M] \{\ddot{Y}_j^{(e)}(t)\}$$

$$= [M] \{\Phi_j\} \omega_j^2 U_j(t) \tag{6-61}$$

or, expressing in terms of the normal coordinates,

$$[Q^{(e)}(t)] = [\grave{M}] [\Phi] [\grave{\Omega}]^2 [\grave{U}(t)] \tag{6-62}$$

where

$$[\grave{U}(t)] = \begin{bmatrix} U_1(t) & 0 & \cdots & 0 \\ 0 & U_2(t) & \cdots & 0 \\ \vdots & \vdots & & \vdots \\ 0 & 0 & \cdots & U_N(t) \end{bmatrix} \tag{6-63}$$

Equation (6-62) represents the complete force response of a tall building to a given earthquake motion. Any other desired force quantity, such as the base shear, the overturning moment, or any local stress, may be obtained from these loads by normal static structural analysis procedures. For example, the base shear force $Q_j(t)$ is given by the sum of the effective earthquake forces for mode j over the height of the structure

$$Q_j(t) = \sum_{i=1}^{N} Q_{ij}^{(e)}(t)$$

$$= \{I_o\}^T \{Q_j^{(e)}(t)\} \qquad (6\text{-}64)$$

By virtue of Equation (6-61), we have

$$Q_j(t) = \{I_o\}^T [\, M \,] \{\Phi_j\} \omega_j^2 U_j(t) \qquad (6\text{-}65)$$

or, using the expression for the modal participation factor δ_j, we obtain

$$Q_j(t) = \delta_j \omega_j^2 U_j(t) \qquad (6\text{-}66)$$

Knowing the statistical characters of the normal coordinates, we can in a straight-forward fashion calculate the base shear force statistics. The expectation of the base shear force for mode j is

$$\mu_{Q_j}(t) = 0 \qquad (6\text{-}67)$$

The mean-square function of $Q_j(t)$ is

$$\sigma^2_{Q_j}(t) = \delta_j^2 \, \omega_j^4 \, \sigma^2_{U_j}(t) \tag{6-68}$$

Using the expression for $\sigma^2_{U_j}(t)$, we obtain

$$\sigma^2_{Q_j}(t) = \beta \, \delta_j^4 \, \omega_j^4 \, I_j(t) \tag{6-69}$$

where $I_j(t)$ is given by Equation (6-40).

It must be recognized, however, that the above discussion gives the base shear for each mode in the structure. The total base shear force at any time may be obtained by adding the modal contributions at that time; thus, the total response history is given by the sum of the modal response, namely

$$Q_T(t) = \sum_{j=1}^{N} Q_j(t) \tag{6-70}$$

Thus, the mean-square function of the total base shear force is obtained

$$\sigma^2_{Q_T}(t) = \sum_{i=1}^{N} \sum_{j=1}^{N} R_{Q_i Q_j}(t) \tag{6-71}$$

By use of Equation (6-66), we have

$$\sigma^2_{Q_T}(t) = \sum_{i=1}^{N} \sum_{j=1}^{N} \delta_i \, \delta_j \, \omega_i^2 \, \omega_j^2 \, R_{U_i U_j}(t) \tag{6-72}$$

For a structure with a small damping ratio, we can simplify the above expression to

$$\sigma^2_{Q_T}(t) = \sum_{j=1}^{N} \delta_j^2 \omega_j^4 \sigma^2_{U_j}(t) \tag{6-73}$$

This equation can also be written in the following form:

$$\sigma^2_{Q_T}(t) = \beta \sum_{j=1}^{N} \delta_j^4 \omega_j^4 I_j(t) \tag{6-74}$$

where $I_j(t)$ is given by Equation (6-40).

So far, we have established the response statistics, such as the mean-square response of the relative displacement, the mean-square response of the story shear force, the mean-square response of the total base shear force, the probability of the response exceeding an inadmissible amount, etc., of a linear lumped multi-story shear building to earthquakes which are simulated by nonstationary modulated Gaussian random processes. We shall present examples in representing tall buildings to obtain some numerical results in the following chapter.

CHAPTER VII

NUMERICAL EXAMPLES

The dynamic response analysis of a multi-story building structure subjected to earthquakes is presented in the preceeding chapter. In the following, two six-story shear buildings with equal column heights are considered. In structure I, the k_j's are assumed to be constant throughout the structure, while in structure II, as proposed by Penzien [40], the k_j's are chosen such that the fundamental mode of vibration is of an inverted triangle shape. These two structures with different stiffness ratios are chosen because the effect of stiffness on their response can be examined. The values of k_j/k_1 and m_j/m_1 are listed in Table 6. Thus, the corresponding mass matrix, stiffness matrix and damping matrix for structure I are

$$[M]_I = \begin{bmatrix} 1 & 0 & 0 & 0 & 0 & 0 \\ 0 & 1 & 0 & 0 & 0 & 0 \\ 0 & 0 & 1 & 0 & 0 & 0 \\ 0 & 0 & 0 & 1 & 0 & 0 \\ 0 & 0 & 0 & 0 & 1 & 0 \\ 0 & 0 & 0 & 0 & 0 & 1 \end{bmatrix} m_1$$

$$[K]_I = \begin{bmatrix} 2 & -1 & 0 & 0 & 0 & 0 \\ -1 & 2 & -1 & 0 & 0 & 0 \\ 0 & -1 & 2 & -1 & 0 & 0 \\ 0 & 0 & -1 & 2 & -1 & 0 \\ 0 & 0 & 0 & -1 & 2 & -1 \\ 0 & 0 & 0 & 0 & -1 & 1 \end{bmatrix} k_1$$

and

$$[C]_I = \begin{bmatrix} 1 & 0 & 0 & 0 & 0 & 0 \\ 0 & 1 & 0 & 0 & 0 & 0 \\ 0 & 0 & 1 & 0 & 0 & 0 \\ 0 & 0 & 0 & 1 & 0 & 0 \\ 0 & 0 & 0 & 0 & 1 & 0 \\ 0 & 0 & 0 & 0 & 0 & 1 \end{bmatrix} c_1$$

respectively.

Similarly, for structure II

$$[M]_{II} = [M]_I$$

$$[K]_{II} = \begin{bmatrix} 41 & -20 & 0 & 0 & 0 & 0 \\ -20 & 38 & -18 & 0 & 0 & 0 \\ 0 & -18 & 33 & -15 & 0 & 0 \\ 0 & 0 & -15 & 26 & -11 & 0 \\ 0 & 0 & 0 & -11 & 17 & -6 \\ 0 & 0 & 0 & 0 & -6 & 6 \end{bmatrix} k_1/21$$

and

$$[\,C\,]_{II} = [\,C\,]_{I}$$

The corresponding eigenvalues and eigenvectors are computed. The ratios ω_j/ω_1 are listed in Table 7, and the mode shapes are sketched in Figures 35 and 36. The normal modal matrices can be obtained from Equations (5-11) and (5-16) and are listed in Table 8. Table 9 lists the modal participation factors δ_j for both structures.

In all cases, the period of the fundamental mode of vibration is considered to be 2.0 seconds. This is equivalent to saying that ω_1 is equal to π/second or 0.5 cps. The damping ratio for the fundamental mode is chosen to be 0.10. The corresponding damping factors for higher modes are listed in Table 10.

For the earthquake ground motion, ensembles I and II are used for our analysis. Computer programs are written to carry out the computations for response statistics. The following results are obtained:

1. The mean-square response of the relative displacement $Y_j(t)$ of the structures is computed using Equation (6-38). Table 11 lists mean-square values of the relative displacement of the top floor $Y_6(t)$ of the structures with $\gamma = 0.0$ and $\gamma = 0.05$. These numerical results show that the introduction of structural damping produces a reduction in the response.

2. Figures 37 through 40 show the time histories of the mean-square response of the relative displacements of structure I and structure II subjected to inputs I and II. It is noted that each floor

reaches its maximum response nearly at the same time. Also we note that the time at which the mean-square response reaches its maximum is just a few seconds behind the time at which the mean-square of the input reaches the maximum.

3. The mean-square response of story shear forces $V_j(t)$ are computed by means of Equation (6-57). Figures 41 through 44 show the mean-square response of story shear forces of structures I and II to earthquake inputs I and II. These curves show the interesting result that the mean-square function of story shear force has its maximum at the second story for structure I, and at the first story for structure II regardless of the input. This result is due to the difference in stiffness distribution of structures I and II.

4. Figures 45 and 46 illustrate the mean-square response of the total base shear force $Q_T(t)$. It is noted that structure I has to resist larger total base shear force than structure II regardless of the input.

5. The probability density function of the response can be computed by knowing the corresponding mean-square values. It is evidently a time dependent quantity. Figure 47 illustrates the probability density functions of the relative displacements of structure I to input I at the time at which the mean-square response reaches its maximum. It is observed that the probability density near the mean is larger for the first story than for any other story. The same conclusion actually holds also for structure II.

6. The probability density functions of the relative displacement at the top story of structure I to input I for different times are

plotted in Figure 48. These curves show that at t = 3 seconds, the probability is the smallest near the mean value.

7. The upper bounds of probability of relative displacements $Y_j(t)$ exceeding $y_j^{(D)}$ are shown in Figure 49. These curves show that they are time dependent and vary from story to story. Similar conclusion can be made for structure II.

CHAPTER VIII

INVESTIGATION OF NONLINEAR STRUCTURES

Review of Existing Analysis Techniques

At the present time, there are three basic methods which can be used to treat the problem of the response of stochastically excited nonlinear structures [57,75]. These are the Fokker-Planck approach, the perturbation approach and the statistical linearization approach. In this section, some major advantages and limitations of these methods are reviewed. In the next section, the response of nonlinear building structures will be investigated by using these methods.

The Fokker-Planck approach is the only one, of these three methods, which gives an exact solution. However, some limitations currently placed on this analysis are:

1. The generalized excitations are uncorrelated white Gaussian processes.

2. Neither the generalized damping forces nor the generalized inertia forces are coupled.

3. The ratio of the spectral density of every generalized excitation to the corresponding generalized damping coefficient is the same constant.

Cauchey [56] showed that the stationary Fokker-Plancker equation can be solved and the first probability density function of the Markovian response process can be obtained under these assumptions.

In the perturbation approach, the solution is expanded in powers of a small nonlinearity parameter. Substituting the assumed solution form into the original equations of motion and equating coefficients of like powers of the nonlinearity parameter then yields a set of linear differential equations for the terms in the solution expansion. A first-order approximation is obtained by solving two linear systems. The first is the system which is obtained by setting all nonlinearities equal to zero, and the second is a system having an excitation which is a function of the solution of the first system. However, application of this approach can become quite complex due to the fact that the first-order correlation must be obtained from the solution of an equation with non-Gaussian excitation. The only important limitation on this approach is the requirement that the system to be analyzed must contain some finite amount of linear viscous dissipation so that the solution of the linearized equation will be bounded.

The technique of statistical linearization is based on the idea of replacing the nonlinear system by a related linear system in such a way that the difference between the two systems is minimized in some statistical sense.

We will use these approaches to investigate the feasibility of analyzing a nonlinear structural model subjected to the simulated nonstationary random process characterized by Equation (3-6).

Response Analysis of a Nonlinear Structural Model

The equation of motion of a single-degree-of-freedom nonlinear system subjected to earthquake excitation is governed by the differential

equation

$$m \ddot{Y} + c \dot{Y} + Q(Y) = P(t) \tag{8-1}$$

where

$$P(t) = - m \ddot{X}_g - c \dot{X}_g$$

in which X_g is the ground displacement.

Since $P(t)$ is a nonstationary Gaussian process specified by Equation (6-19) which is neither shot noise nor white noise, the Fokker-Planck approach cannot be applied to Equation (8-1). However, we shall use other alternative approaches, namely, the perturbation method and the statistical linearization approach to analyze the problem.

Perturbation Approach

Assume the nonlinear term is governed by a Duffing type of nonlinearity and the governing equation can be transform into the form

$$\ddot{Y} + 2\xi \omega_o \dot{Y} + \omega_o^2(Y + \epsilon Y^3) = F(t) \tag{8-2}$$

where

$$F(t) = P(t)/m$$

$$= - \ddot{X}_g - 2\xi \omega_o \dot{X}_g \tag{8-3}$$

and where ϵ is a parameter which is sufficiently small that the perturbation scheme is applicable.

Assume that the solution may be expressed as a power series in ϵ. That is,

$$Y(t) = Y_o(t) + \epsilon\, Y_1(t) + \epsilon^2\, Y_2(t) + \cdots . \tag{8-4}$$

Substituting Equation (8-4) into Equation (8-2) and grouping terms having the same power of ϵ leads to a set of linear equations for Y_o, Y_1, Y_2, ...

$$\ddot{Y}_o + 2\xi\omega_o\dot{Y}_o + \omega_o^2 Y_o = F(t) \tag{8-5}$$

$$\ddot{Y}_1 + 2\xi\omega_o\dot{Y}_1 + \omega_o^2 Y_1 = -\,\omega_o^2 Y_o^3 \tag{8-6}$$

The solution of $Y_o(t)$ can be expressed as

$$Y_o(t) = \int_{-\infty}^{\infty} F(t-\tau)\, h(\tau)\, d\tau$$

or

$$Y_o(t) = \int_{o}^{t} F(\tau)\, h(t-\tau)\, d\tau \tag{8-7}$$

where $h(t)$ is the impulse response function corresponding to $\epsilon = 0$. Similarly, the solution of $Y_1(t)$ is

$$Y_1(t) = -\int_{o}^{t} \omega_o^2 Y_o^3(\tau)\, h(t-\tau)\, d\tau \tag{8-8}$$

Equation (8-7) will be used to compute various statistical properties of the response $Y(t)$.

The mean function of $Y(t)$ is obtained by taking the expectation of Equation (8-4). This is

$$E[Y(t)] = E[Y_o(t)] + \epsilon\, E[Y_1(t)] + \epsilon^2\, E[Y_2(t)] + \cdots \tag{8-9}$$

From Equations (3-37) and (6-9), we conclude that

$$E[F(t)] = 0 \tag{8-10}$$

Thus,

$$E[Y_o(t)] = 0 \tag{8-11}$$

The expectation of $Y_1(t)$ can be obtained from Equation (8-8)

$$E[Y_1(t)] = - \int_0^t \omega_o^2 \, E[Y_o^3(\tau)] \, h(t-\tau) \, d\tau \tag{8-12}$$

Substituting Equations (8-11) and (8-12) into Equation (8-9) and considering the first order solution in the perturbation approach, we obtain

$$E[Y(t)] = - \epsilon \int_0^t \omega_o^2 E[Y_o^3(\tau)] \, h(t-\tau) \, d\tau \tag{8-13}$$

Substituting Equation (8-7) into Equation (8-13), we have

$$E[Y(t)] = - \epsilon \, \omega_o^2 \int_0^t \int_0^\tau \int_0^\tau \int_0^\tau E[F(\tau_1) \, F(\tau_2) \, F(\tau_3)]$$

$$\times \, h(t-\tau) \, h(t-\tau_3) \, h(t-\tau_2) \, h(t-\tau_1) \, d\tau_1 \, d\tau_2 \, d\tau_3 \, d\tau \tag{8-14}$$

The autocorrelation of the response, computed to the first order of ϵ, is

$$E[Y(t_1) \, Y(t_2)] = E[Y_o(t_1) \, Y_o(t_2)] + \epsilon \, E[Y_o(t_1) \, Y_1(t_2)]$$

$$+ \epsilon \, E[Y_o(t_2) \, Y_1(t_1)] \tag{8-15}$$

Equation (8-15) can also be written in the following form:

$$R_Y(t_1,t_2) = R_{Y_o}(t_1,t_2) + \epsilon[R_{Y_oY_1}(t_1,t_2) + R_{Y_1Y_o}(t_1,t_2)] \quad (8\text{-}16)$$

Using Equations (8-7) and (8-8), we obtain

$$R_{Y_o}(t_1,t_2) = \int_0^{t_2}\int_0^{t_1} R_F(\tau_1,\tau_2)\, h(t_1-\tau_1)\, h(t_2-\tau_2)\, d\tau_1\, d\tau_2 \quad (8\text{-}17)$$

$$R_{Y_oY_1}(t_1,t_2) = -\omega_o^2 \int_0^{t_2}\int_0^{t_1} R_{F\,Y_o^3}(\tau_1,\tau_2)\, h(t_1-\tau_1)\, h(t_2-\tau_2)\, d\tau_1\, d\tau_2$$

$$= -\omega_o^2 \int_0^{t_2}\int_0^{t_1}\int_0^{\tau_2}\int_0^{\tau_2}\int_0^{\tau_2} E[F(\tau_1)\, F(\tau_3)\, F(\tau_4)\, F(\tau_5)]$$

$$\times\, h(t_1-\tau_1)\, h(t_2-\tau_2)\, h(\tau_2-\tau_3)\, h(\tau_2-\tau_4)\, h(\tau_2-\tau_5)$$

$$\times\, d\tau_5\, d\tau_4\, d\tau_3\, d\tau_2\, d\tau_1 \quad (8\text{-}18)$$

Similarly

$$R_{Y_1Y_o}(t_1,t_2) = -\omega_o^2 \int_0^{t_2}\int_0^{t_1}\int_0^{\tau_1}\int_0^{\tau_1}\int_0^{\tau_1} E[F(\tau_2)\, F(\tau_3)\, F(\tau_4)\, F(\tau_5)]$$

$$\times\, h(t_1-\tau_1)\, h(t_2-\tau_2)\, h(\tau_1-\tau_3)\, h(\tau_1-\tau_4)\, h(\tau_1-\tau_5)$$

$$\times\, d\tau_3\, d\tau_4\, d\tau_5\, d\tau_1\, d\tau_2 \quad (8\text{-}19)$$

Although the mean function and the correlation function of $Y(t)$ can be written in integral expressions, the calculation is obviously tedious. Therefore, using the perturbation approach to solve nonlinear structures subjected to the simulated random process is still not practical. We shall try to investigate the feasibility of the statistical linearization approach to this kind of problem.

Statistical Linearization Approach

A nonlinear system which is characterized by a Duffing type of nonlinearity has equation of motion

$$m \ddot{Y} + c \dot{Y} + k(Y + \epsilon Y^3) = P(t) \tag{8-20}$$

where

$$P(t) = - m \ddot{X}_g - c \dot{X}_g$$

In order to obtain an approximate solution of Equation (8-20), let us consider an auxiliary system which is described by a linear differential equation of the form

$$m \ddot{Y} + c \dot{Y} + k_e Y = P(t) \tag{8-21}$$

The error of linearization, a random process, is

$$\Delta = k(Y + \epsilon Y^3) - k_e Y \tag{8-22}$$

which is the difference between Equations (8-21) and (8-20). We have to minimize the error in the mean-square sense. This requires that

$$\frac{\partial}{\partial k_e} E [\Delta^2] = 0 \tag{8-23}$$

Substituting Equation (8-22) into (8-23) and interchanging the order of differentiation and expectation, we obtain

$$E[k(Y + \epsilon Y^3)Y] - k_e E[Y^2] = 0 \tag{8-24}$$

Solving for the equivalent stiffness k_e, we find

$$k_e = \frac{k E[Y^2(t) + \epsilon Y^4(t)]}{E[Y^2(t)]}$$

$$= k \left\{ 1 + \epsilon \frac{E[Y^4(t)]}{E[Y^2(t)]} \right\} \tag{8-25}$$

Let

$$\bar{N}(t) = \frac{E[Y^4(t)]}{E[Y^2(t)]}$$

then,

$$k_e = k [1 + \epsilon \bar{N}(t)] \tag{8-26}$$

At this stage, it is understood from literature that if $P(t)$ is a Gaussian white noise, $\bar{N}(t)$ will be independent of time and

$$\bar{N}(t) = 3\sigma_Y^2$$

where σ_Y^2 is the mean-square value obtained from Equation (8-21). In this case, the equation of motion becomes

$$\ddot{Y} + 2\xi \omega_o \dot{Y} + \omega_o^2(1 + \epsilon \bar{N})Y = P(t)/m \tag{8-27}$$

The stochastic properties of the response can be obtained from linear theory. However, in our problem, $P(t)$ is a nonstationary random process as is $Y(t)$. Thus, the second and the fourth order moments are function of time. Therefore, the equation of motion becomes

$$\ddot{Y} + 2\xi\,\omega_o\dot{Y} + \omega_o^2[1 + \epsilon\,\bar{N}(t)]Y = -\ddot{X}_g - 2\xi\,\omega_o\,\dot{X}_g \qquad (8\text{-}28)$$

This is the Hill-type [76] stochastic differential equation. The solution has not been available yet.

Obviously, multi-degree-of-freedom nonlinear systems are essentially more complicated than one-degree-of-freedom systems. So long as the difficulties pointed out in this investigation for one-degree-of-freedom systems have been solved, the response analyses of multi-degree-of-freedom systems will become meaningful.

CHAPTER IX

CONCLUSIONS AND RECOMMENDATIONS

Conclusions

The main conclusions of the present investigation are:

1. Earthquake ground motion can be represented by a nonstationary modulated Gaussian random process in which the stationary random process is expressed directly in terms of random functions.

2. The probability density function of the random frequencies of earthquake acceleration is obtainable from the autocorrelation function of ground acceleration.

3. The parameters of the simulation earthquake acceleration model can be determined statistically from the past earthquake records.

4. The simulation random process satisfies Levy's criteria for simulation processes. Thus, it is a suitable stochastic model for representing earthquake accelerations.

5. The normal mode method is applicable to the tall building model in which the viscous damping force is proportional to the absolute velocity of the floor.

6. The forcing function for the multi-story building structure is a linear combination of ground acceleration and ground velocity. Thus, the correlations of ground acceleration and ground velocity are employed in the response analysis.

7. The responses, such as relative displacements, story shear

forces and total base shear forces, of the multi-story buildings under the simulated earthquake excitation are Gaussian random processes with zero mean. Thus, mean-square functions of the response specify such processes.

8. The mean-square response of a structure differs only a negligible amount for the following particular values: $\gamma = 0.00$, $\xi_1 = 0.10$; $\gamma = 0.05$, $\xi_1 = 0.10$. Generally, in a practical situation values of the viscous damping ratio would be encountered which would be less than 0.10. It can therefore be expected that the structural damping may not be negligible in many of these cases.

9. Those structures with equal stiffness ratios have to resist larger total base shear forces than those with the fundamental mode of vibration being of an inverted triangle shape.

10. The time at which the mean-square response reaches its maximum is just a few seconds behind the time at which the mean-square of the input reaches its maximum.

11. The maximum mean-square value of the story shear force varies from story to story for structures with different stiffness ratios.

12. The probability density functions of the response are obtainable from the corresponding mean-square values.

13. From the bound for the probability of the response $Z(t)$ exceeding an inadmissible amount $h\,\sigma_Z(t)$, we conclude that the smaller the ratio $\sigma_Z(t)/z^{(D)}$, the smaller the probability that $|Z(t)|$, at t, is in excess of $z^{(D)}$. Thus, in designing a structure, we had better choose $\sigma_Z(t)/z^{(D)}$ as small as possible for all significant t.

14. The Fokker-Planck approach fails when applied to nonlinear structures subjected to the simulated ground motion.

15. The response analysis of the Duffing-type nonlinear structure under the simulated input process becomes tedious in calculation when using perturbation techniques.

16. Using the statistical linearization technique to analyze the Duffing-type nonlinear structures subjected to the simulated earthquakes results in solving Hill-type stochastic differential equa-equations.

Recommendations

The following recommendations are made for the future work:

1. Response analyses of multi-story buildings subjected to three-dimensional ground motion.

2. Response analyses of structures, such as bridges, towers and dams subjected to the simulated earthquake excitation.

3. Response analyses of multi-story buildings which are modeled by combined translation and rotation of floors subjected to the simulated ground motion.

4. Obtaining response statistics of the Duffing-type nonlinear structures subjected to the simulated earthquake excitation.

In addition, the simulation procedures for the input process presented in this research can also be extended to any type of stochastic disturbance, such as wind loading on multi-story structures.

APPENDIX A

TABLES

Table 1. Characterization of Eight Past Earthquake Accelerations.

Record Number	Location and Date	Component	Duration (sec.)	Time to Abs. Max. (sec.)	Abs. Max. (g)
1	El Centro California May 19, 1940	NS	29.16	2.02	0.33
2	El Centro California May 19, 1940	EW	29.82	1.90	0.23
3	Taft California July 21, 1952	N21°E	30.23	6.58	0.17
4	Taft California July 21, 1952	S69°E	30.00	8.96	0.18
5	Olympia Washington April 29, 1965	S4°E	36.00	7.11	0.18
6	Olympia Washington April 29, 1965	S86°W	36.00	6.32	0.19
7	San Fernando California February 9, 1971	S74°W	25.72	8.25	1.27
8	San Fernando California February 9, 1971	S16°E	25.72	7.75	1.25

Table 2. Values of N_o and N_m of Eight Past Earthquake Accelerations.

Record Number	Number of Zero Crossings Per Second N_o	Number of Maximum Per Second N_m	$\lambda = \frac{N_o}{N_m}$
1	8.2	6.6	1.242
2	7.6	6.3	1.206
3	8.0	6.0	1.334
4	7.2	6.1	1.118
5	10.2	9.0	1.134
6	10.8	8.2	1.318
7	12.2	10.4	1.174
8	11.8	10.8	1.092

Table 3. Estimated Parameters α and b.

Record Number	N	t_1 (sec.)	t_2 (sec.)	b (g)	α ($sec.^{-1}$)
1	7	1.52	2.52	0.2564	0.495
2	6	1.40	2.40	0.1981	0.526
3	6	6.08	7.08	0.0427	0.152
4	6	8.46	9.46	0.0328	0.112
5	9	6.61	7.61	0.0373	0.141
6	8	5.82	6.82	0.0450	0.158
7	10	7.75	8.75	0.2190	0.121
8	11	7.25	8.25	0.2252	0.129

Table 4. Estimated Parameters μ_d and ω_d.

Record Number	τ' (sec.)	ω_d ($sec.^{-1}$)	μ_d ($sec.^{-1}$)
1	0.09	17.45	7.25
2	0.10	15.71	7.25
3	0.10	15.71	7.25
4	0.09	17.45	7.25

Table 5. Values Used for the Simulation of Earthquake Motion.

Pseudo-Earthquake Motion	Values for Parameters			
	b (0.1g)	α ($sec.^{-1}$)	ω_d ($sec.^{-1}$)	μ_d ($sec.^{-1}$)
Ensemble I	2.564	0.495	17.45	7.25
Ensemble II	0.427	0.152	15.71	7.25

Table 6. Mass Distribution, Spring Constants, and Damping Factors for Idealized Structures.

Floor (j)	m_j/m_1 and c_j/c_1	k_j/k_1	
		Structure I	Structure II
6	1	1	6/21
5	1	1	11/21
4	1	1	15/21
3	1	1	18/21
2	1	1	20/21
1	1	1	21/21

Table 7 Natural Frequencies of Vibration.

Mode Number (j)	ω_j/ω_1	
	Structure I	Structure II
1	1.00	1.00
2	2.94	2.45
3	4.71	3.87
4	6.22	5.29
5	7.35	6.71
6	8.09	8.12

Table 8. Normal Modes ($/\sqrt{m_1}$)

Mode Number	1	2	3	4	5	6
Structure I	0.118	0.369	-0.519	0.551	-0.457	0.258
	0.249	0.551	-0.369	-0.133	0.519	-0.457
	0.365	0.457	0.258	-0.519	-0.133	0.551
	0.459	0.133	0.551	0.258	-0.369	-0.519
	0.522	-0.258	0.133	0.457	0.551	0.369
	0.554	-0.519	-0.457	-0.369	-0.258	-0.133
Structure II	0.105	0.236	-0.359	0.465	-0.539	0.545
	0.209	0.414	-0.467	0.302	0.108	-0.681
	0.315	0.473	-0.197	-0.349	0.558	0.454
	0.420	0.355	0.323	-0.479	-0.575	-0.182
	0.524	0.000	0.593	0.563	0.233	0.044
	0.629	-0.651	-0.396	-0.154	-0.036	-0.004

Table 9. Modal Participation Factors ($\sqrt{m_1}$)

Mode Number	1	2	3	4	5	6
Structure I	2.267	0.733	-0.403	0.245	-0.147	0.069
Structure II	2.202	0.827	-0.503	0.348	-0.251	0.176

Table 10. Damping Factors of Vibration.

Mode Number	1	2	3	4	5	6
Structure I	0.100	0.034	0.021	0.016	0.014	0.012
Structure II	0.100	0.041	0.026	0.019	0.015	0.012

Table 11. Mean-Square Response of the Relative Displacement $Y_6(t)$ (Input I) ($ft^2 \times 10^{-3}$).

Time (sec.)	Structure I		Structure II	
	$\gamma = 0.00$	$\gamma = 0.05$	$\gamma = 0.00$	$\gamma = 0.05$
0	0.0000	0.0000	0.0000	0.0000
1	1.1631	1.1498	1.4146	1.3984
2	3.1196	3.0833	3.7941	3.7500
3	3.8810	3.8185	4.7201	4.6442
4	3.3962	3.3166	4.1306	4.0338
5	2.3995	2.3155	2.9183	2.8162
6	1.4411	1.3629	1.7527	1.6576
7	0.7389	0.6722	0.8786	0.8175
8	0.3047	0.2514	0.3705	0.3058

APPENDIX B

FIGURES

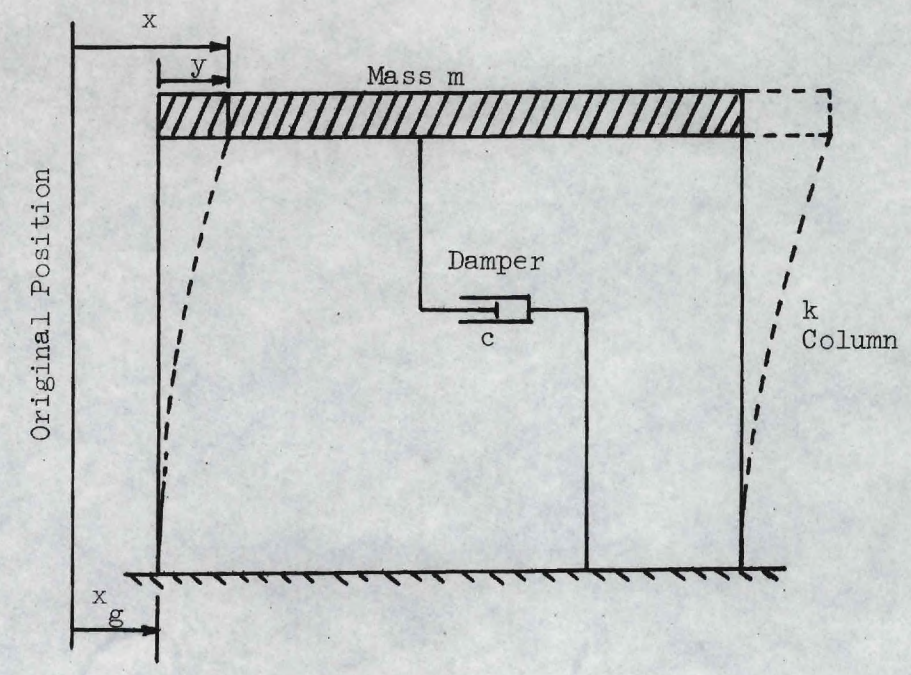

Figure 1. Schematic Representation of One-Story Flexible Structure.

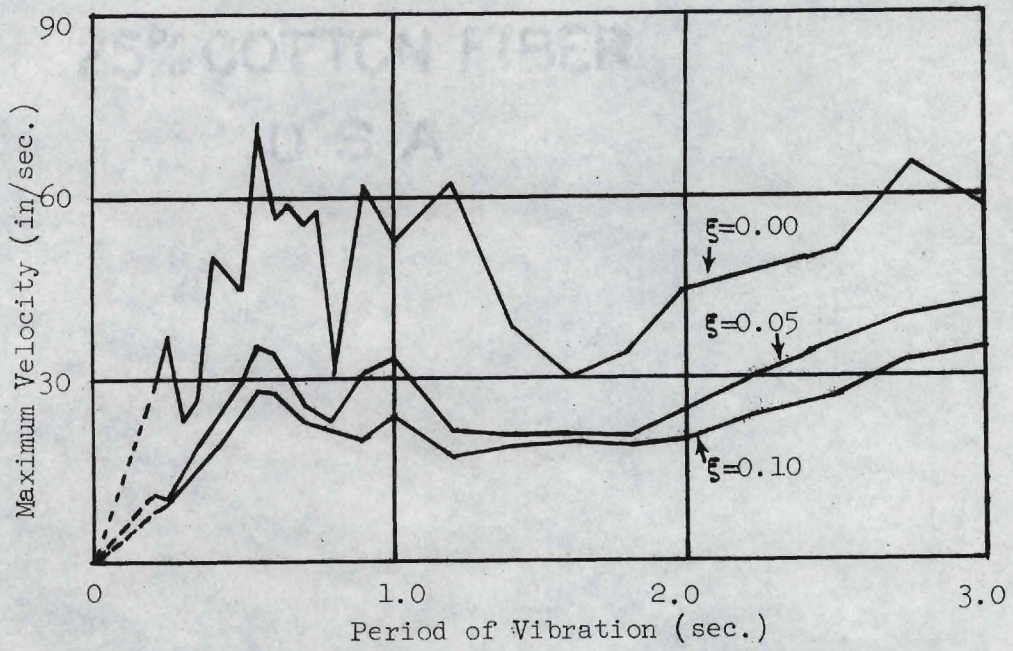

Figure 2. Velocity Response Spectrum for El Centro Earthquake of May 18, 1940 (N-S).

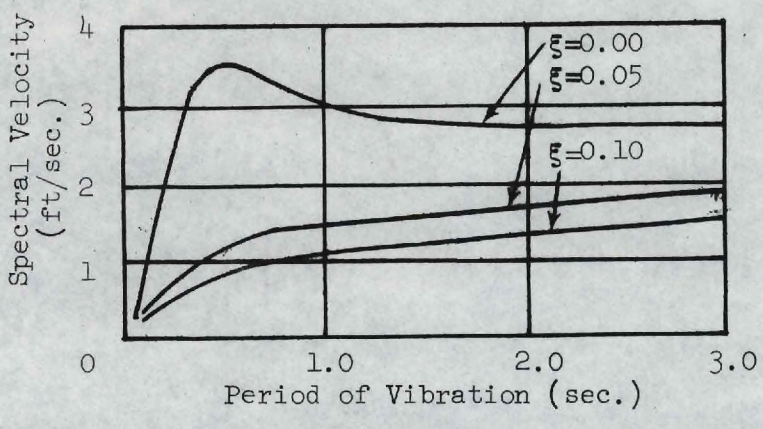

Figure 3. Average Velocity Response Spectrums, 1940 El Centro Intensity.

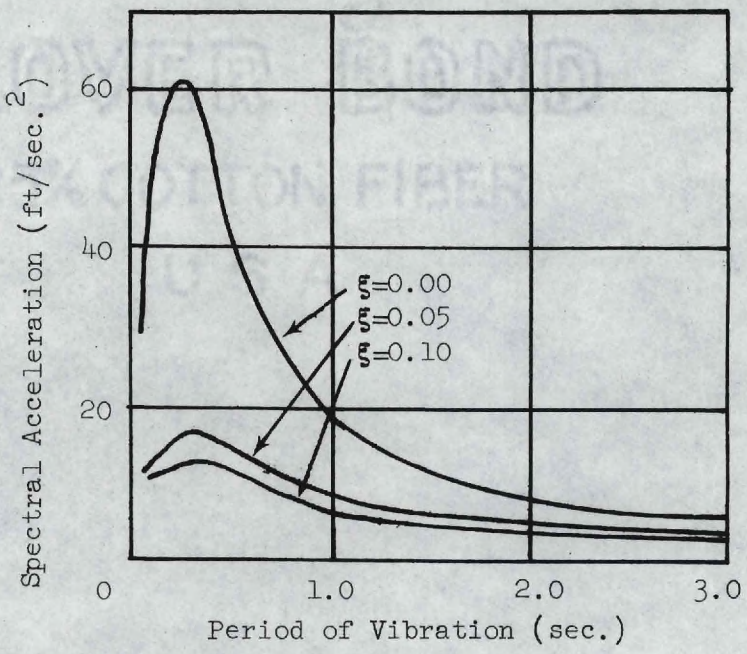

Figure 4. Average Acceleration Response Spectrums, 1940 El Centro Intensity.

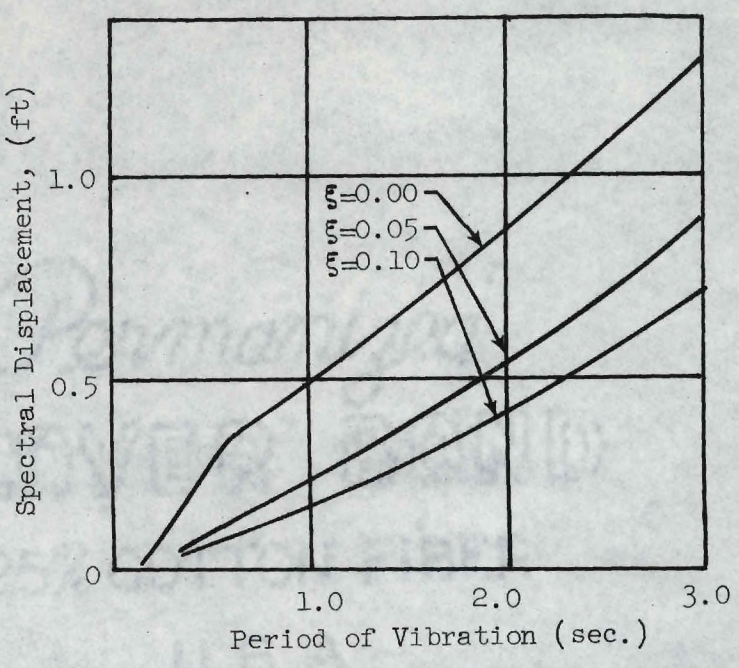

Figure 5. Average Displacement Response Spectrums, 1940 El Centro Intensity.

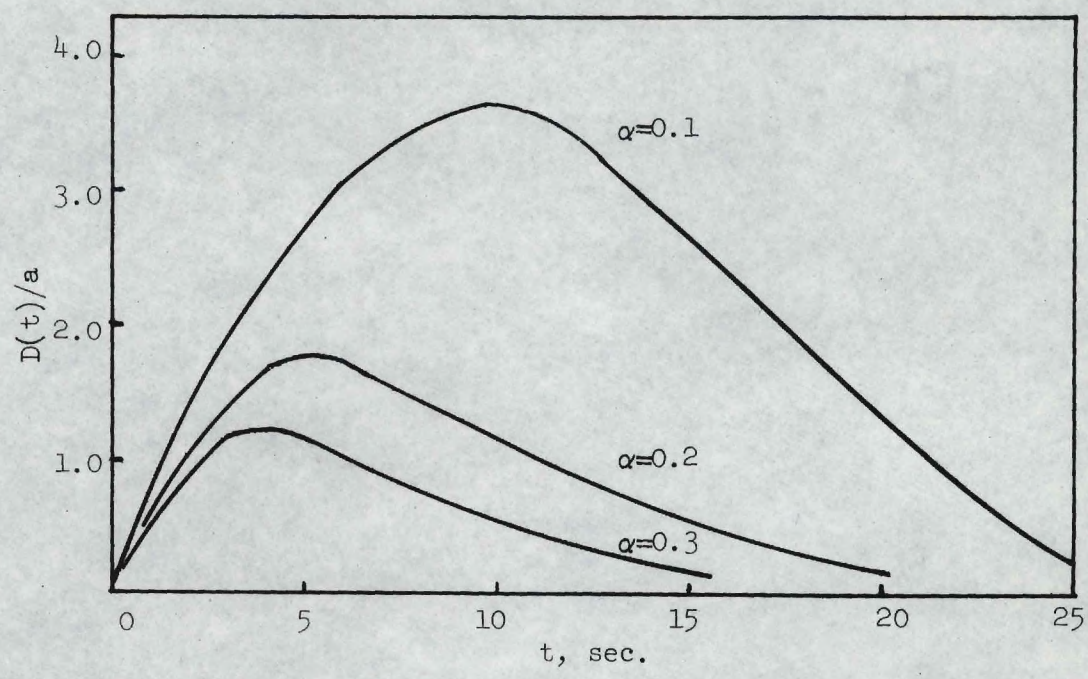

Figure 6. Envelope Functions of the Simulation Process.

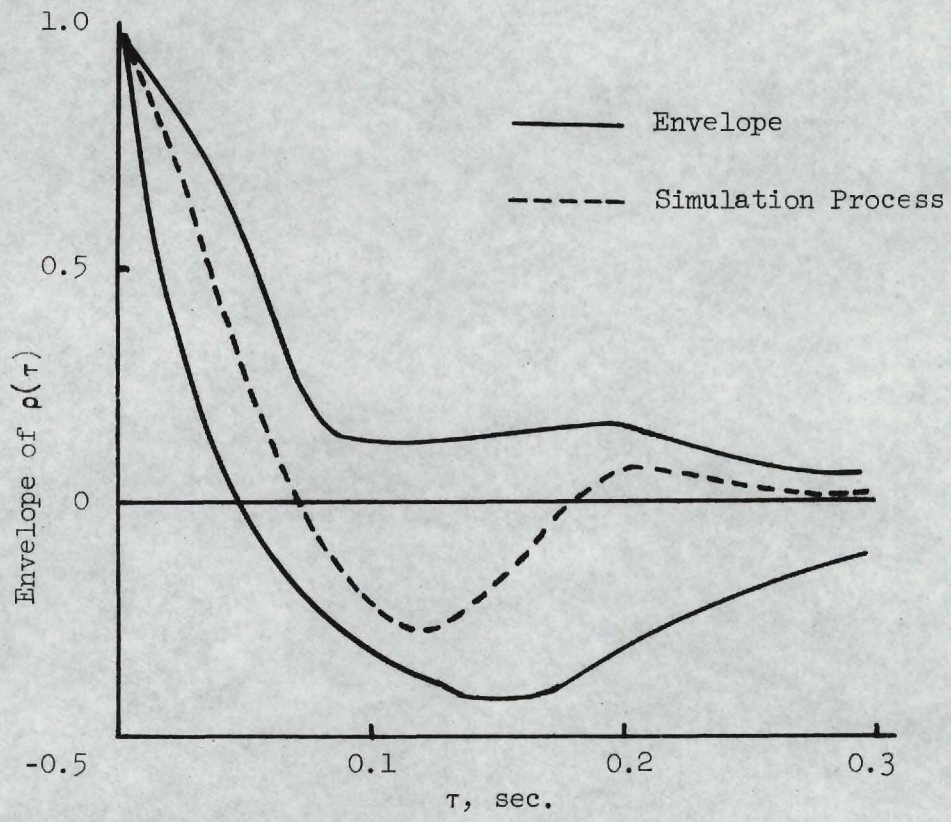

Figure 7. Envelope of Normalized Autocorrelation Functions.

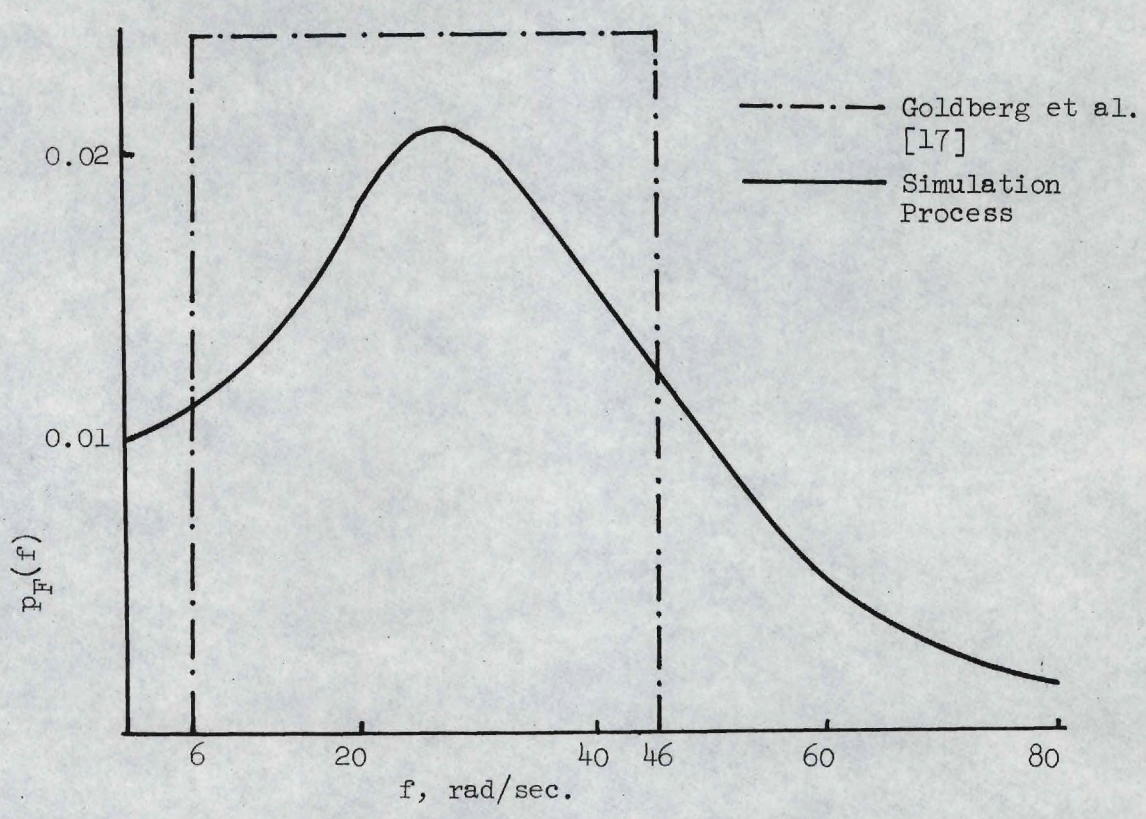

Figure 8. Probability Density Functions of the Random Variables F_j.

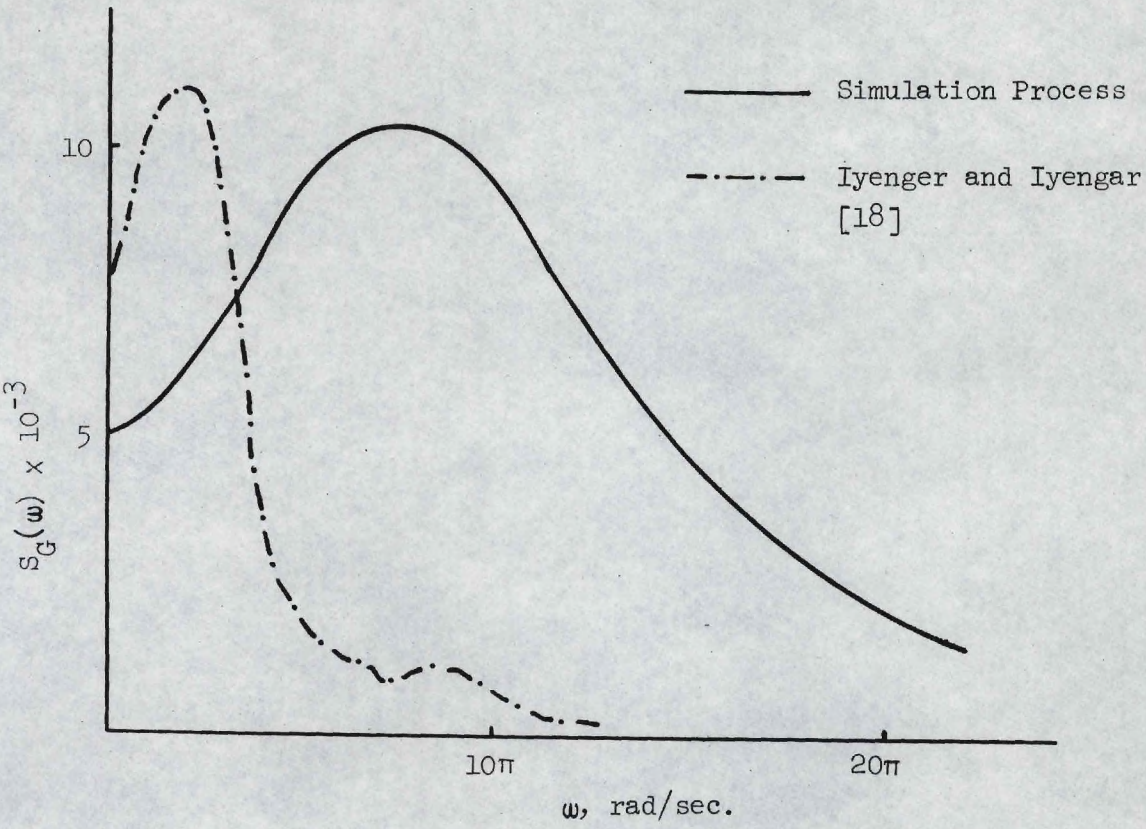

Figure 9. Power Spectral Density Functions of the Stationary Random Process G(t).

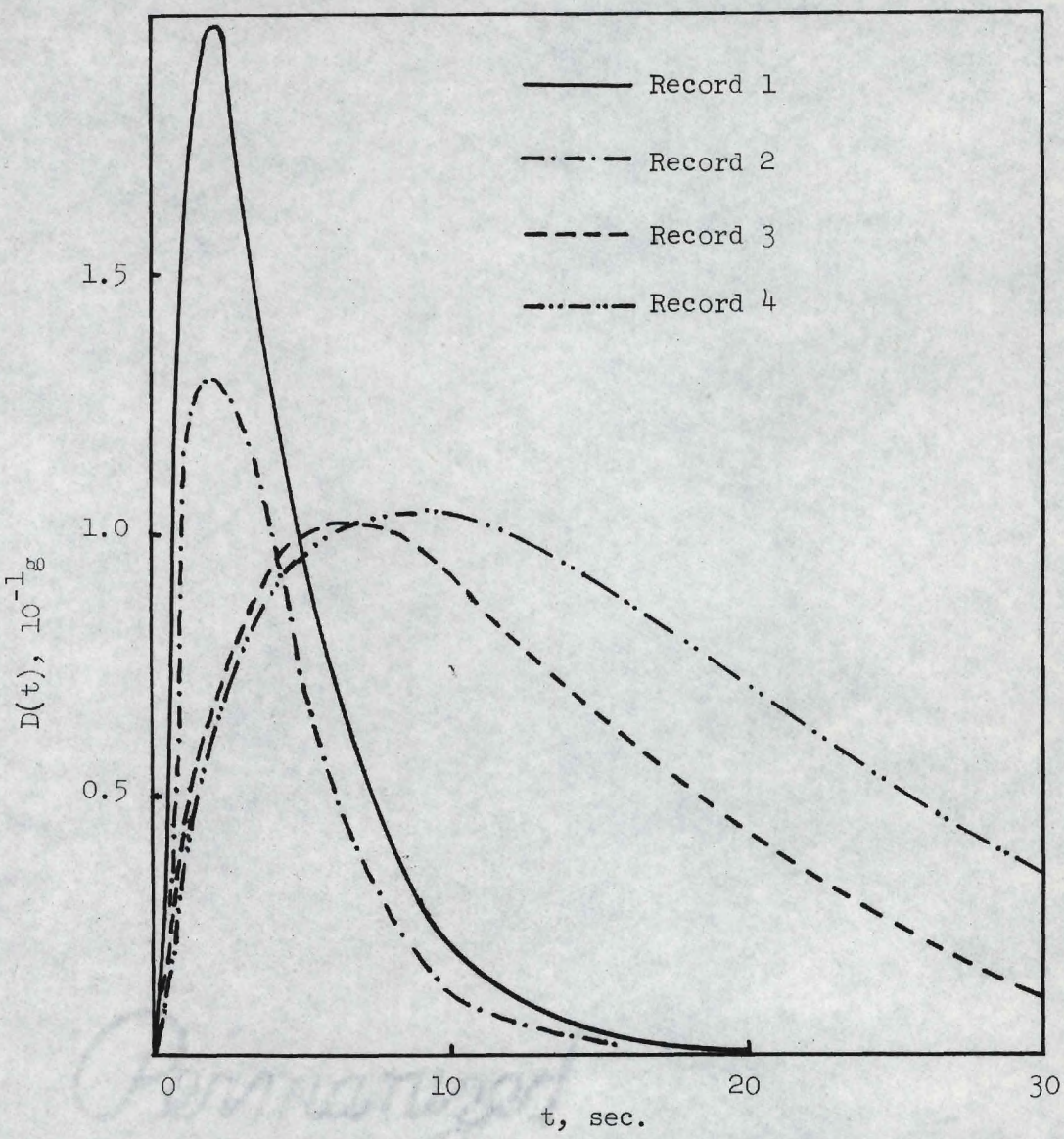

Figure 10. Envelope Functions (RMS) for Records One through Four.

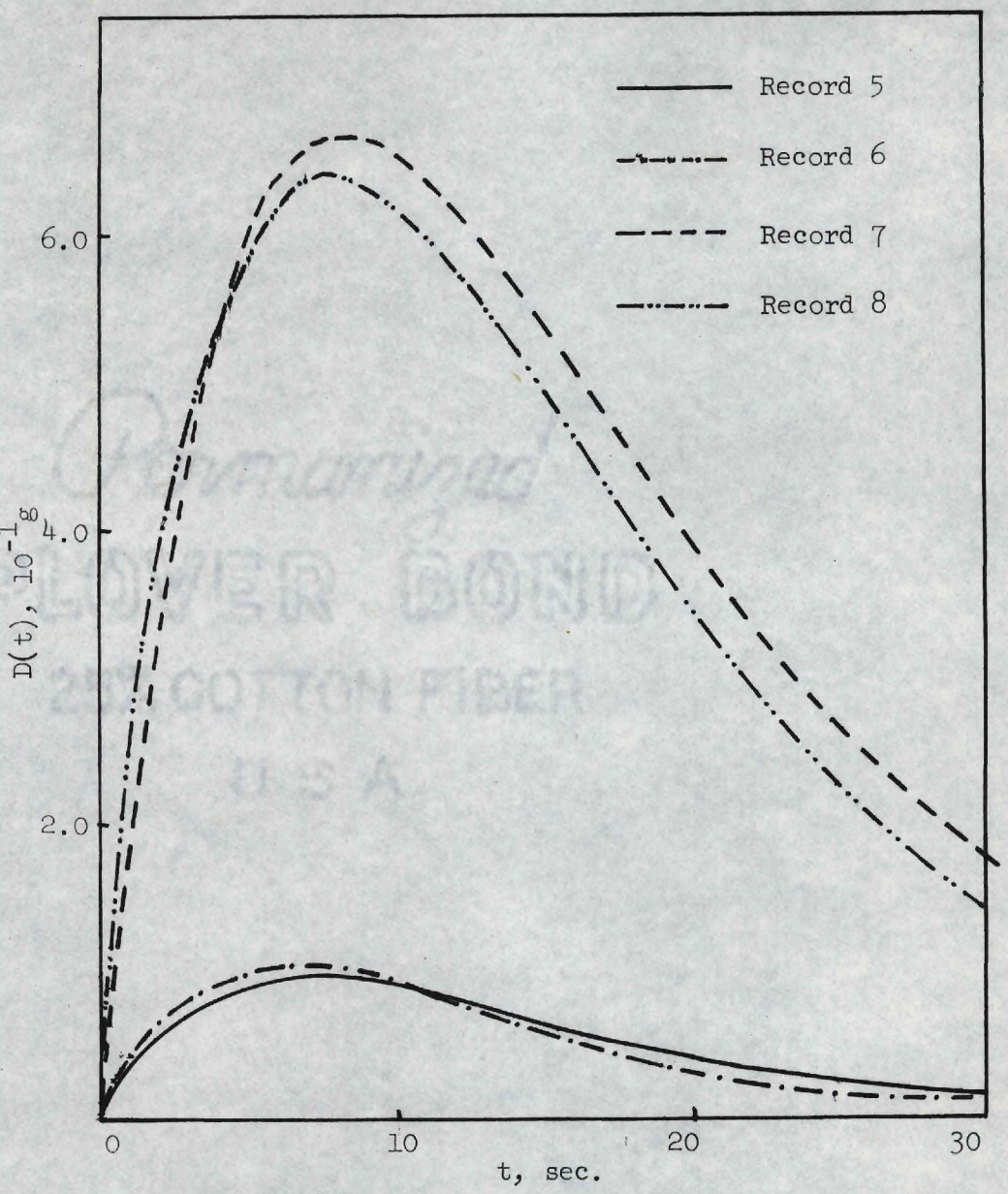

Figure 11. Envelope Functions (RMS) for Records Five through Eight.

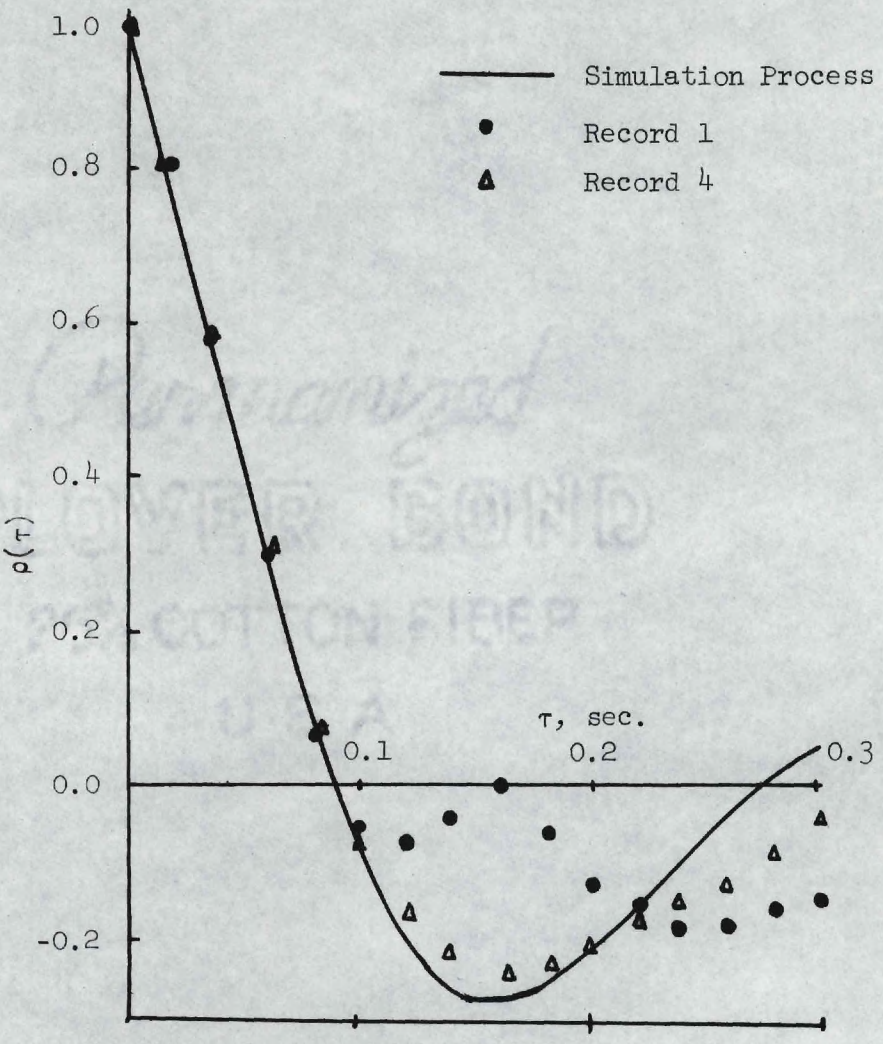

Figure 12. Normalized Autocorrelation Functions for Records One and Four.

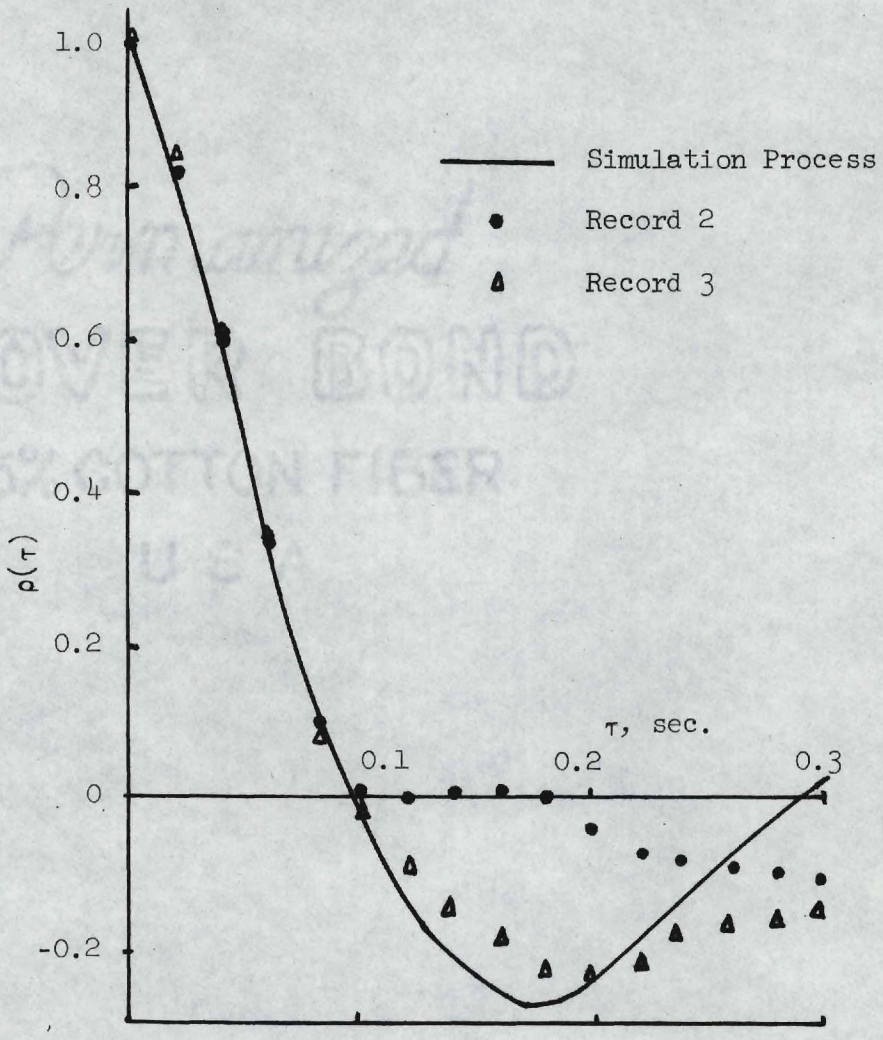

Figure 13. Normalized Autocorrelation Functions for Records Two and Three.

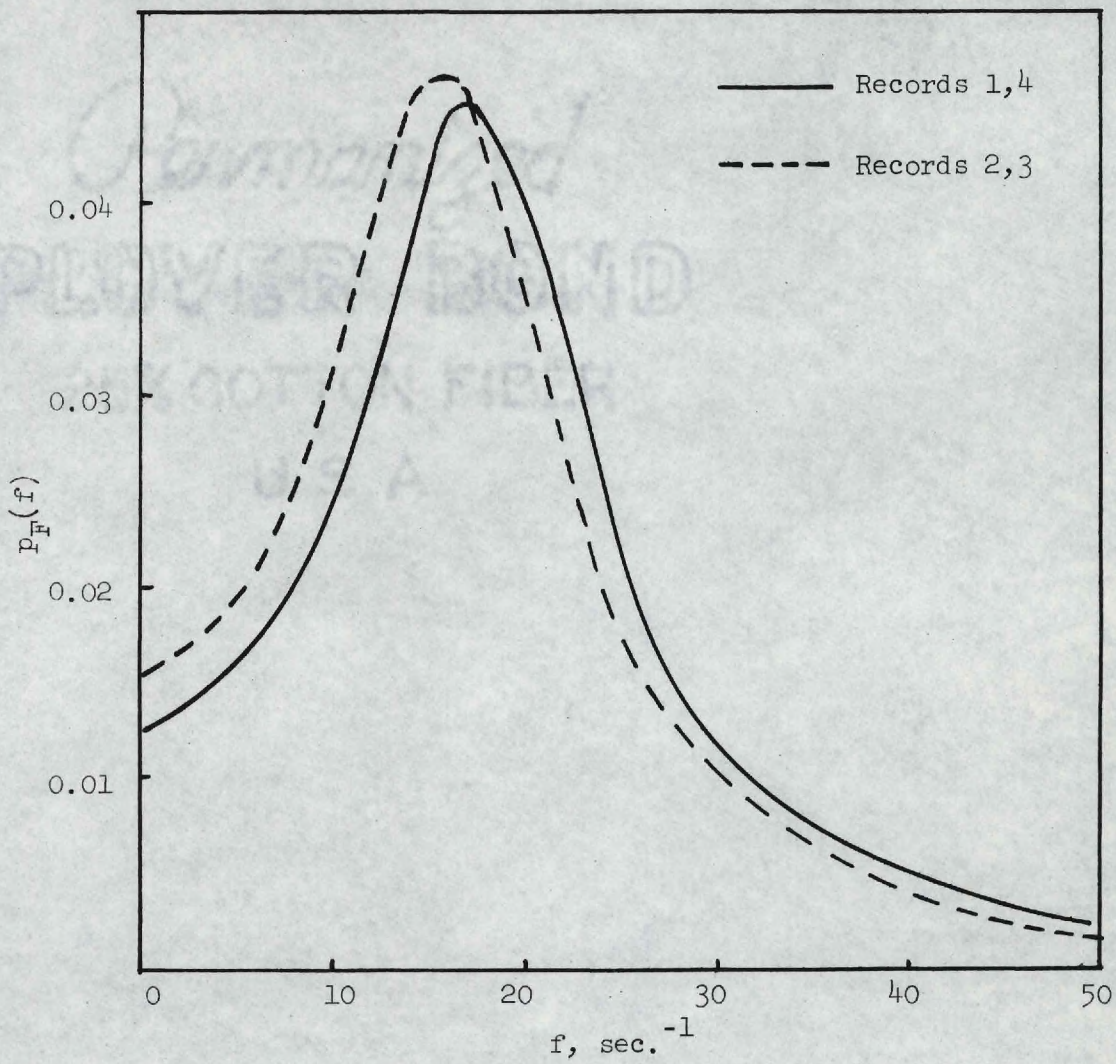

Figure 14. Probability Density Functions of the Random Variables F_j for Records One through Four.

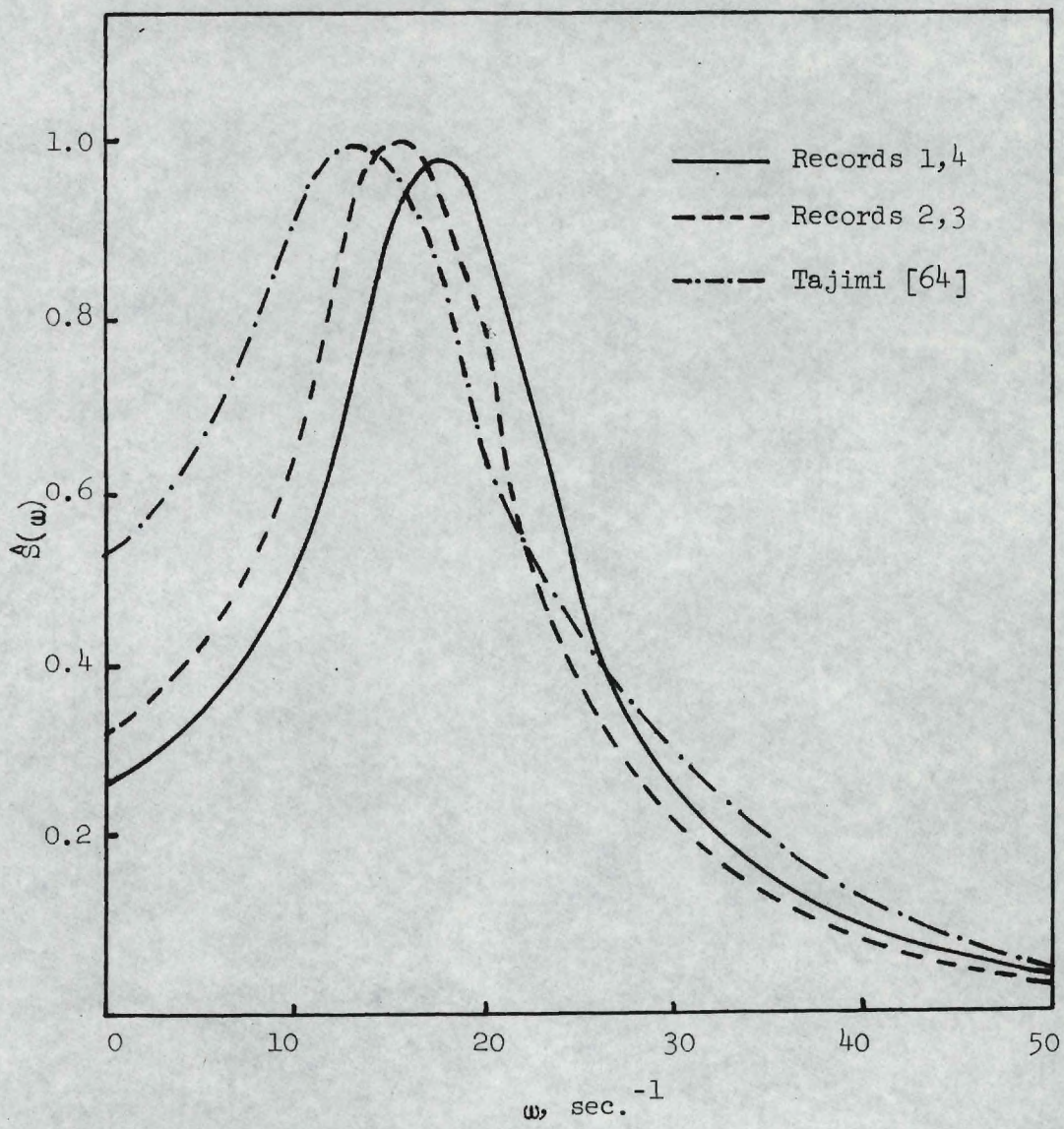

Figure 15. Normalized Spectral Densities of the Stationary Random Processes.

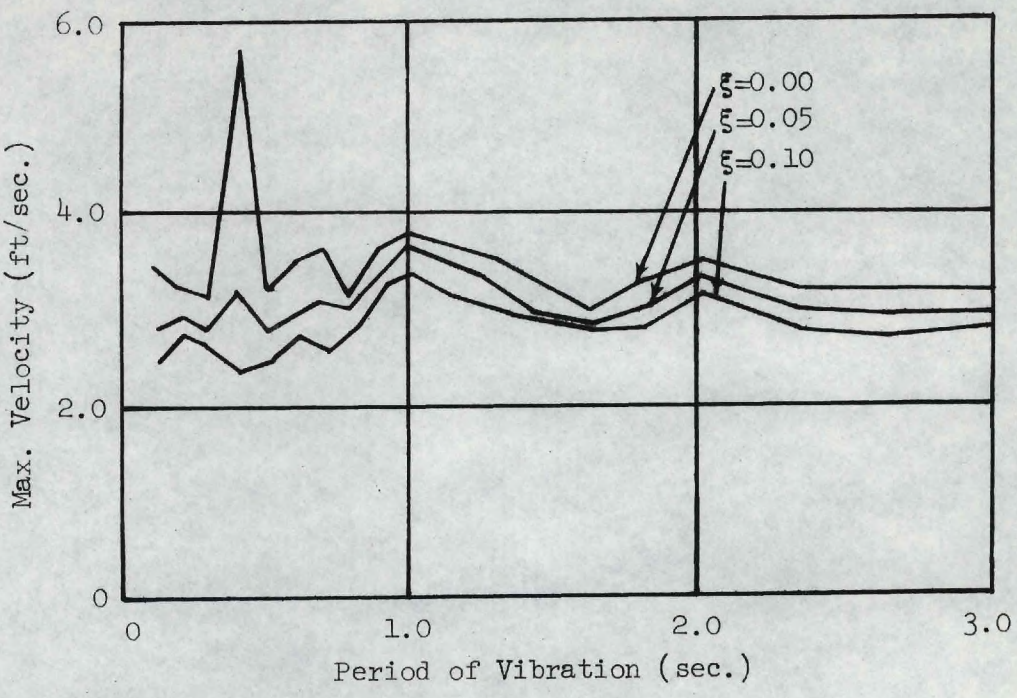

Figure 16. Velocity Response Spectra, Ensemble I, Sample 1.

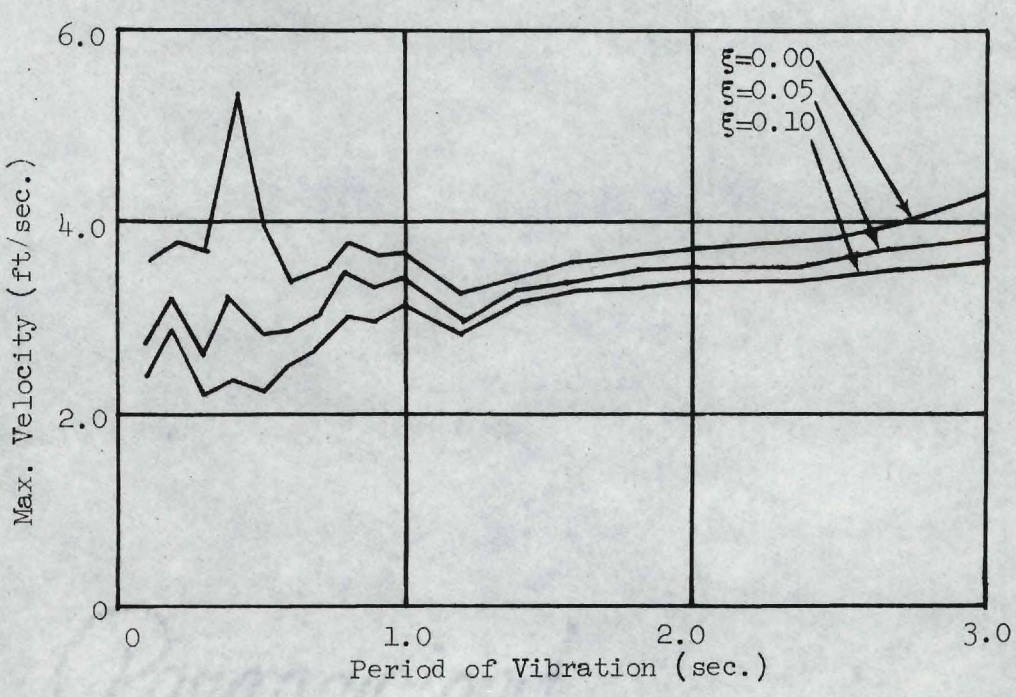

Figure 17. Velocity Response Spectra, Ensemble I, Sample 2.

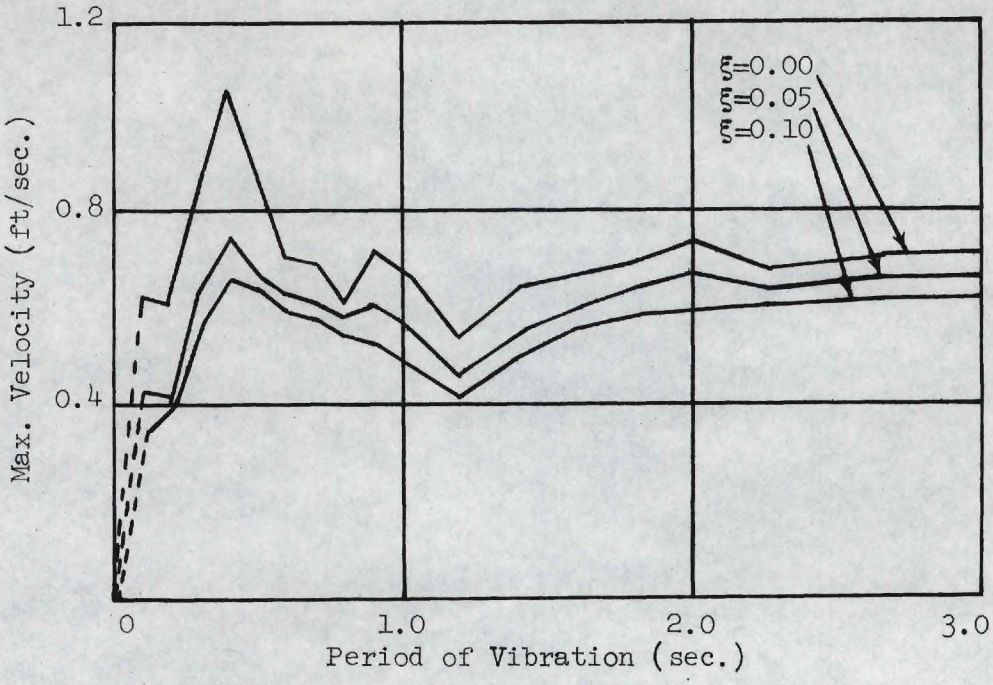

Figure 18. Velocity Response Spectra, Ensemble II, Sample 1.

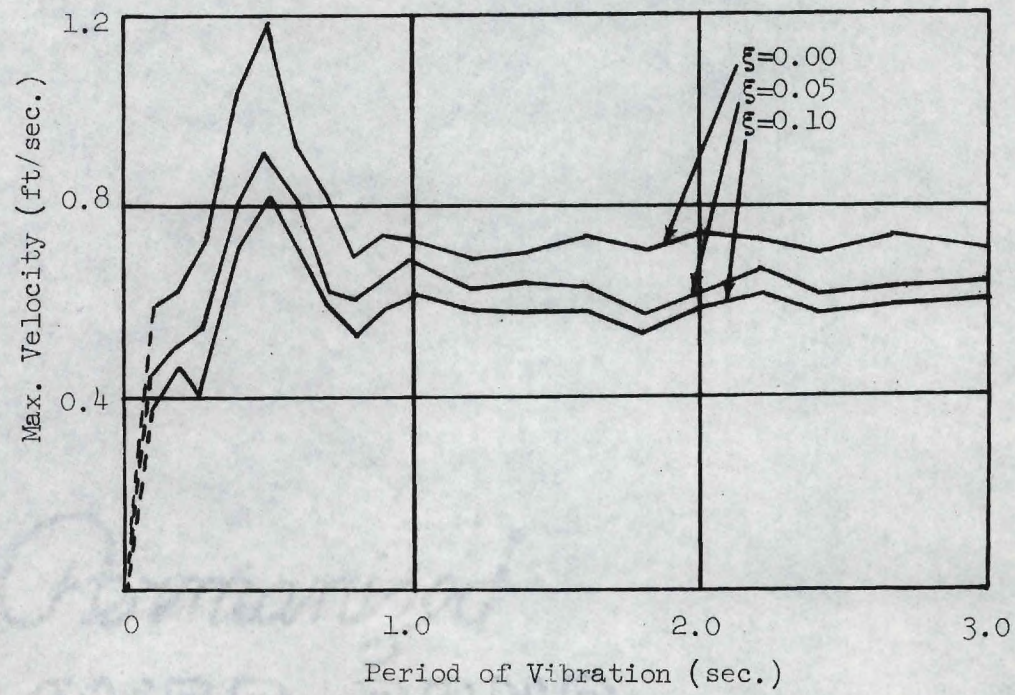

Figure 19. Velocity Response Spectra, Ensemble II, Sample 2.

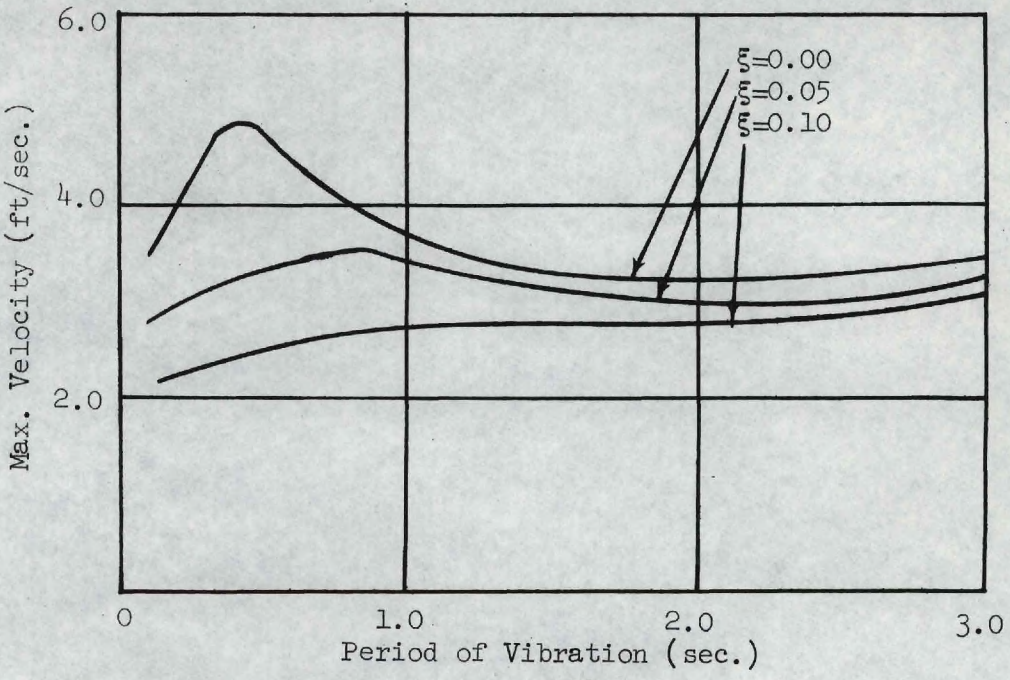

Figure 20. Average Velocity Response Spectra, Ensemble I.

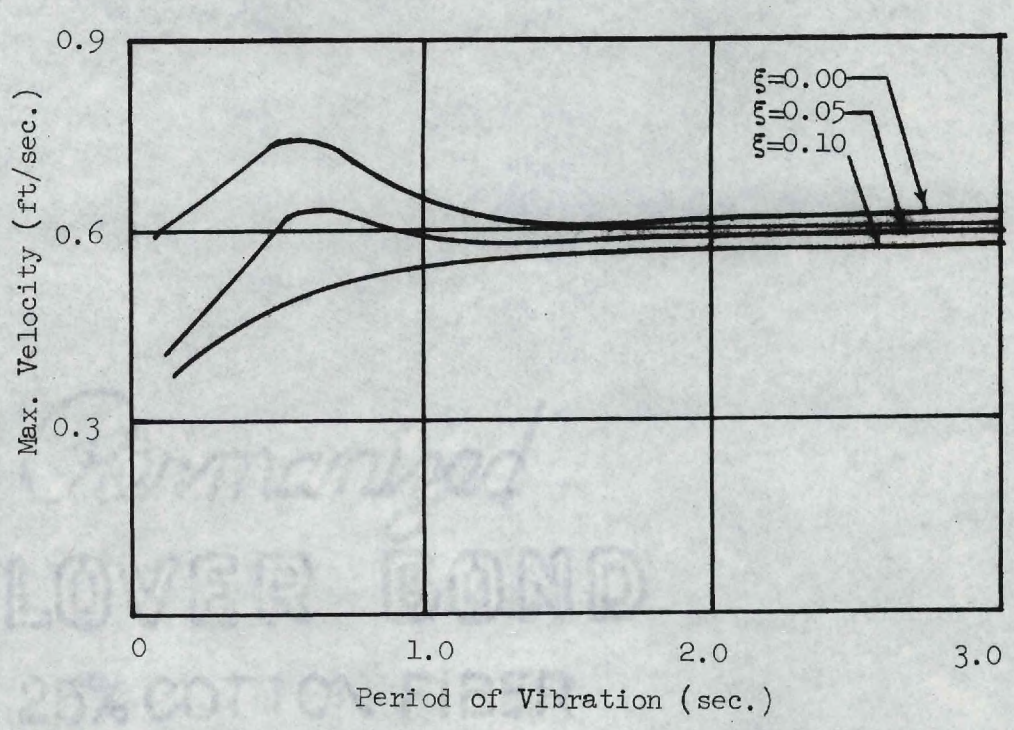

Figure 21. Average Velocity Response Spectra, Ensemble II.

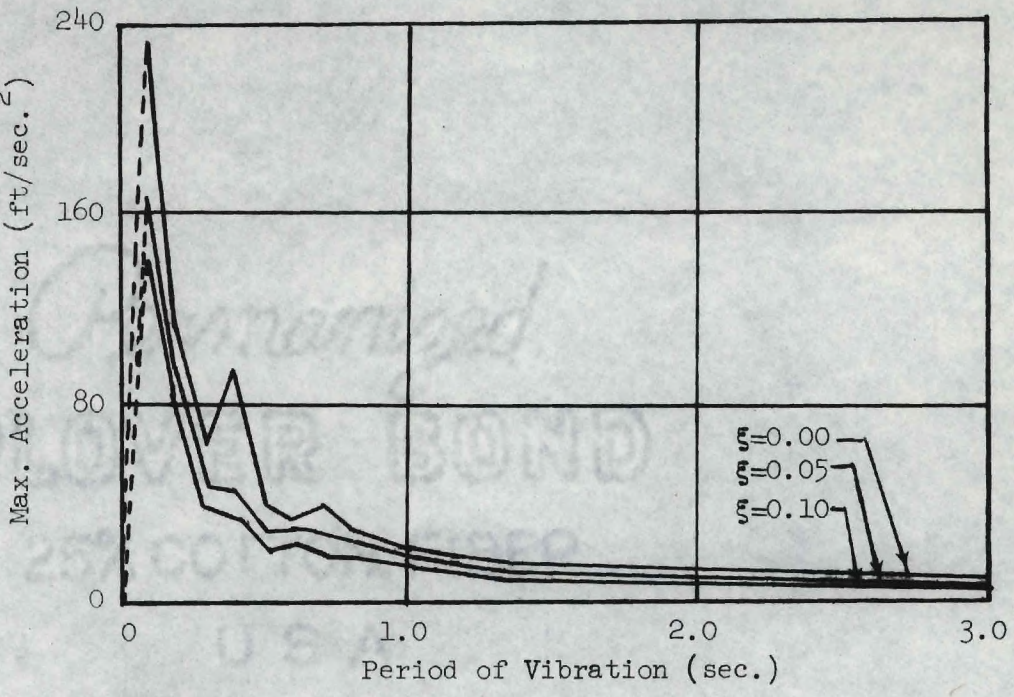

Figure 22. Acceleration Response Spectra, Ensemble I, Sample 1.

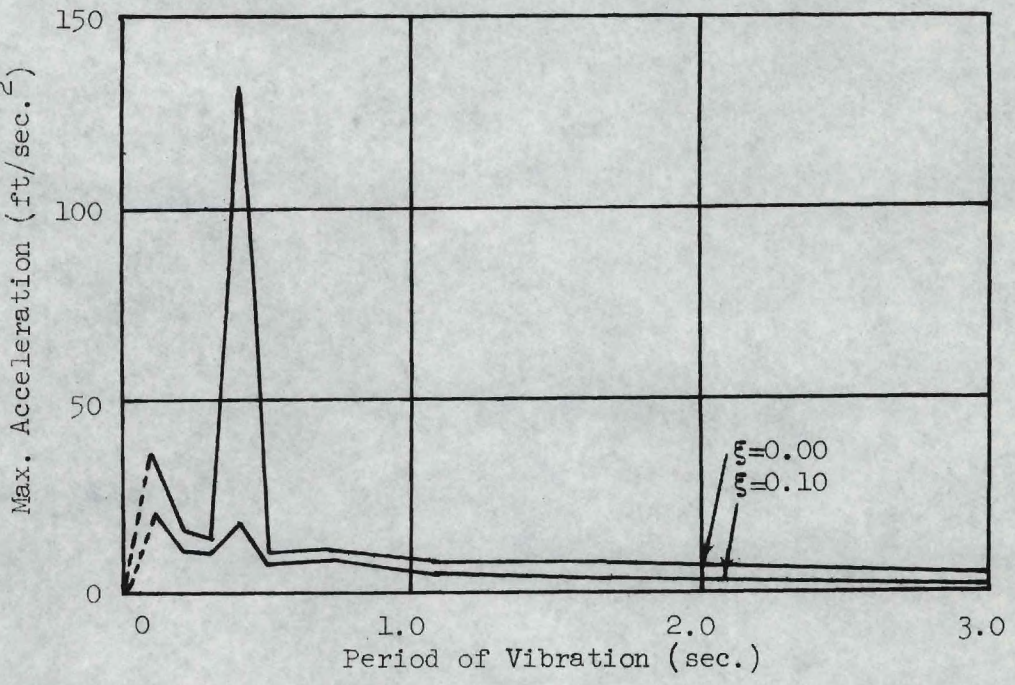

Figure 23. Acceleration Response Spectra, Ensemble II, Sample 1.

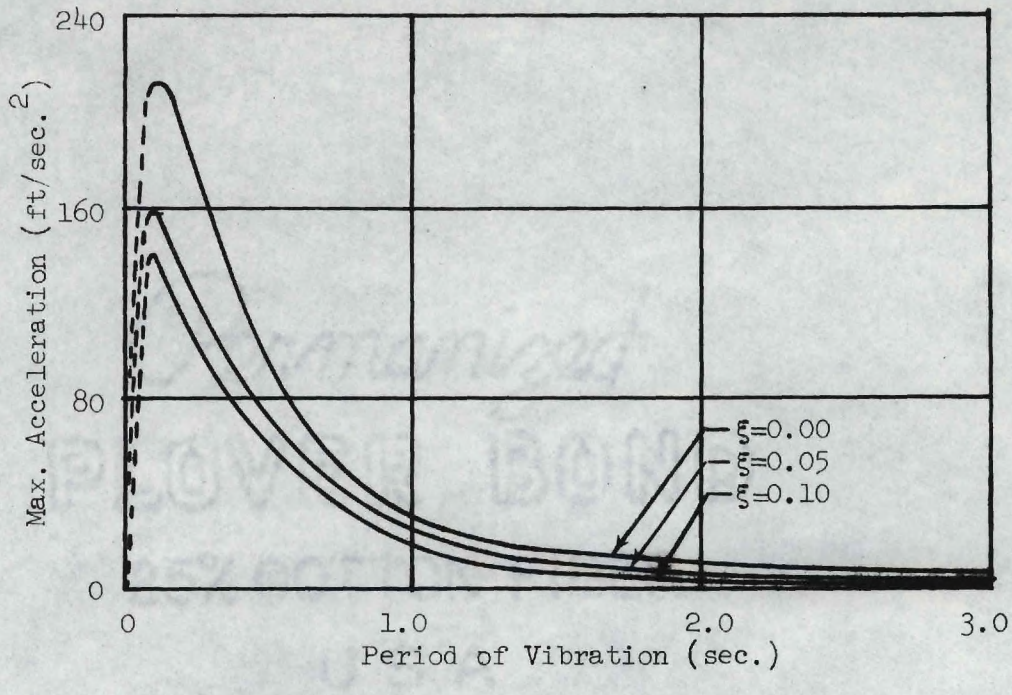

Figure 24. Average Acceleration Response Spectra, Ensemble I.

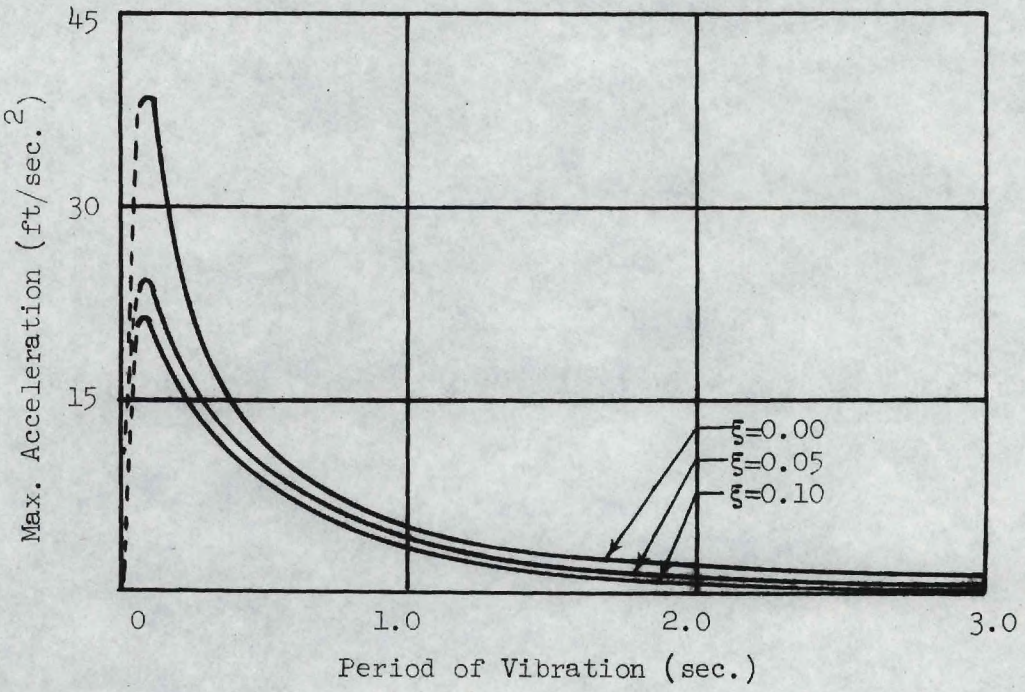

Figure 25. Average Acceleration Response Spectra, Ensemble II.

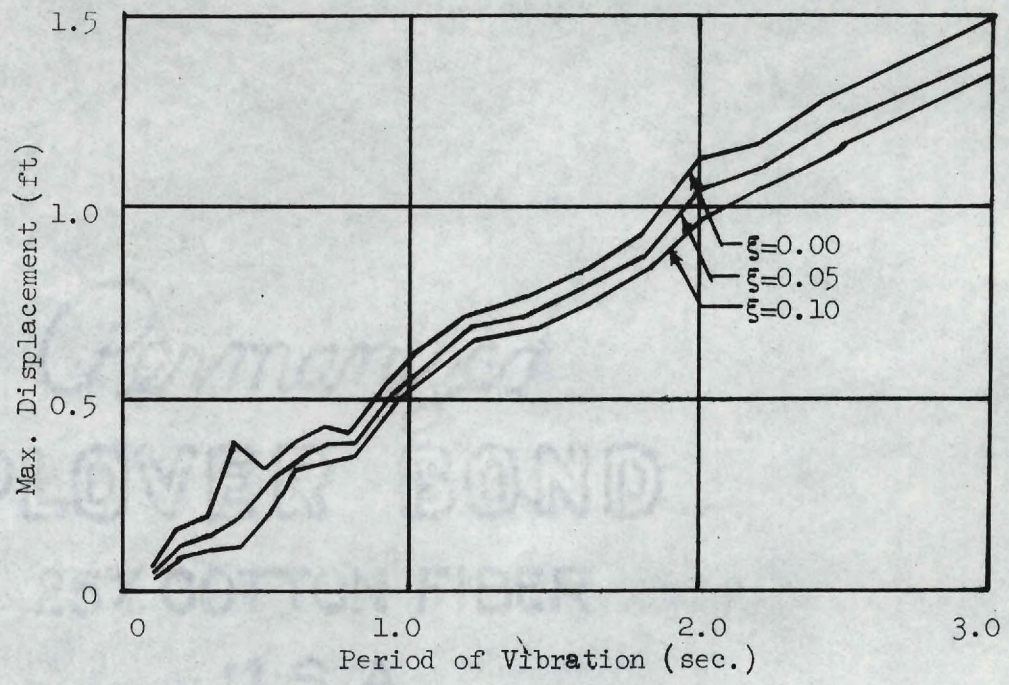

Figure 26. Displacement Response Spectra, Ensemble I, Sample 1.

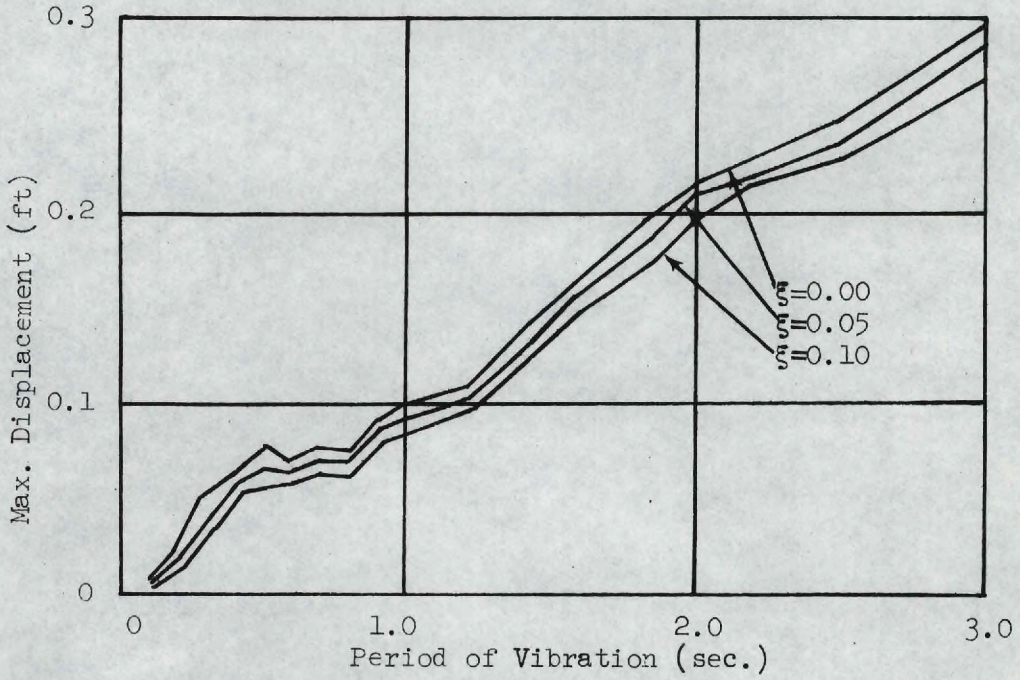

Figure 27. Displacement Response Spectra, Ensemble II, Sample 1.

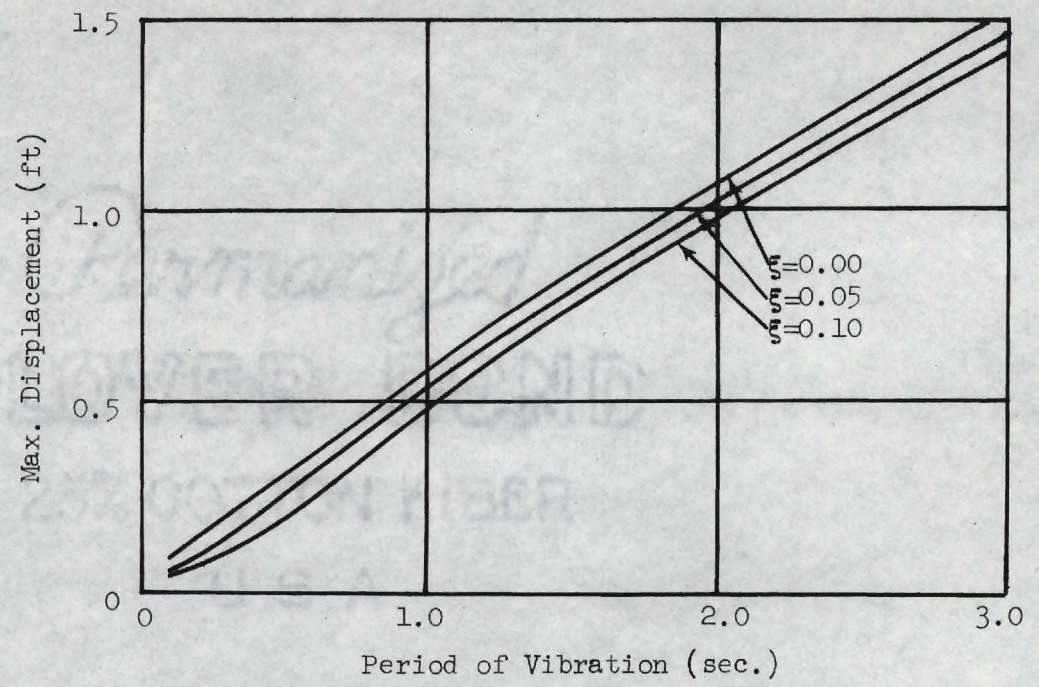

Figure 28. Average Displacement Response Spectra, Ensemble I.

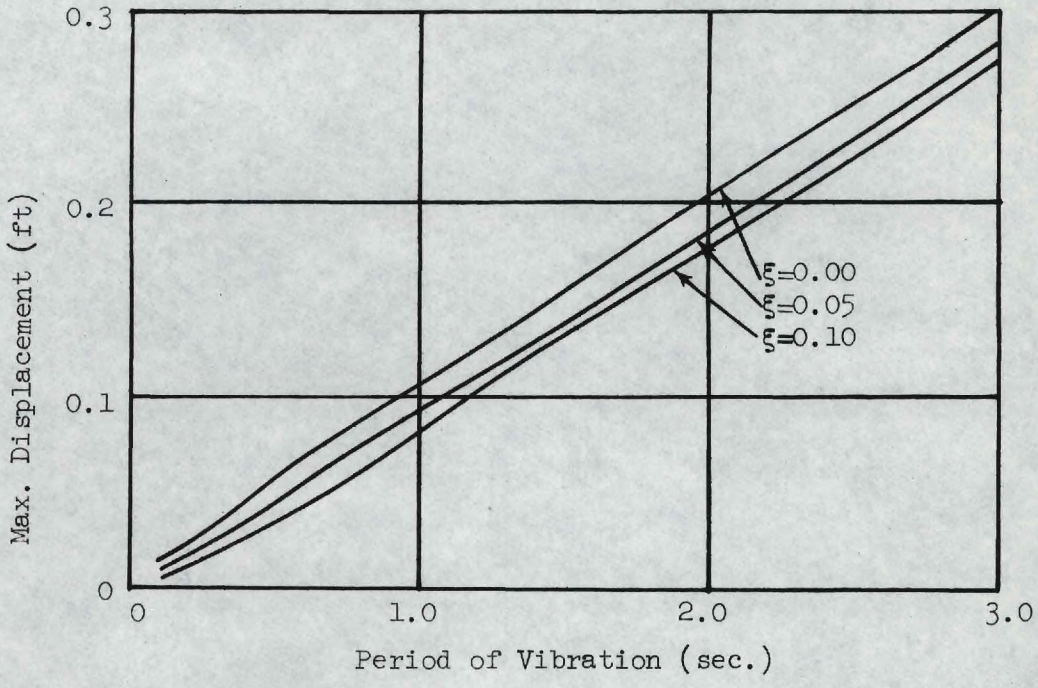

Figure 29. Average Displacement Response Spectra, Ensemble II.

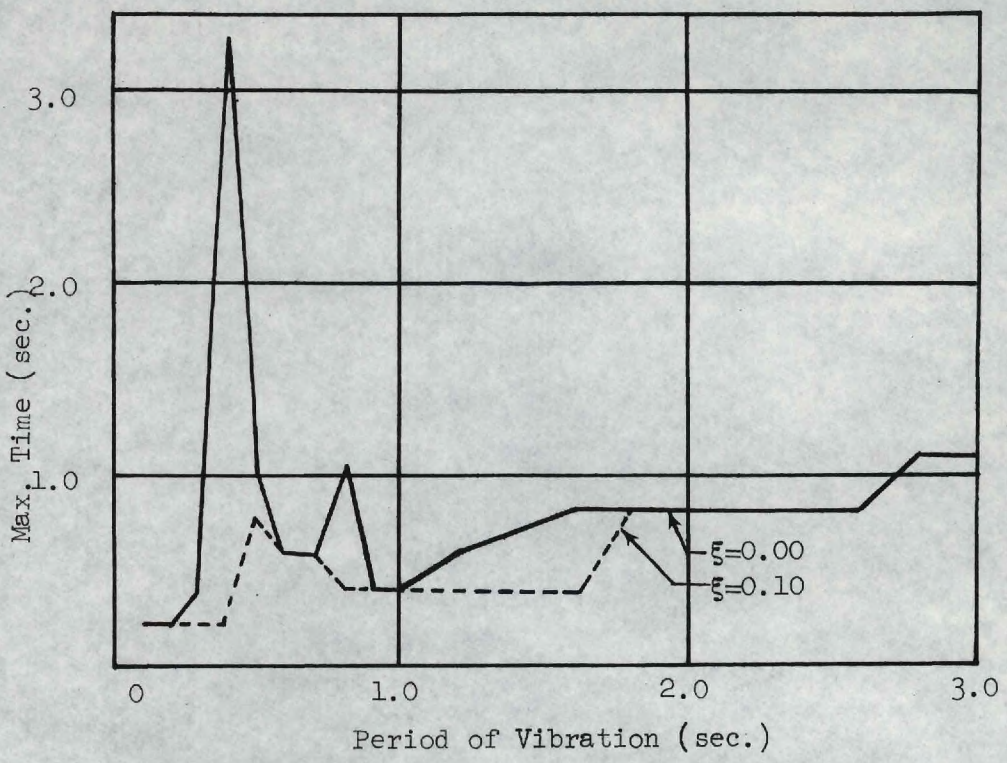

Figure 30. Time Response Spectra, Ensemble I, Sample 1.

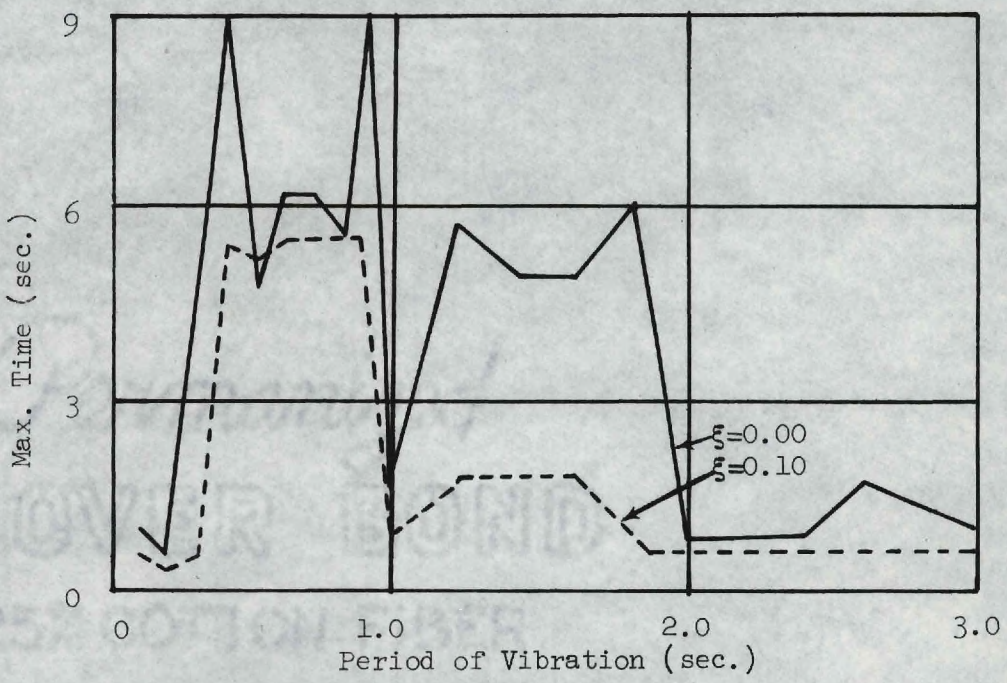

Figure 31. Time Response Spectra, Ensemble II, Sample 1.

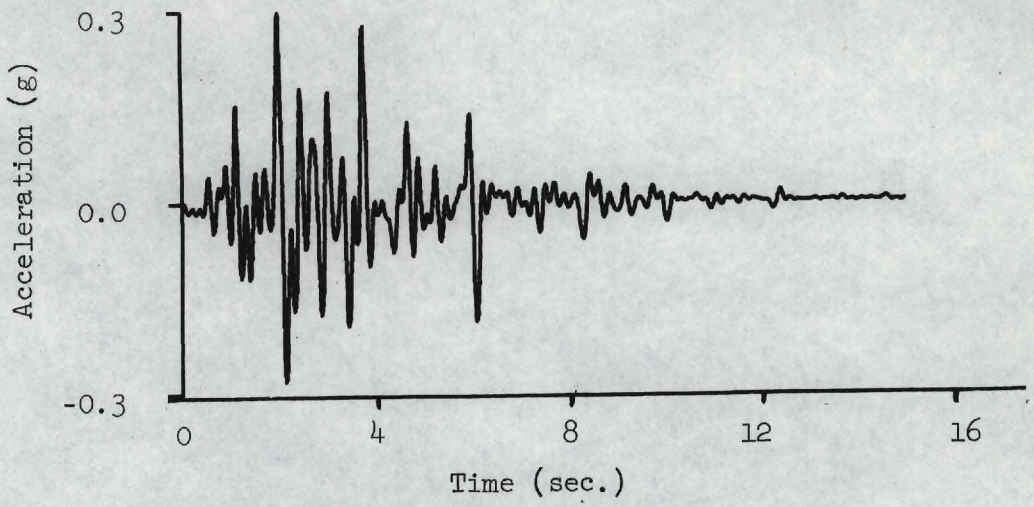

Figure 32. Artificial Accelerogram, Ensemble I.

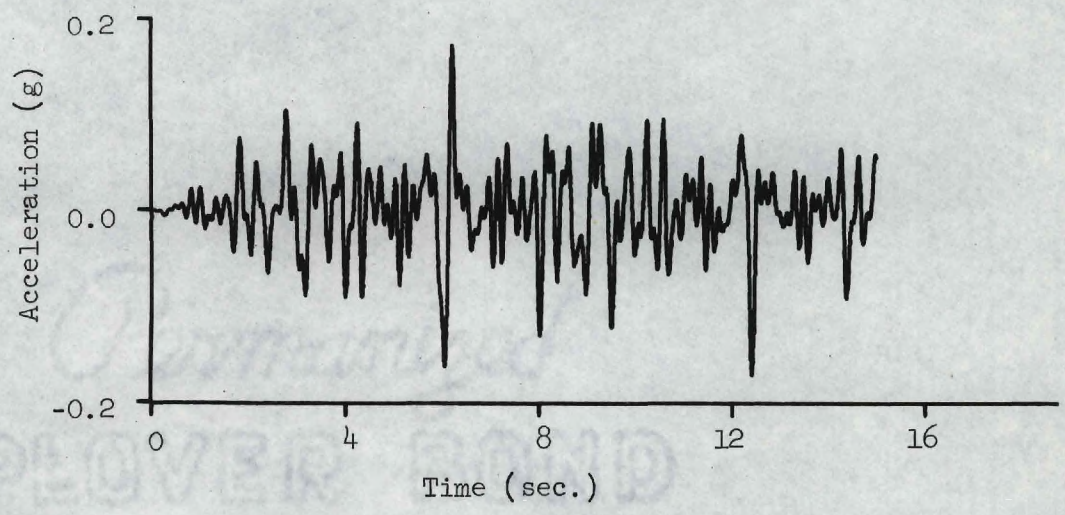

Figure 33. Artificial Accelerogram, Ensemble II.

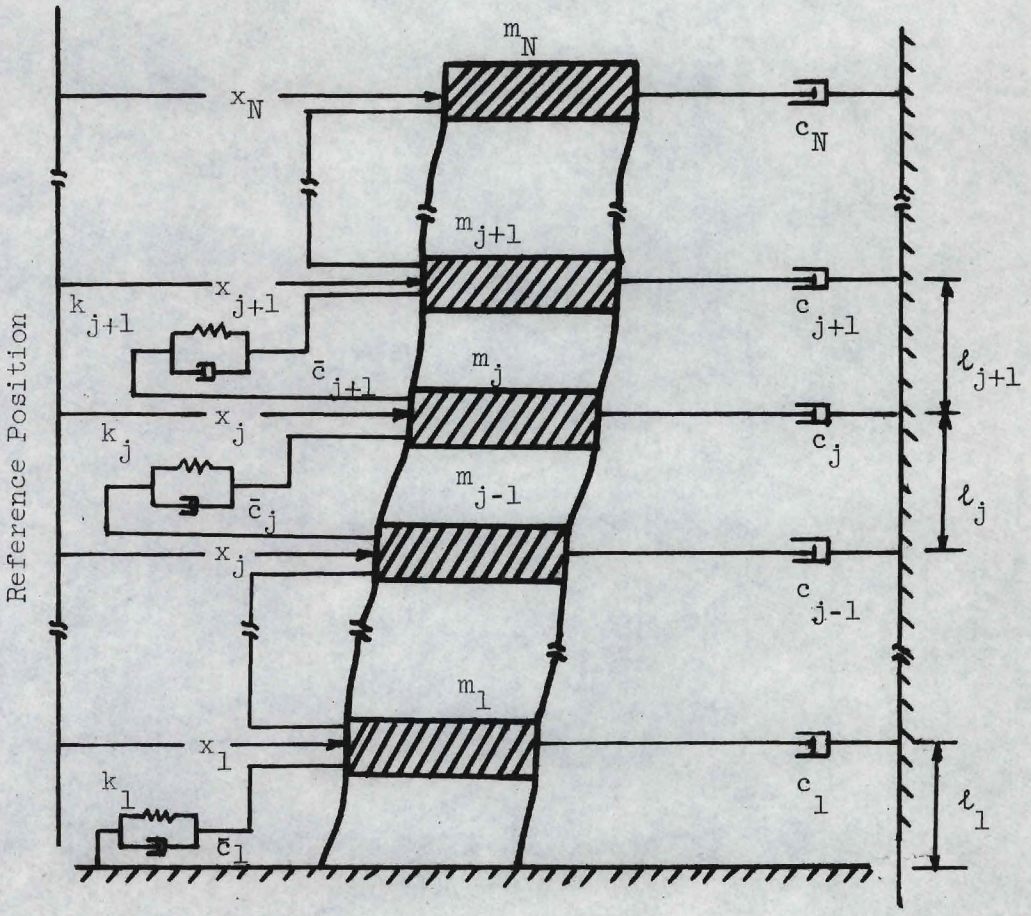

Figure 34. A Shear-type Multi-story Building.

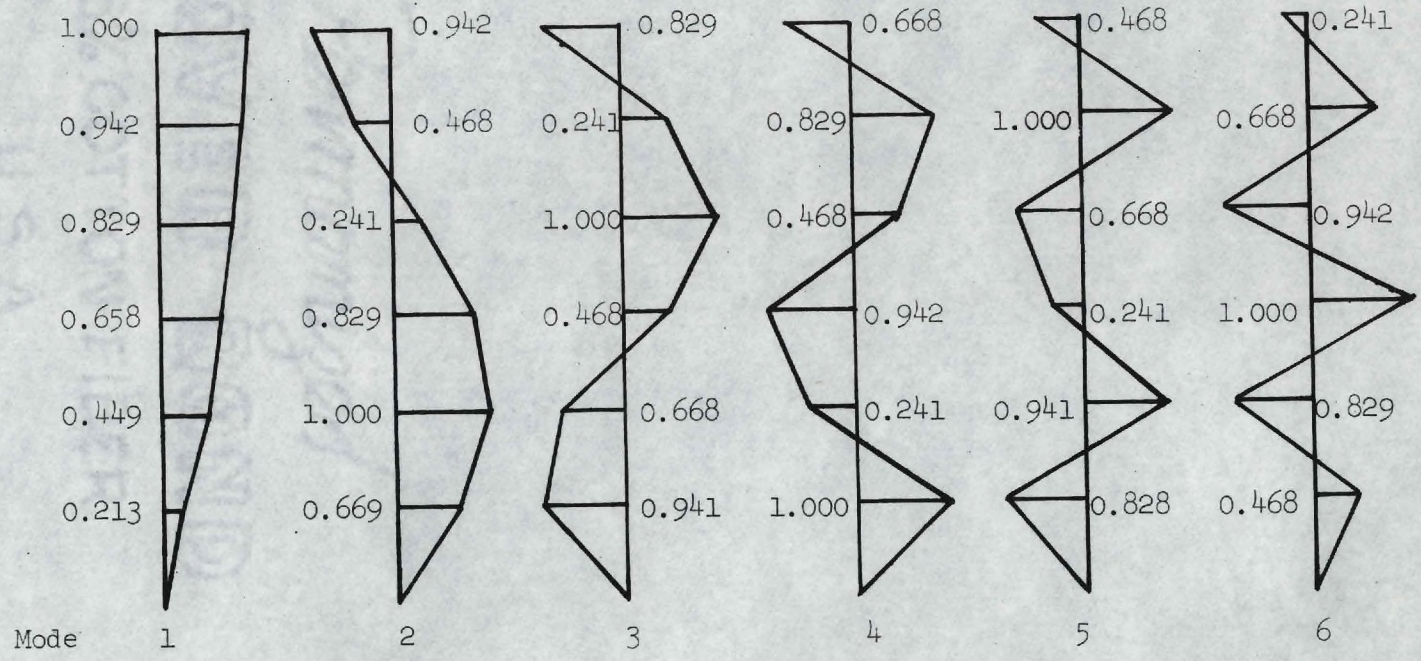

Figure 35. Mode Shapes of Structure I.

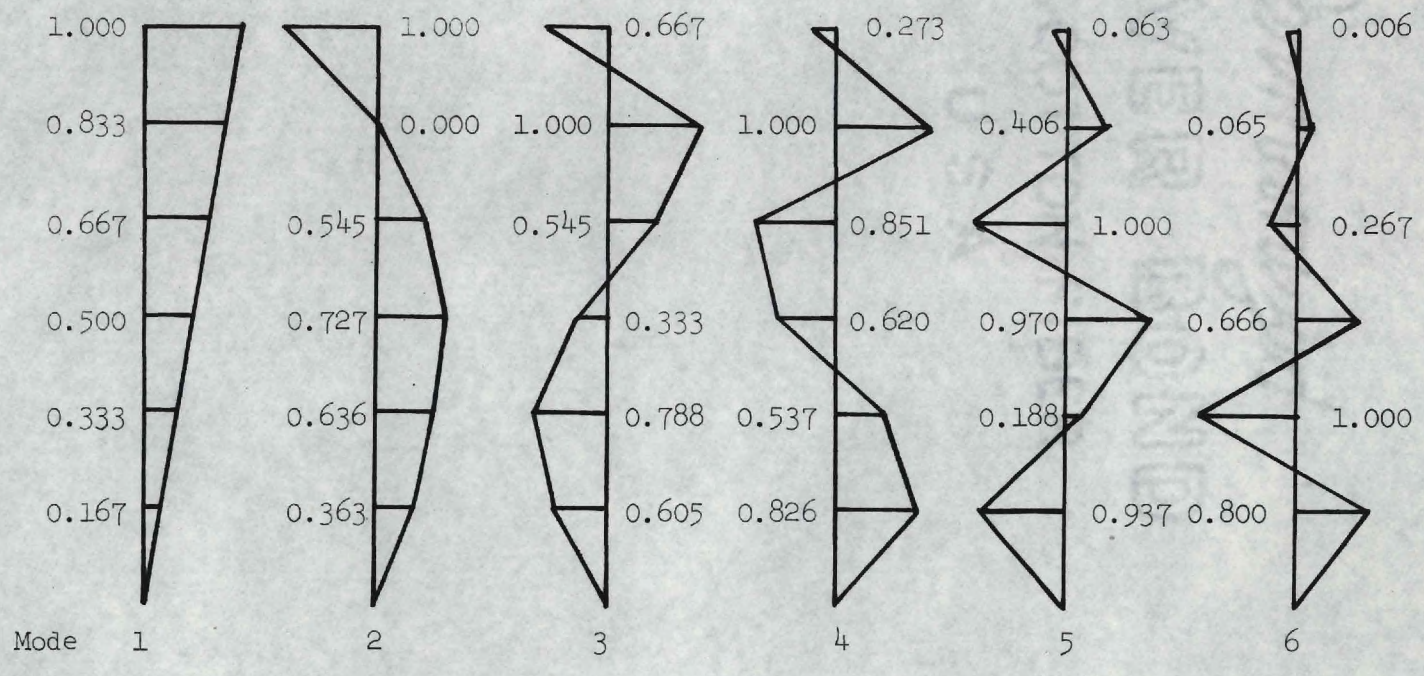

Figure 36. Mode Shapes of Structure II.

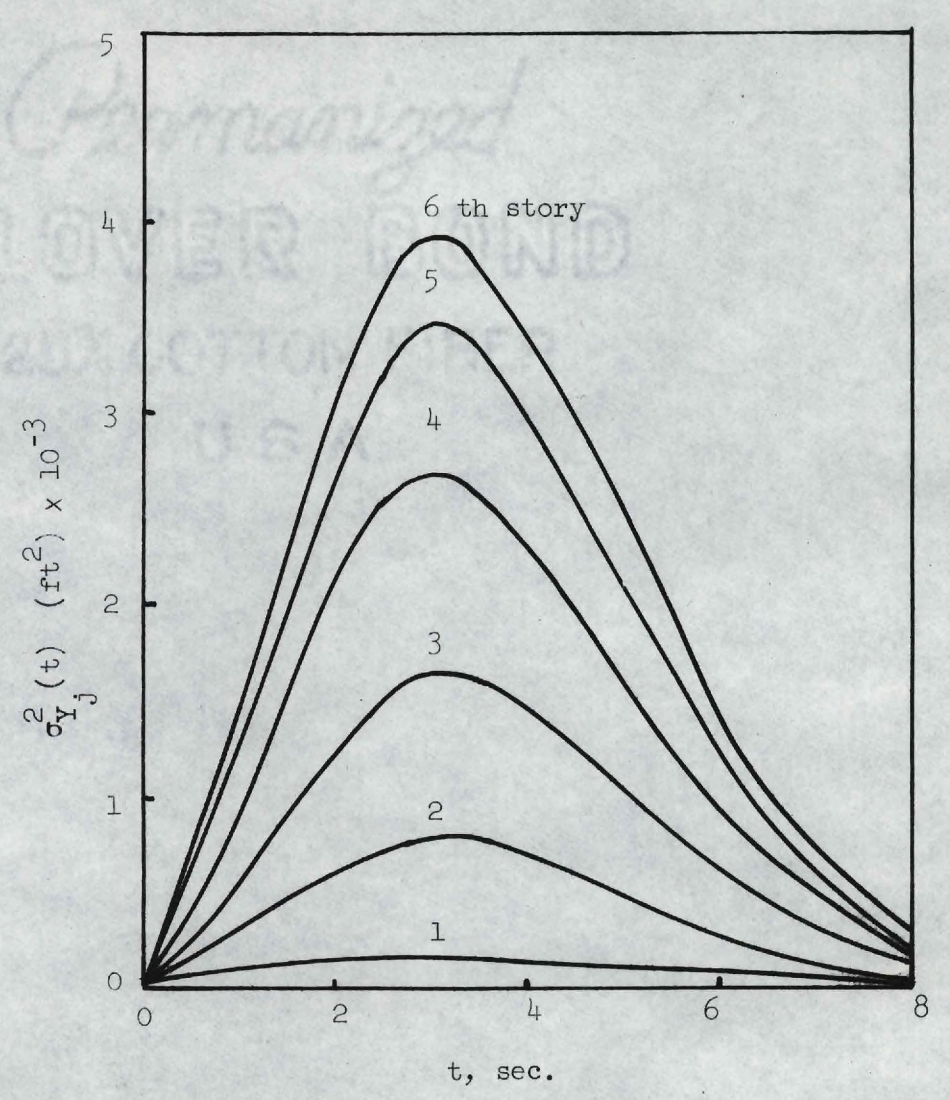

Figure 37. Variances of Relative Displacements $Y_j(t)$ (Input I, Structure I).

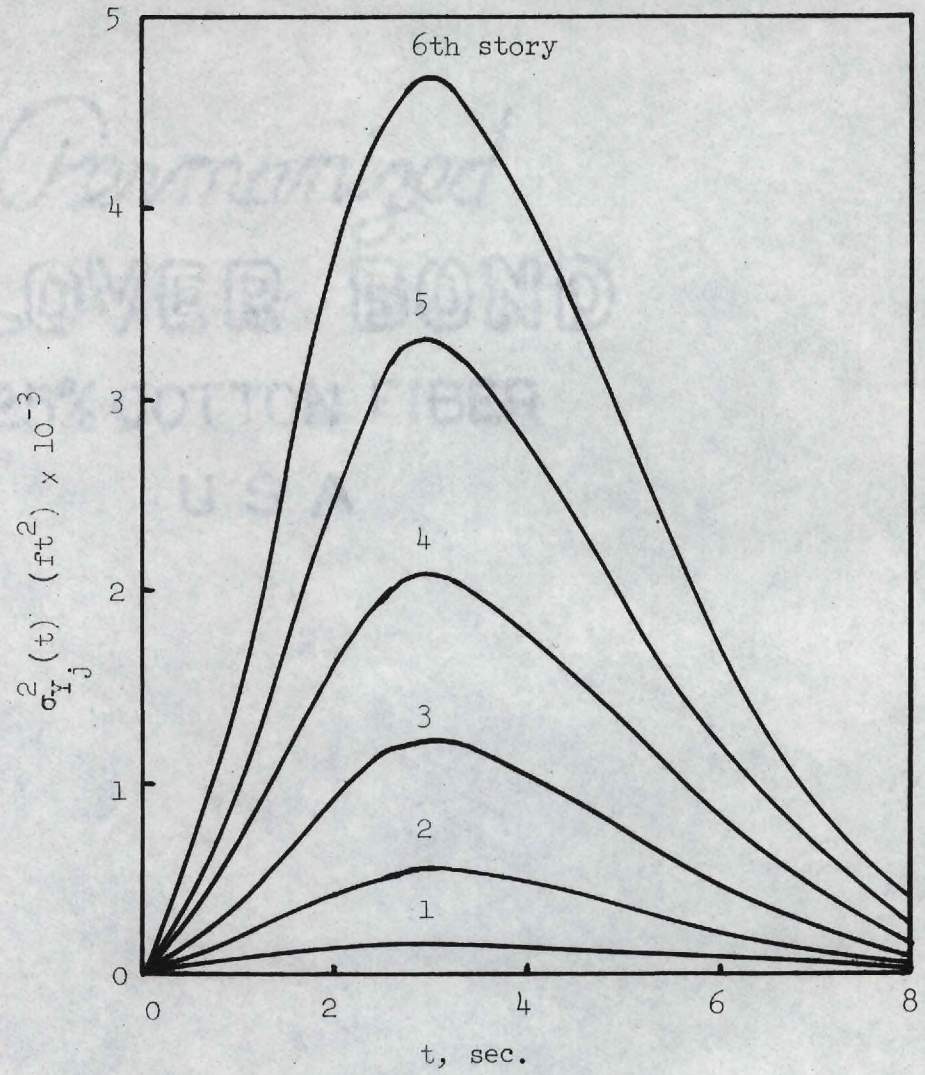

Figure 38. Variances of Relative Displacements $Y_j(t)$ (Input I, Structure II).

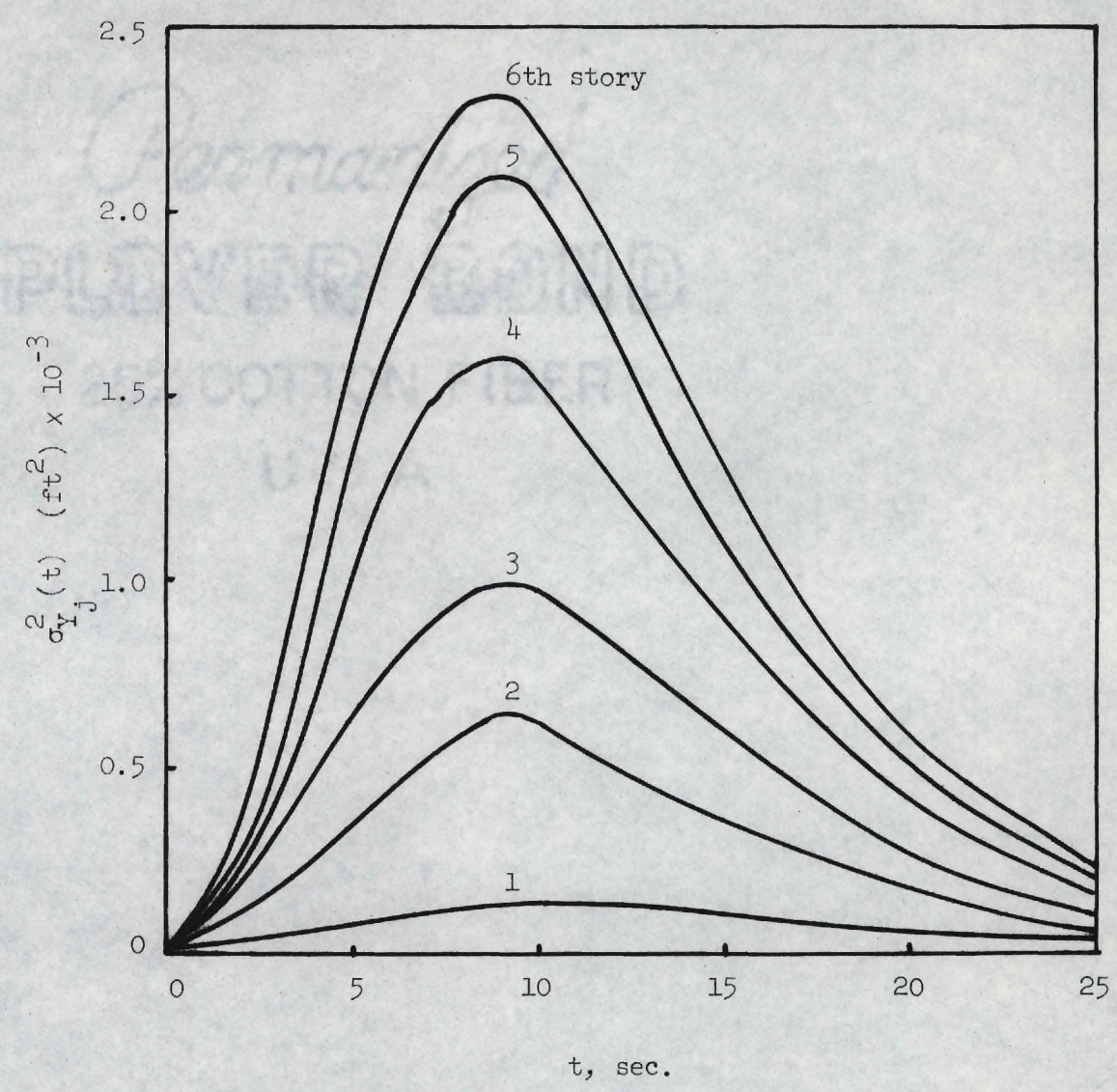

Figure 39. Variances of Relative Displacements $Y_j(t)$, (Input II, Structure I).

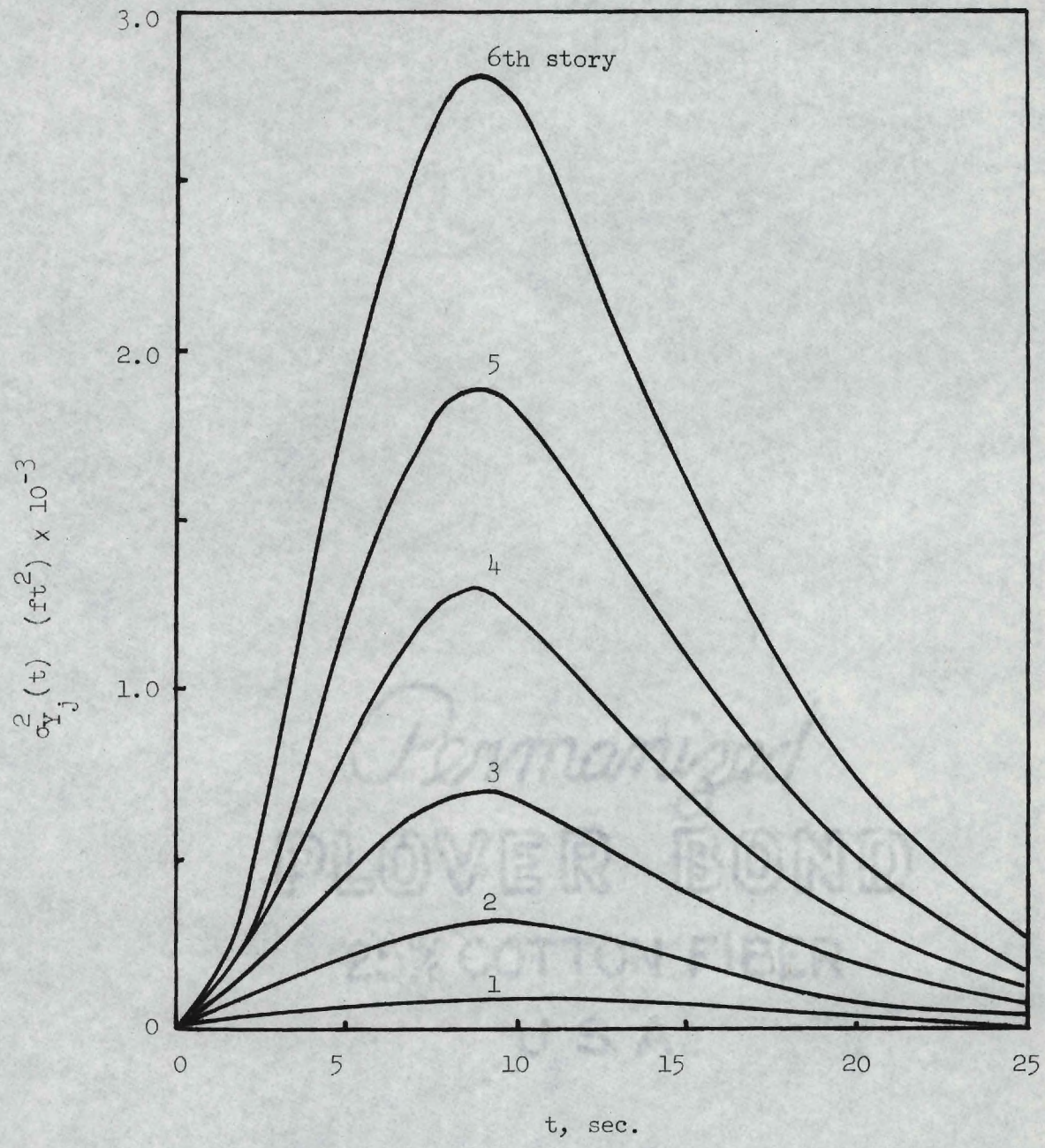

Figure 40. Variances of Relative Displacements $Y_j(t)$ (Input II, Structure II).

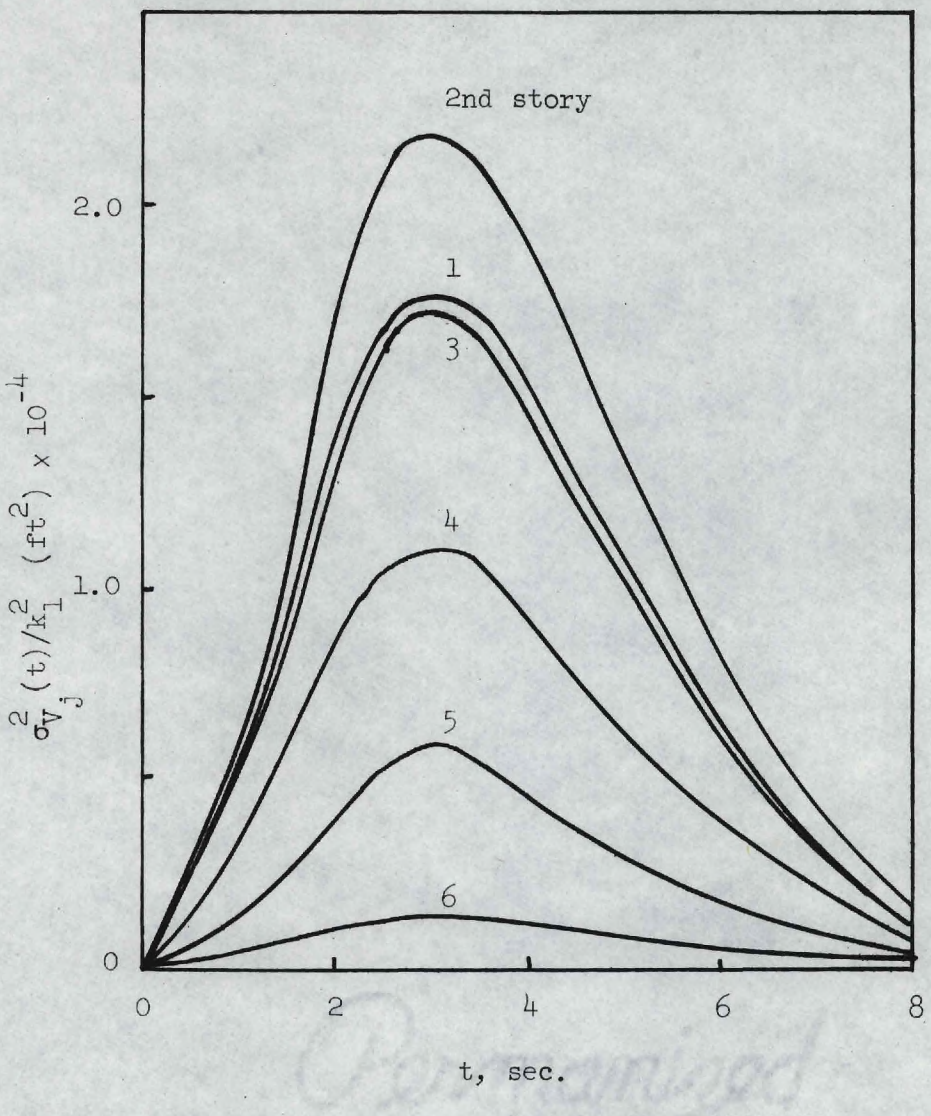

Figure 41. Variances of Story Shear Forces $V_j(t)$ (Input I, Structure I).

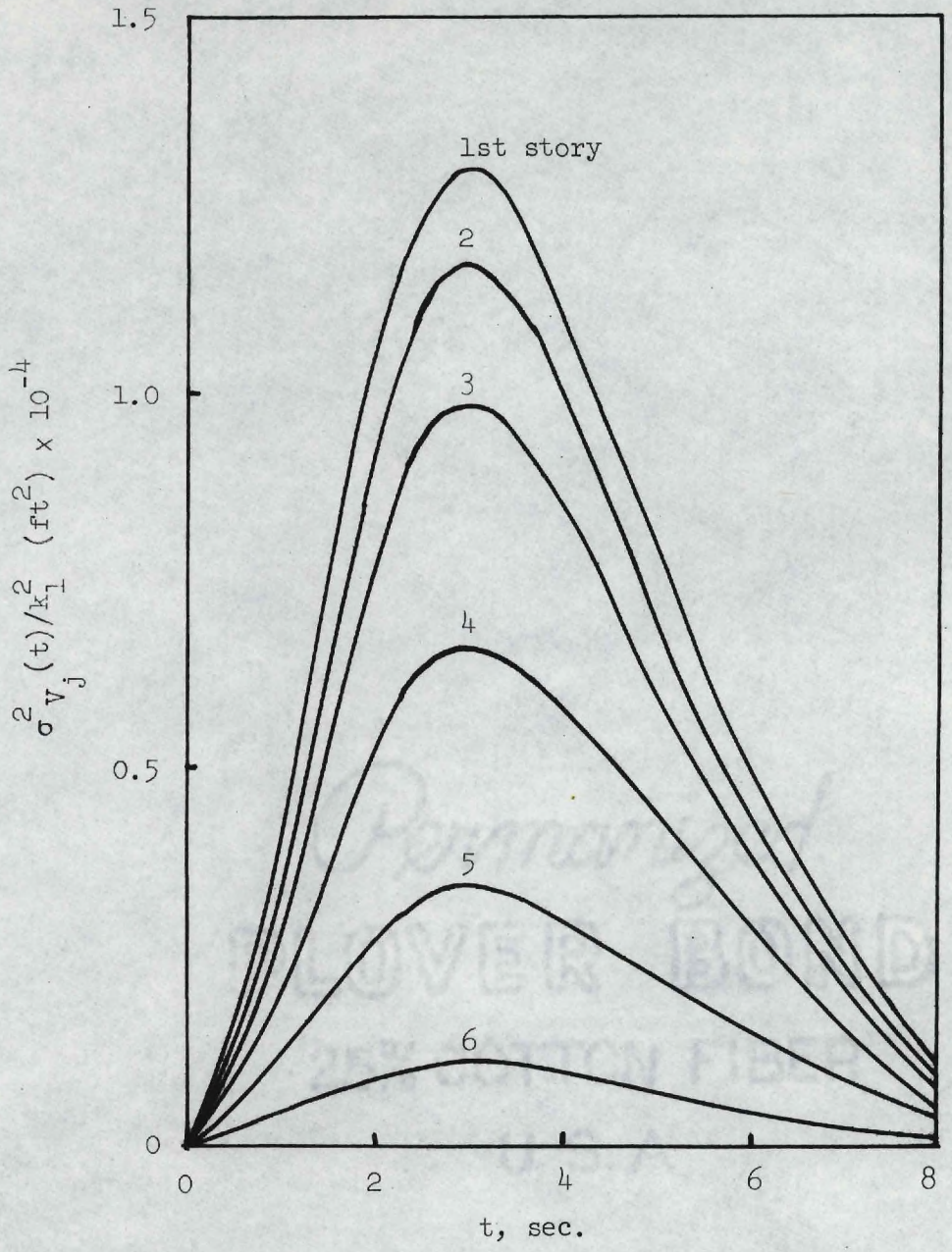

Figure 42. Variances of Story Shear Forces $V_j(t)$ (Input I, Structure II).

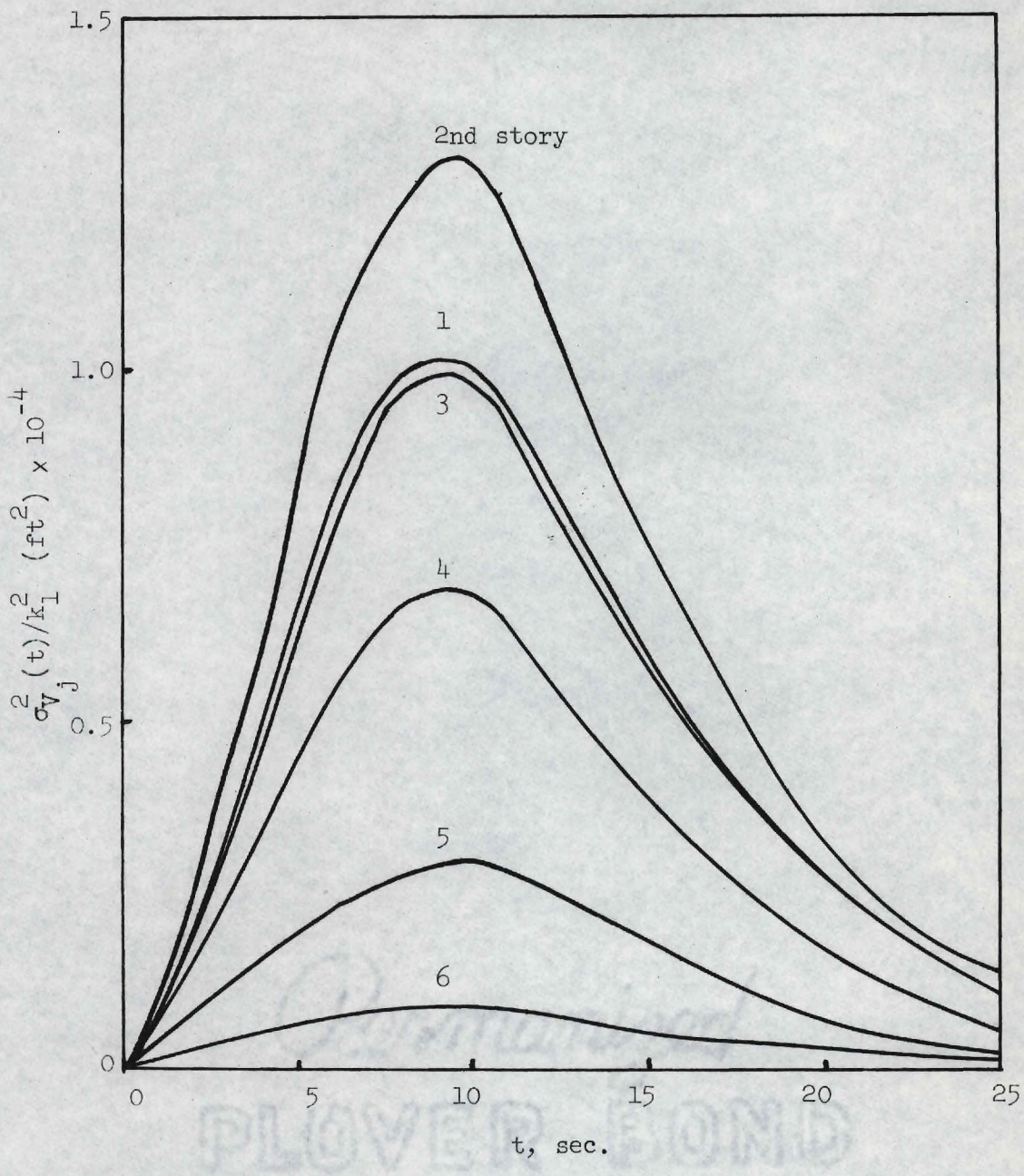

Figure 43. Variances of Story Shear Forces $V_j(t)$ (Input II, Structure I).

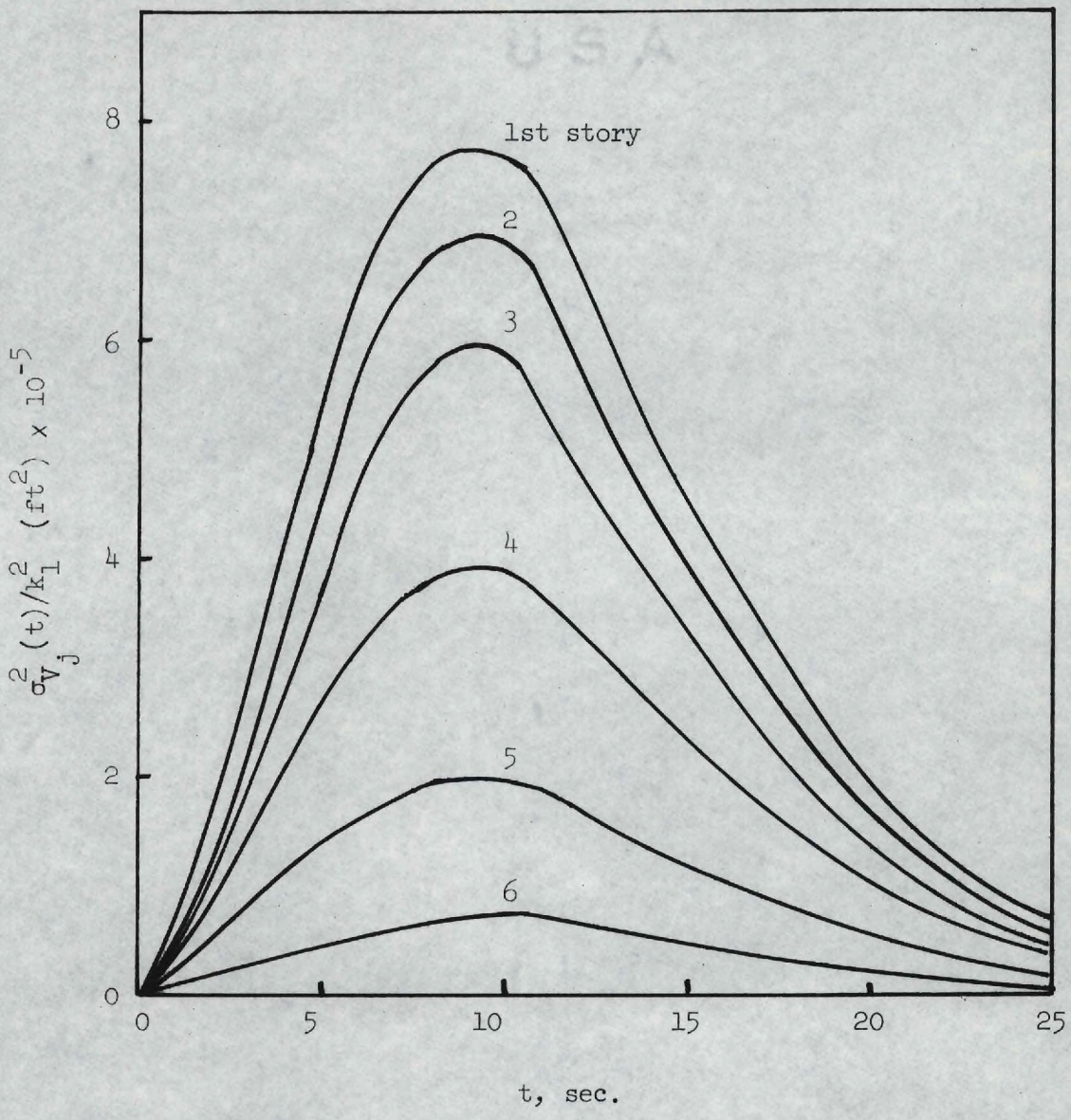

Figure 44. Variances of Story Shear Forces $V_j(t)$ (Input II, Structure II).

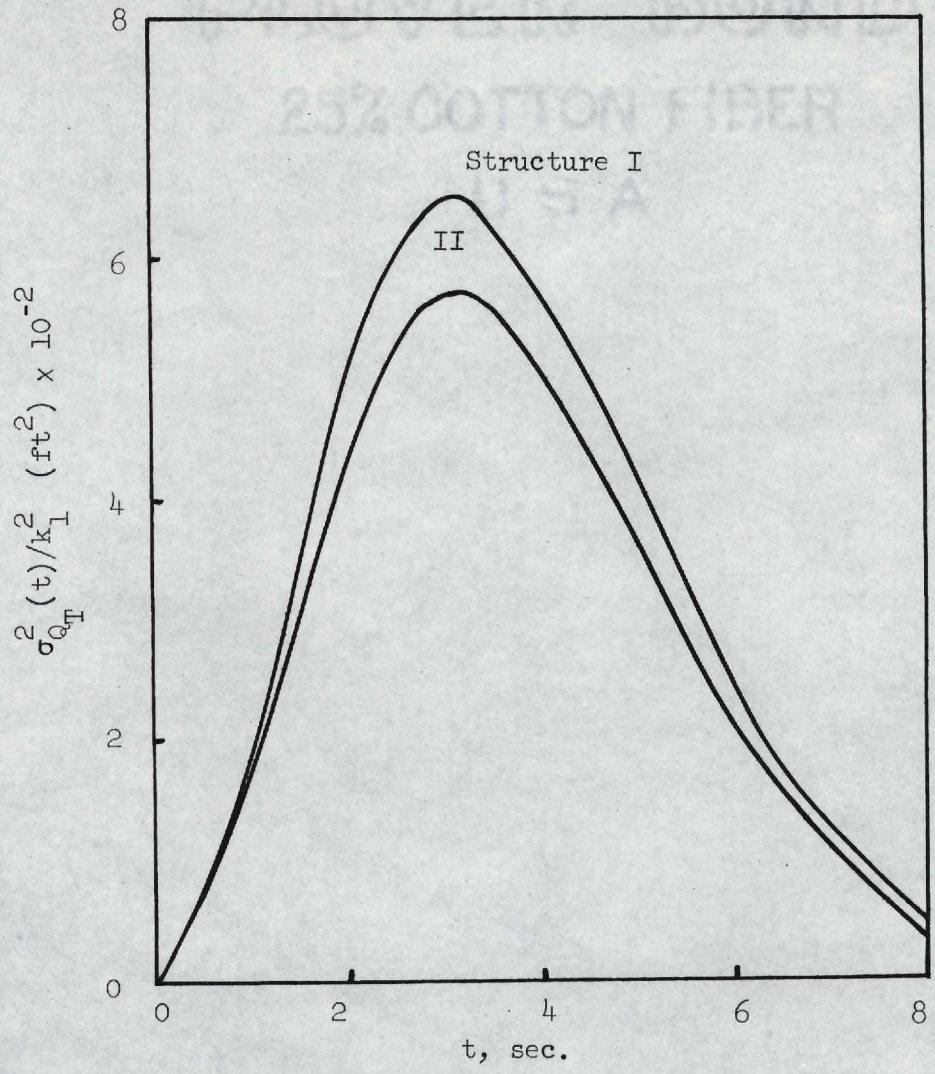

Figure 45. Variances of Total Base Shear Forces $Q_T(t)$ (Input I).

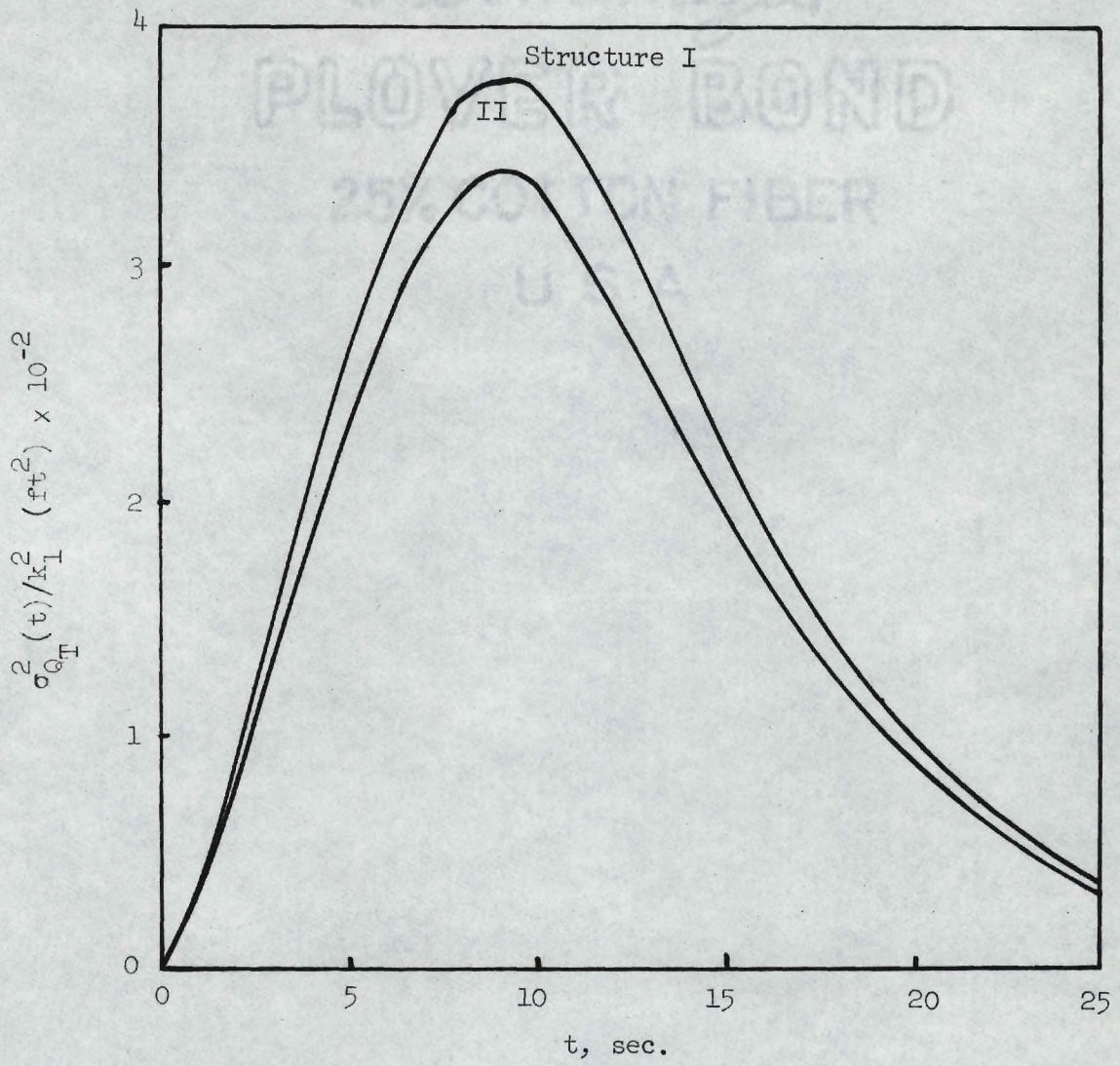

Figure 46. Variances of Total Base Shear Forces $Q_T(t)$ (Input II).

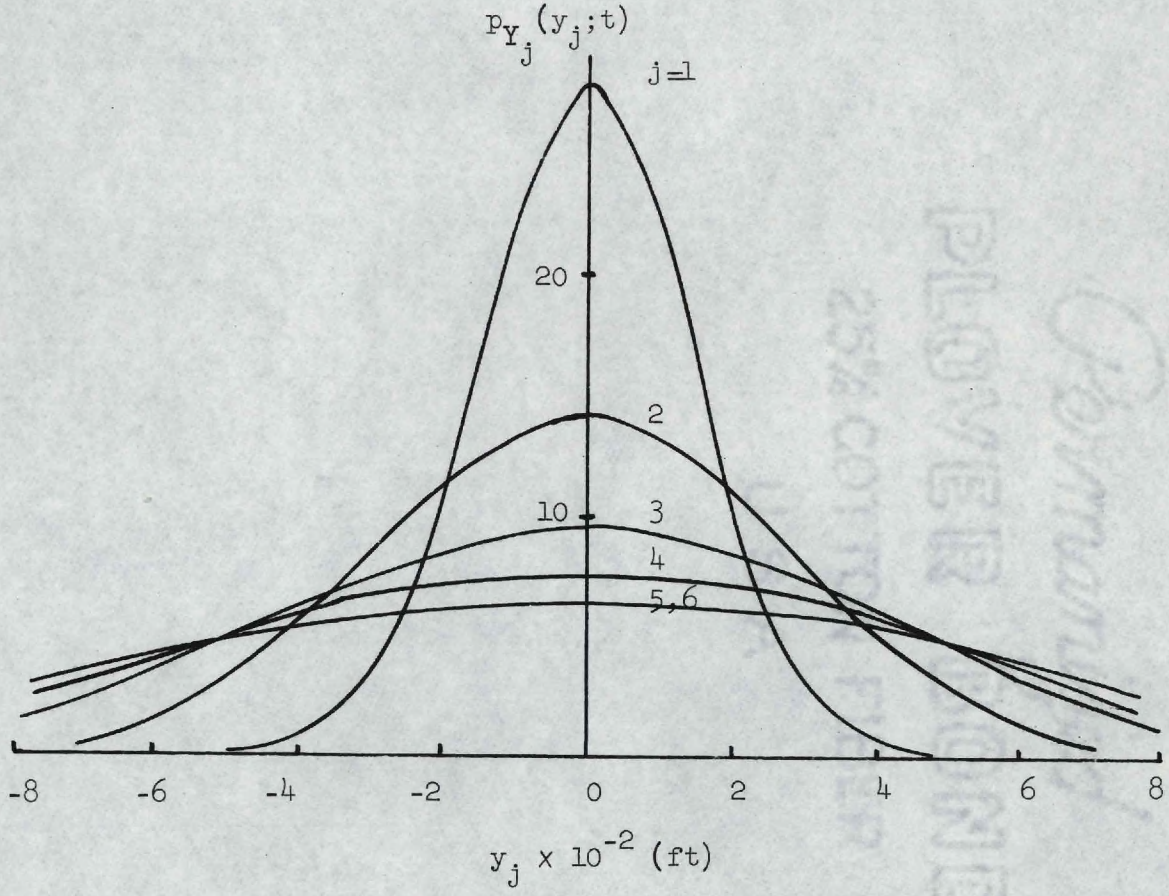

Figure 47. Probability Density Functions of Relative Displacements $Y_j(t)$ at t=3 sec. (Input I, Structure I).

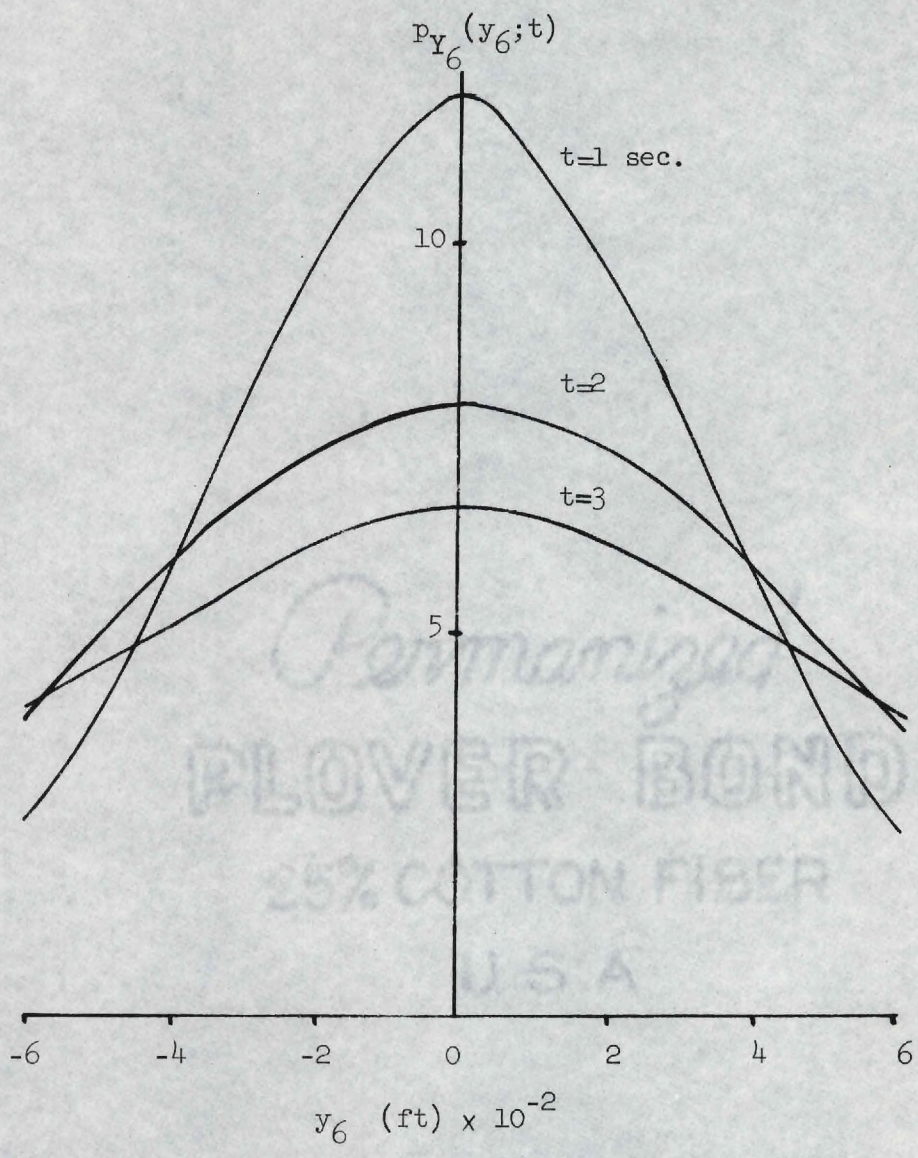

Figure 48. Probability Density Functions of Relative Displacements $Y_6(t)$ (Input I, Structure I).

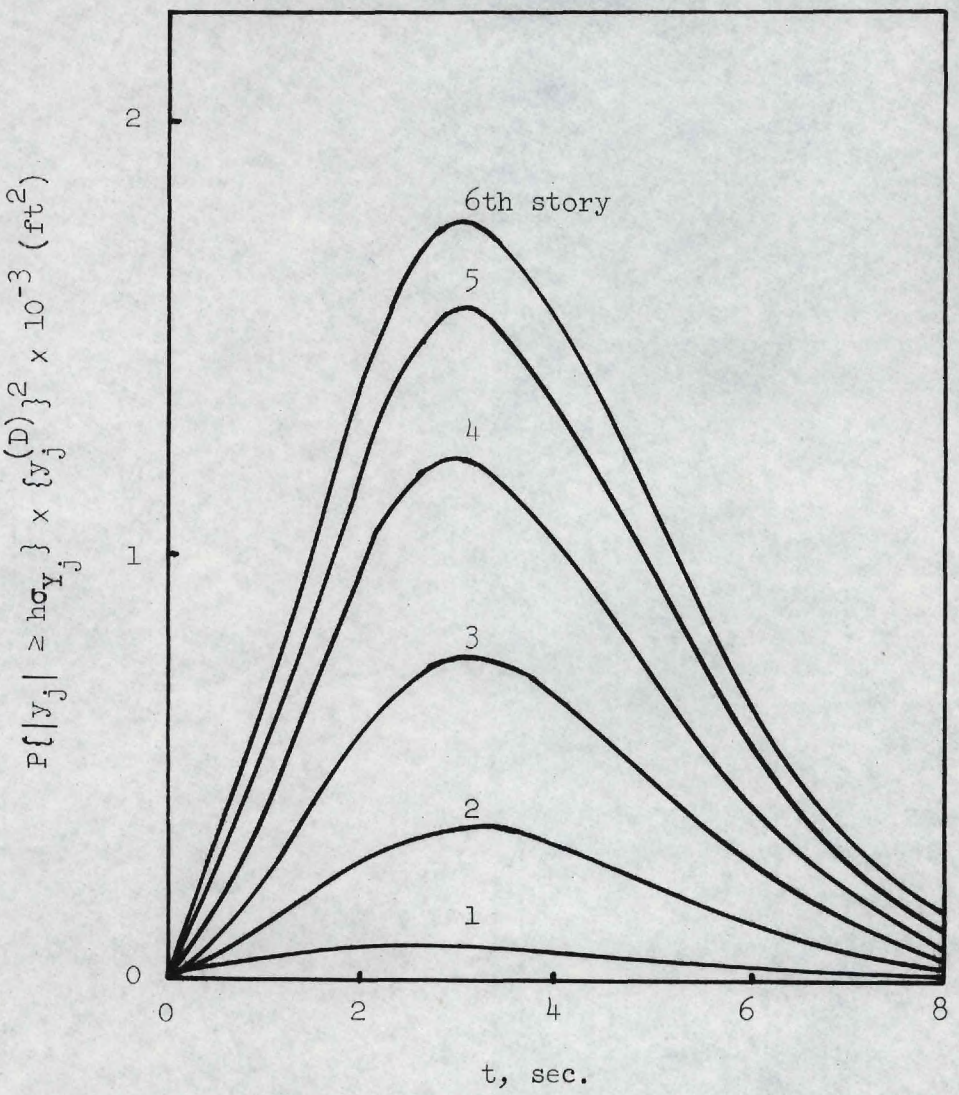

Figure 49. Upper Bounds of Probability of Relative Displacements $Y_j(t)$ Exceeding $y_j^{(D)}$ (Input I, Structure I).

REFERENCES

1. Housner, G. W., "Characteristics of Strong Motion Earthquakes", Bulletin of the Seismological Society of America, Vol. 37, No. 1, January 1947, pp. 19-31.

2. Bycroft, G. N., "White Noise Representation of Earthquakes", Journal of the Engineering Mechanics Division, ASCE, Vol. 86, No. EM2, April 1960, pp. 1-16.

3. Housner, G. W., "Behavior of Structures During Earthquakes", Journal of the Engineering Mechanics Division, ASCE, Vol. 85, No. EM4, October 1959, pp. 109-129.

4. Rosenblueth, E. and Bustamante, J. I., "Distribution of Structural Response to Earthquakes", Journal of the Engineering Mechanics Division, ASCE, Vol. 88, No. EM3, June 1962, pp. 75-106.

5. Lin, Y. K., Probabilistic Theory of Structural Dynamics, McGraw-Hill Book Company, Inc., New York, 1967.

6. Lin, Y. K., "Application of Nonstationary Shot Noise in the Study of System Response to a Class of Nonstationary Excitations", Journal of Applied Mechanics, ASME, Vol. 30, Series E, December 1963, pp. 555-558.

7. Amin, M. and Ang, A. H. S., "Nonstationary Stochastic Model of Earthquake Motions", Journal of the Engineering Mechanics Division, ASCE, Vol. 94, No. EM2, April 1968, pp. 559-584.

8. Shinozuka, M. and Sato, Y., "Simulation of Nonstationary Random Process", Journal of the Engineering Mechanics Division, ASCE, Vol. 93, No. EM1, February 1967, pp. 11-40.

9. Levy, R., "Random Processes for Earthquake Simulation", Journal of the Engineering Mechanics Division, ASCE, Vol. 97, No. EM2, April 1971, pp. 495-517.

10. Ruiz, P. and Penzien, J., "Stochastic Seismic Response of Structures", Journal of the Engineering Mechanics Division, ASCE, Vol. 97, No. EM2, April 1971, pp. 441-456.

11. Kanai, K., "Semi-empirical Formula for the Seismic Characteristics of the Ground", Bulletin of the Earthquake Research Institute, University of Tokyo, June 1957, pp. 307-325.

12. Cauchey, T. K. and Stumpf, H. J., "Transient Response of a Dynamic System Under Random Excitation", Journal of Applied Mechanics, ASME, Vol. 28, Series E, December 1961, pp. 563-566.

13. Penzien, J., Kaul, M. K. and Berge, B., "Stochastic Response of Offshore Towers to Random Sea Waves and Strong Motion Earthquakes", Journal of Computers and Structures, Vol. 2, 1972, pp. 733-756.

14. Housner, G. W. and Jennings, P. C., "Generation of Artificial Earthquakes", Journal of the Engineering Mechanics Division, ASCE, Vol. 90, No. EM1, February 1964, pp. 113-150.

15. Moyal, J. E., "Stochastic Processes and Statistical Physics," Journal of the Royal Statistical Society (London), Series B, Vol. 2, No. 11, 1949, pp. 150-210.

16. Bogdanoff, J. L., Goldberg, J. E. and Bernard, M. C., "Response of Simple Structures to a Random Earthquake-type Disturbance", Bulletin of the Seismological Society of America, Vol. 51, No. 2, April 1961, pp. 293-310.

17. Goldberg, J. E., Bogdanoff, J. L. and Sharpe, D. R., "The Response of Simple Nonlinear Systems to a Random Disturbance of Earthquake Type", Bulletin of the Seismological Society of America, Vol. 54, No. 1, February 1964, pp. 263-276.

18. Iyengar, R. N. and Iyengar, K. T., "A Nonstationary Random Process Model for Earthquake Accelerograms", Bulletin of the Seismological Society of America, Vol. 59, No. 3, June 1969, pp. 1163-1188.

19. Iyengar, R. N. and Iyengar, K. T., "Probabilistic Response Analysis to Earthquake", Journal of the Engineering Mechanics Division, ASCE, Vol. 96, No. EM3, June 1970, pp. 207-225.

20. Roberts, J. B., "The Covariance Response of Linear Systems to Nonstationary Random Excitation", Journal of Sound and Vibration, Vol. 14, No. 3, February 1971, pp. 385-400.

21. Barnoski, R. L. and Maurer, J. R., "Transient Characteristics of Simple Systems to Modulated Random Noise", Journal of Applied Mechanics, ASME, Vol. 40, Series E, March 1973, pp. 73-77.

22. Jennings, P. C., Housner, G. W. and Tsai, N. C., "Simulated Earthquake Motions for Design Purposes", Proceedings of the Fourth World Conference on Earthquake Engineering, Chile, 1969, pp. 145-160.

23. Saragoni, G. R. and Hart, G. C., "Simulation of Artificial Earthquakes", International Journal of Earthquake Engineering

and Structural Dynamics, Vol. 2, 1974, pp. 249-267.

24. Newmark, N. M. and Rosenblueth, E., Fundamentals of Earthquake Engineering, Prentice-Hall Book Co., N. J., 1971.

25. Hurty, W. C. and Rubinstein, M. F., Dynamics of Structures, Prentice-Hall Book Co., Inc., N. J., 1964.

26. Lazan, B. J., Damping of Materials and Members in Structural Mechanics, Pergamon Press Inc., New York, 1968.

27. Pian, T. H., "Structural Damping" in Random Vibration, Ed. by Crandall, S. H., MIT Press, 1958, pp. 91-108.

28. Meirovitch, L., Analytical Methods in Vibrations, Macmillan Book Co., 1967.

29. Crandall, S. H. and Mark, W. D., Random Vibration in Mechanical Systems, Academic Press Co., New York, 1963.

30. Hudson, D. E., "Some Problems in the Application of Spectrum Techniques to Strong-Motion Earthquake Analysis", Bulletin of the Seismological Society of America, Vol. 52, No. 2, April 1962, pp. 417-430.

31. Klotter, K., "Nonlinear Vibrations", in Handbook of Engineering Mechanics, Ed. by Flügge, W., McGraw-Hill Book Co., New York, 1962.

32. Clough, R. W. and Penzien, J., Dynamics of Structures, McGraw-Hill Book Co., New York, 1975, Chapter 8, 15.

33. Caughey, T. K., "Equivalent Linearization Techniques", Journal of the Acoustical Society of America, Vol. 35, No. 11, November 1963, pp. 1706-1711.

34. Crandall, S. T., "Perturbation Techniques for Random Vibration of Nonlinear Systems", Journal of the Acoustical Society of America, Vol. 35, No. 11, November 1963, pp. 1700-1705.

35. Biggs, J. M., Introduction to Structural Dynamics, McGraw-Hill Book Co., New York, 1964.

36. Rayleigh, L., The Theory of Sound, Vol. 1, Dover Book Co., New York, 1945.

37. Caughey, T. K. and O'Kelly, M. E. J., "Classical Normal Modes in Damped Linear Dynamic Systems", Journal of Applied Mechanics, ASME, Vol. 32, Series E, September 1965, pp. 583-588.

38. Bert, C. W., "Material Damping", Journal of Sound and Vibration, Vol. 29, No. 2, 1973, pp. 129-153.

39. Eringen, A. C., "Response of Tall Buildings to Random Earthquakes", Proceedings of the Third U. S. National Congress on Applied Mechanics, ASME, June 1958, pp. 141-151.

40. Penzien, J., "Elasto-plastic Response of Idealized Multistory Structures Subjected to a Strong Motion Earthquake", Proceedings of the Second World Conference on Earthquake Engineering, Japan, 1960, pp. 739-760.

41. Saul, W. E., Fleming, J. F. and Lee, S. L., "Dynamic Analysis of Bilinear Inelastic Multistory Shear Buildings", Proceedings of the Third World Conference on Earthquake Engineering, New Zealand, 1965, pp. 533-551.

42. Shinozuka, M. and Henry, L., "Random Vibration of a Beam Column", Journal of the Engineering Mechanics Division, ASCE, Vol. 91, No. EM5, February 1965, pp. 123-143.

43. Amin, M. and Ang, A. H. S., "Significance of Nonstationarity of Earthquake Motions", Proceedings of the Fourth World Conference on Earthquake Engineering, Chile, 1969, pp. 97-114.

44. Douglas, B. M. and Weir, P., "Multistory Building Response Determined from Ground-Velocity Records", Bulletin of the Seismological Society of America, Vol. 62, No. 1, February 1972, pp. 357-367.

45. Blume, J. A., "The Motion and Damping of Buildings Relative to Seismic Response Spectra", Bulletin of the Seismological Society of America, Vol. 60, No. 1, February 1970, pp. 231-259.

46. Jennings, R. L. and Newmark, N. M., "Elastic Response of Multistory Shear Beam Type Structures Subjected to Strong Ground Motion", Proceedings of the Second World Conference on Earthquake Engineering, Japan, 1960, pp. 699-717.

47. Penzien, J. and Kaul, M. K., "Response of Offshore Towers to Strong Motion Earthquakes", International Journal of Earthquake Engineering and Structural Dynamics, Vol. 1, June 1972, pp. 55-68.

48. Nigam, N. C. and Housner, G. W., "Elastic and Inelastic Response of Framed Structures During Earthquakes", Proceedings of the Fourth World Conference on Earthquake Engineering, Chile, 1969.

49. Clough, R. W., Benuska, K. L. and Wilson, E. L., "Inelastic Earthquake Response of Tall Buildings", Proceedings of the Third World Conference on Earthquake Engineering, New Zealand, 1965, pp. 68-89.

50. Clough, R. W. and Benuska, K. L., "Nonlinear Earthquake Behavior of Tall Buildings", Journal of the Engineering Mechanics Division, ASCE, Vol. 93, No. EM3, June 1967, pp. 129-155.

51. Newmark, N. M., "Current Trends in the Seismic Analysis and Design of High-Rise Structures", in Earthquake Engineering, Ed. by Wiegel, R. L., Prentice-Hall Book Co., 1970, pp. 403-424.

52. Penzien, J. and Liu, S. C., "Nondeterministic Analysis of Nonlinear Structures Subjected to Earthquake Excitations", Proceedings of the Fourth World Conference on Earthquake Engineering, Chile, 1969, pp. A-4-89 - A-4-104.

53. Kaul, M. K. and Penzien, J., "Stochastic Seismic Analysis of Yielding Offshore Towers", Journal of the Engineering Mechanics Division, ASCE, Vol. 100, No. EM5, October 1974, pp. 1025-1038.

54. Meyer, C., "Inelastic Dynamic Analysis of Tall Buildings", International Journal of Earthquake Engineering and Structural Dynamics, Vol. 2, 1974, pp. 325-342.

55. Ni, C. M. and Lee, L. H., "Finite Earthquake-Response of Inelastic Structures", Journal of the Engineering Mechanics Division, ASCE, Vol. 98, No. EM6, December 1972, pp. 1529-1545.

56. Caughey, T. K., "Derivation and Application of the Fokker-Planck Equation to Discrete Nonlinear Dynamic Systems Subjected to White Random Excitation", Journal of the Acoustical Society of America, Vol. 35, No. 11, 1963, pp. 1683-1692.

57. Iwan, W. D. and Yang, I. M., "Application of Statistical Linearization Techniques to Nonlinear Multi-Degree-of-Freedom Systems", Journal of Applied Mechanics, ASME, Vol. 39, Series E, June 1972, pp. 559-562.

58. Penzien, J., "Applications of Random Vibration Theory in Earthquake Engineering", in Earthquake Engineering, Ed. by Wiegel, R. L., Prentice-Hall Book Co., N. J., 1970, pp. 335-347.

59. Vervon, J. M., "Response of a Single-Degree-of-Freedom System to Modulated White Noise", Journal of Applied Mechanics, ASME, Vol. 40, Series E, March 1973, pp. 296-297.

60. Hasselman, T., "Linear Response to Nonstationary Random Excitation", Journal of the Engineering Mechanics Division, ASCE, Vol. 98, No. EM3, June 1972, pp. 519-530.

61. Papoulis, A., Probability, Random Variables and Stochastic Processes, McGraw-Hill Book Co., New York, 1965.

62. Barstein, M. F., "The Application of Probability Methods for Design-the Effect of Seismic Forces on Engineering Structures", Proceedings of the Second World Conference on Earthquake Engineering, Japan, 1960, pp. 1467-1481.

63. Hildebrand, F. B., Methods of Applied Mathematics, Prentice-Hall Book Co., N. J., 1960, Chapter 3.

64. Tajimi, H., "A Statistical Method of Determining the Maximum Response of a Building Structure During an Earthquake", Proceedings of the Second World Conference on Earthquake Engineering, Japan, 1960, pp. 781-797.

65. Coast and Geodetic Survey (Annual), United States Earthquakes, Washington, D. C., U. S. Government Printing Office.

66. Jennings, P. C., Engineering Features of the San Fernando Earthquake, (February 9, 1971), Earthquake Engineering Research Laboratory, California Institute of Technology, June 1974.

67. Cartwright, D. E. and Longuet-Higgins, M. S., "The Statistical Distribution of the Maxima of a Random Function", Proceedings of the Royal Society of London, Series A, Vol. 237, 1956, pp. 212-232.

68. Bolotin, V. V., "Statistical Theory of the Aseismic Design of Structures", Proceedings of the Second World Conference on Earthquake Engineering, Japan, 1960, pp. 1365-1374.

69. Merrit, R. C. and Housner, G. W., "Effect of Foundation Compliance on Earthquake Stresses in Multistory Buildings", Bulletin of the Seismological Society of America, Vol. 44, No. 4, October 1954, pp. 551-569.

70. Weinberger, H. F., Partial Differential Equations, Xerox, New York, 1965, Chapter 5.

71. Berg, G. V. and Housner, G. W., "Integrated Velocity and Displacement of Strong Earthquake Ground Motion", Bulletin of the Seismological Society of America, Vol. 51, No. 2, April 1961, pp. 175-189.

72. Bolotin, V. V., Statistical Methods in Structural Mechanics, Holden-Day, Inc., San Francisco, 1969, Chapter 5.

73. Cramér, H., Mathematical Methods of Statistics, Princeton University Press, 1946.

74. Clough, R. W., "Earthquake Response of Structures", in Earthquake Engineering, Ed. by Wiegel, R. L., Prentice-Hall Co., N. J., 1970, pp. 307-334.

75. Caughey, T. K., "Nonlinear Theory of Random Vibrations", in Advances in Applied Mechanics, Ed. by Yih, C. S., Vo. 2, Academic Press, 1971, pp. 209-253.

76. Lepore, J. A. and Stoltz, R. A., "Stability of Cylindrical Shells Under Random Excitation", Journal of the Engineering Mechanics Division, ASCE, Vol. 100, No. EM3, June 1974, pp. 531-546.

VITA

Tzu-I Hsu was born in Taiwan, China, on September 10, 1947. He received his Bachelor's Degree in Civil Engineering from National Taiwan University, Taipei, Taiwan, in June, 1969. During the period from July, 1969, to August, 1970, he participated in the Reserve Officer Training Program of the Army of the Republic of China. In September, 1970, he entered the Graduate School of Civil Engineering, National Taiwan University. He received his Master's Degree in Civil Engineering in June, 1972.

He entered the Georgia Institute of Technology as a doctoral student in the School of Engineering Science and Mechanics in September, 1972.

On July 25, 1973, he married Day-Luan Yang of Taiwan, China.